

# Radioligand Development for PET Imaging of $\beta$ -Amyloid ( $A\beta$ )-Current Status

Lisheng Cai<sup>\*</sup>, Robert B. Innis and Victor W. Pike

Molecular Imaging Branch, National Institute of Mental Health, National Institutes of Health, Bethesda, MD 20892, USA

**Abstract:** Two of the main pathological hallmarks of Alzheimer's disease (AD) are neuritic plaques and neurofibrillary tangles. Significant evidence supports a critical and probable causative role of  $\beta$  amyloid ( $A\beta$ ) plaque formation. Since neuroprotective treatments are typically most effective at early stages of injury, the detection and measurement of  $A\beta$  load in living brain should be performed at early and perhaps even presymptomatic stages of AD. Two primary targets of molecular imaging research with positron emission tomography (PET) are to develop surrogate markers (radioligands) for assessing disease progression and for monitoring the efficacy of developmental therapeutics. Here, we review the current status of radioligand development for PET imaging of  $A\beta$  aggregates. General structure-activity relationships have emerged, including the identification of at least three different ligand binding sites in various  $A\beta$  aggregates and recognition of the general structural requirements for ligand binding at each site. Also a few radioligands applicable to imaging  $A\beta$  plaques in living human brain with positron emission tomography (PET) have emerged, including [<sup>11</sup>C]PIB, [<sup>11</sup>C]SB-13 and [<sup>18</sup>F]FDDNP.

**Keywords:** PET imaging,  $\beta$ -amyloid, radioligand, assay, Alzheimer's disease.

## 1. INTRODUCTION TO ALZHEIMER'S DISEASE (AD)

Alzheimer's disease (AD) is a major cause of dementia and currently afflicts about four million Americans [1] and more than thirty million people worldwide [2]. The most significant risk factor is age, with about 5% prevalence at 65 and 20-30% at 85 years [3]. Histopathologically, AD is characterized by neuronal loss and also the presence of senile plaques (SP), diffuse plaques (DP), neurofibrillary tangles (NFT), neuropil threads (NT), and dystrophic neurites (DN) [4]. Clinical treatments mainly control symptoms by providing temporary improvement and reducing the rate of cognitive decline. Agents useful for reducing the signs of dementia include cholinesterase inhibitors, such as donepezil, rivastigmine and galantamine, and the NMDA receptor antagonist, memantine [5]. Other psychotropic agents useful for the treatment of associated neuropsychiatric symptoms and behavioral disturbances are also available [6].

AD is a genetically complex and heterogeneous disorder. Mutations in three genes (APP, PSEN1 and PSEN2) are known to cause familial early-onset AD [7-9]. Although there is no evidence that autosomal dominant inheritance of mutated genes causes late-onset AD, genetics does appear to play a role in the development of this more common form. Thus, in the early 1990s, Corder *et al.* found increased risk for late-onset AD with inheritance of one or two copies of the apolipoprotein E epsilon4 (APOE  $\epsilon$ 4) allele on chromosome 19 [10,11]. Different alleles of particular genes produce variations in inherited characteristics, such as for eye color or blood type. In this case, variations are in the gene

that directs the manufacture of the APOE protein. This protein helps carry blood cholesterol throughout the body [12], among other functions [13]. It is found in glial cells and neurons of healthy brains [14-16], but is also associated in excess amount with plaques found in brains of people with AD [17]. Three common alleles of the APOE gene are  $\epsilon$ 2,  $\epsilon$ 3 and  $\epsilon$ 4. The finding that an increased risk of AD is linked with inheritance of the  $\epsilon$ 4 allele has helped explain some of the variation in age of onset of AD based on whether people have inherited zero, one, or two copies of this allele [18,19]. The more  $\epsilon$ 4 alleles that are inherited, the lower the age of AD onset. The relatively rare  $\epsilon$ 2 allele may protect some people against the disease; it seems to be associated with a lower risk for AD and a later age of onset. The  $\epsilon$ 3 allele is the most common version found in the general population and may play a neutral role in AD.

$\beta$ -Amyloid ( $A\beta$ ) peptides (*e.g.*  $A\beta$ 40 and  $A\beta$ 42) mainly constitute the various deposits (*e.g.* plaques and their precursors) appearing in brains of AD subjects. These peptides are cleaved from amyloid precursor protein (APP) by three types of enzymes,  $\alpha$ -,  $\beta$ - and  $\gamma$ -secretases (Fig. 1). Both  $\alpha$ - and  $\gamma$ -secretases are involved in cleaving APP while the function of  $\beta$ -secretases, such as BACE1 and BACE2, appears to be only involved in the production of  $A\beta$ .

Previous studies in transgenic (Tg) mice with a mutated human APP gene, suggested that an interaction between APOE and  $A\beta$  is somehow linked to plaque formation. In newer studies, Tg mice with the mutated APP gene were used to create mice in which their APOE gene had been removed and replaced either with the human  $\epsilon$ 3 or  $\epsilon$ 4 allele [20-22]. Mice with the APP mutation and no mouse APOE genes had fewer  $A\beta$  deposits and no neuritic plaques. When either of the human APOE genes ( $\epsilon$ 2,  $\epsilon$ 3) was present, the pattern of  $A\beta$  deposition changed. There was  $A\beta$  deposition in the hippocampus but few neuritic plaques appeared until

<sup>\*</sup>Address correspondence to this author at the Molecular Imaging Branch, National Institute of Mental Health, National Institutes of Health, Bethesda, MD 20892, USA; E-mail: caill@intra.nimh.nih.gov

late age. In mice with the human  $\epsilon 4$  risk-factor gene, there was more  $A\beta$  deposited as well as a large increase in the amount of fibrillar  $A\beta$  compared to mice with the human  $\epsilon 3$  allele. Thus, the  $\epsilon 4$  allele may be critical for the formation of plaques and consequent nerve cell damage and death [23]. It was shown that the neurotoxic effects of the  $\epsilon 4$  allele are mediated *via* dysregulation of calcium homeostasis. The search for other genetic factors in AD continues [7,24,25].

Although the pathology of AD clearly remains unknown, a number of hypotheses have arisen, based on amyloid cascade (Fig. 1) [5], tau-tangle [26], inflammatory response/microglial activation [27,28], oxidative stress [29-31] or stroke infarct phenomena [32]. Correlation between elevated levels of  $A\beta$  peptides in brain and cognitive decline has been established [33]. The leading 'amyloid cascade hypothesis' states that over-accumulation of  $A\beta$  initiates a sequence of events that lead to neuron death and precipitation of protein aggregates, at first  $A\beta$  plaques and then NFTs.  $A\beta$  precipitation is considered to result from either its over-production or its slow digestion. The accumulation of  $A\beta$  in the AD brain reduces secretion of APP [34]. Since secreted APP has been proposed to have a neuroprotective function,  $A\beta$  deposits may thereby indirectly increase  $A\beta$  toxicity.

Post modification of  $A\beta$  peptides has also been reported to have significant effect on the pathology of AD disease. Metalloelements coordination of Cu and Fe have been demonstrated to co-localize with some of amyloid plaques [35]. Their potential role in the plaque formation and oxidative stress has been studied *in vitro* [36,37]. The Cu-adducts show catecholase activity, catechol oxidase activity, or tyrosinase activity ascribed to a binuclear form of the  $Cu^{II}_2\mu\eta^1:\eta^1$ -peroxo,  $Cu^{II}_2\mu\eta^2:\eta^2$ -peroxo, or  $Cu^{II}_2$ -bis- $\mu$ -oxo intermediates [38,39]. In a similar sense, the Cu bonding domain is known on the extracellular surface region of APP protein other than  $A\beta$ -sequence, which favors Cu(I) coordination [40]. It is also suggested that AD is a Cu deficiency disease [41]. This Cu deficiency may lead to a microglial mediated inflammatory disease which is neurodegenerative [42].

The evidence that links  $A\beta$  peptides to the pathogenesis of AD is substantial, but the means by which these peptides exert their toxic effects, and where in neuronal cells they act, is far from clear [43]. It should be noted that, in view of accumulating evidence, a recent refinement of the amyloid cascade hypothesis switches the postulated cause of lesion from mature  $A\beta$  plaques to precursor  $A\beta$  oligomers, referred to as  $A\beta$ -derived diffusible ligands, ADDLs [44]. Thus, McLean *et al.* [45] found that soluble  $A\beta$ , but not  $A\beta$  plaque, was significantly correlated with the density of tau-reactive neuritic plaques and with NFTs in the cortex and putamen of post mortem AD brain. Also, Lue *et al.* [46] showed that soluble  $A\beta_{40}$ , but not  $A\beta$  plaque or NFT, was significantly correlated with synaptic loss in post mortem brain specimens from patients with AD. Mucke *et al.* [47] found that Tg mice carrying a wild type version of the human gene for APP had decreasing presynaptic terminals with age in the absence of  $A\beta$  plaques, which correlated with levels of soluble  $A\beta$ . Current development of small molecule ligands has not yet generated any promising leads for ADDLs. Therefore, they will not be discussed here.

## 2. MOTIVATION FOR IMAGING $A\beta$ AGGREGATES WITH POSITRON EMISSION TOMOGRAPHY (PET)

Currently the diagnosis of AD is based on clinical evaluation and patient history [5], combined with structural imaging of the brain, such as magnetic resonance imaging (MRI) [5,48-50]. This clinical and structural imaging assessment is typically sufficient for diagnosis in patients with moderate or severe symptoms but is often inadequate for patients in early stages of AD [3]. Functional imaging using fluorine-18-fluorodeoxyglucose-positron emission tomography (FDG-PET), shows that patients with mild cognitive impairment (MCI) patients have substantial changes in cortical metabolism [6,51-53]. The prospects for a reliable method for assessing  $A\beta$  burden *in vivo* at an earlier stage of the disease, especially at a pre-symptomatic stage, is just emerging, based on the application of positron emission tomography (PET) [54-60] with radioligands for binding sites in  $A\beta$  aggregates, mainly plaques [54]. Understanding the pathological significance of  $A\beta$  plaques and monitoring the effect of anti- $A\beta$  therapy are the primary goals of developing PET radioligands for  $A\beta$  aggregates. The monitoring will be critical for accurate differential diagnosis and treatment follow-up [61,62]. Some therapeutic treatments based on the amyloid cascade hypothesis are already in development [3].

In principle, the development of PET radioligands for  $A\beta$ -containing targets is similar to the development of PET radioligands for other protein targets (*e.g.* neurotransmitter receptors) in terms of the properties sought in candidate radioligands. Key properties are high affinity for a binding site in the protein, selectivity of binding for the target versus binding to other proteins, moderate lipophilicity for good brain entry, low non-specific binding and fast pharmacokinetics, limited molecular mass (< 500 Da) for brain entry, and finally amenability to labeling with a positron-emitter, usually carbon-11 ( $t_{1/2} = 20.4$  min) or fluorine-18 ( $t_{1/2} = 109.7$  min), which emit measurable positrons when they radio-decay. The most popular methods for labeling are by *N*-alkylation reactions, especially  $^{11}C$ -methylation and  $^{18}F$ -fluoroethylation. Furthermore, radioligands should not give rise to radioactive metabolites in brain so that biochemical models may be applied to derive quantitative information on the relative regional densities of the target protein [63].

## 3. LIGAND BINDING SITES IN $A\beta$ PLAQUES

There are three types of binding sites that are firmly established as existing in  $A\beta$  plaques for PET radioligands. We differentiate them by their typical ligands. They are Congo-Red (CR; **1**, Scheme 1), Thioflavin-T (Th-T; **30**, Scheme 4) and FDDNP (**215**, Scheme 14) binding sites. Since there is no method available to synthesize or isolate  $A\beta$  aggregates with a certain profile of binding sites, the characterization of new ligands for  $A\beta$  plaques is a challenging task. The nature and amount of any particular binding site depends on the plaque source, which may be from synthetic aggregation, a Tg rodent or human AD brain. Even for a single source, other sometimes difficult to control factors, such as plaque age, environment and metalloelements, may contribute to differences in the nature and concentration of ligand binding sites. This will become clearer when we discuss the binding of ligands to  $A\beta$  aggregates.

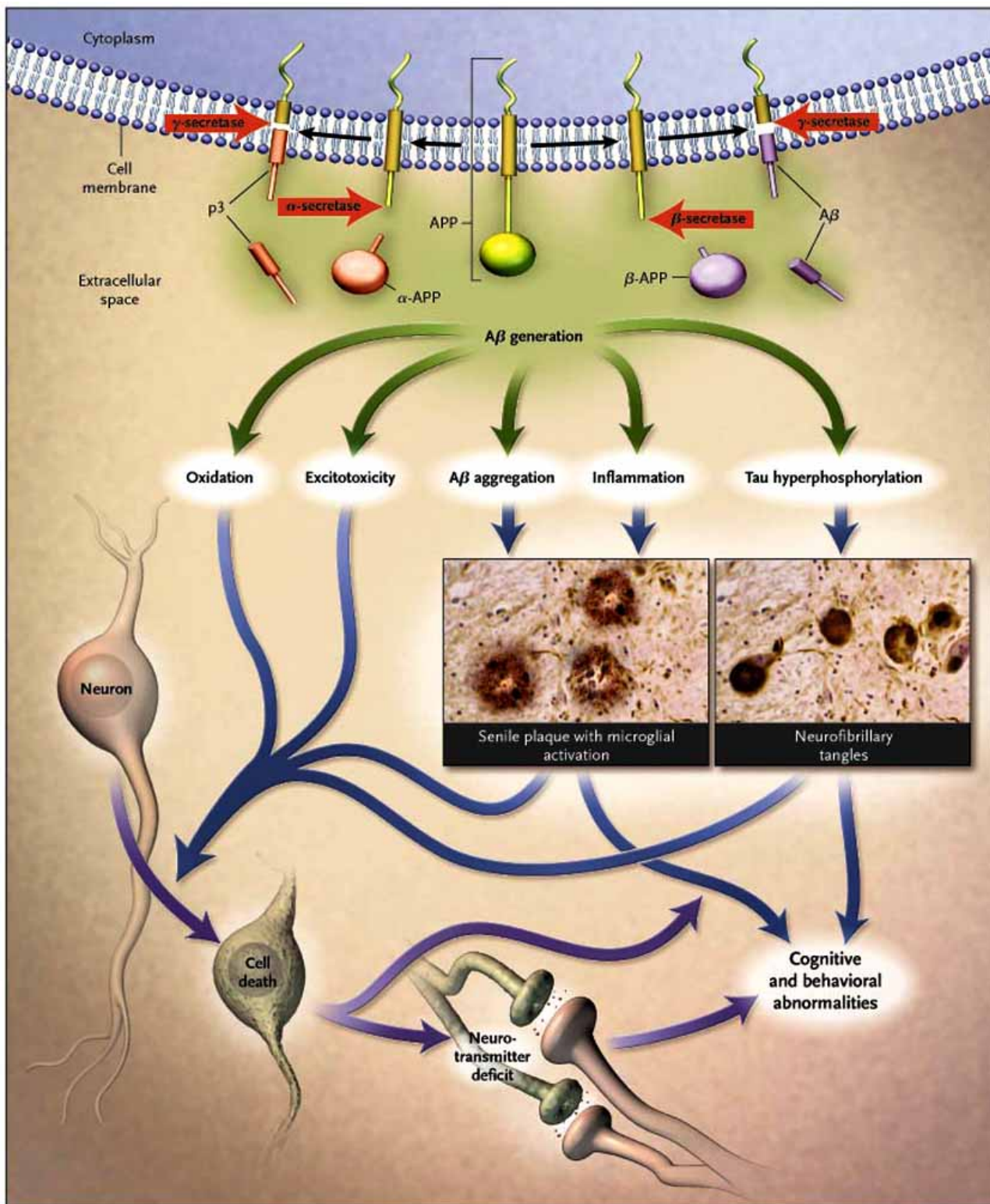


**Fig. (1).** Amyloid cascade hypothesis. This hypothesis, which progresses from the generation of A $\beta$  from APP, through multiple secondary steps, to cell death, forms the main foundation for current and emerging options for the treatment of AD. Adapted with permission [5].

The clearest differentiation between CR and Th-T type binding sites came from the study of Kung *et al.* [64]. CR and Th-T type ligands showed mutually exclusive behavior; when one type of radioligand bound with the A $\beta$  plaque the other kind could not displace it. That is, the binding of these

two ligands is non-competitive and presumably caused by each ligand binding to distinct, non-overlapping sites on the A $\beta$  aggregate. The exact nature of this phenomenon is unknown. Such mutual exclusivity has not been demonstrated for FDDNP-type ligands [65,66]. Since A $\beta$  plaques have

multiple binding sites and those with only one binding site cannot be isolated or synthesized, binding affinities measured for new ligands depend on the protein source, reference radioligand and method of measurement. More details on this aspect will be found in later discussion. Since passage through the blood-brain-barrier (BBB) is an important issue for radioligands to be used in brain, only the Th-T and FDDNP types have been used with PET in human subjects.

Recently, researchers from the Pharma company, Glaxo SmithKline (GSK), have identified more binding sites [67]. Our work has also shown that there are more binding site types in A $\beta$  plaques, since the binding affinities differ according to the selected reference radioligand (Cai *et al.*, unpublished results).

#### 4. *IN VITRO* BINDING ASSAYS

There are essentially three kinds of A $\beta$  aggregates that can be used for the evaluation of new ligands *in vitro*: synthetic aggregates of A $\beta$ 40 and A $\beta$ 42; Tg rodent brain; human brain homogenate or isolated AD A $\beta$ . There are two categories of method for performing binding assays, differing in the radiation detected, either light from fluorescence or radioactivity. The fluorescence method is based on the observation that some ligands change fluorescence properties significantly upon binding with A $\beta$  plaques. A fluorescence titration experiment generates an equilibrium protein-ligand dissociation constant (K<sub>d</sub>), such as that reported for FDDNP [68]. K<sub>d</sub> is inversely proportional to binding affinity (the association constant). Fluorescence ligand displacement may also be used to measure the binding affinities of competing ligands [66]. Thus, Th-T, upon binding with A $\beta$  aggregate changes its fluorescence properties dramatically and provides a unique monitoring tool. Binding inhibition constants (K<sub>i</sub> values), which are also inversely proportional to binding affinity, may be readily determined for ligands that compete with the binding of Th-T. However, *in vitro* binding assays based on radioligand titration and displacement have greater scope and constitute the most common approach for determining binding affinities. A variety of reference radioligands has been used. The choice of reference radioligand for assay of a particular set of ligands depends on the properties of the radioligand, the source of A $\beta$  to be used and the solvent acceptable for the assay and test compounds. [<sup>125</sup>I]TZDM (TZDM: **70**, Scheme 5, Table 5), because of its high lipophilicity and extensive nonspecific binding in human brain tissue, is unsuitable for experiments using human AD tissue as protein source [65]. [<sup>3</sup>H]PIB (PIB: **32**, Scheme 4, Table 3) (85% after one year at -70°C) and [<sup>125</sup>I]IMPY (IMPY: **199**, Scheme 13, Table 20) are not very stable in solution, especially in open air and room temperature (Cai *et al.*, unpublished results).

#### 5. LIGAND BINDING CONSTANTS ACCORDING TO BINDING SITES

##### 5.1. Congo Red (CR) Type Ligands

The structures of ligands in this group of (**1-29**) are defined in Schemes 1-3 with Table 1. Their binding and LogD parameters are given in Table 2. Two structural features are important for the binding of CR (**1**) to A $\beta$  deposits. One is the separation of its two negative charges by a fixed distance

and the other is the biaryl core organic framework. Titration of radiolabeled CR with A $\beta$ 40 aggregates gave K<sub>d</sub> values ranging from 1,100 to 1,500 nM, which are lower than those from a radioligand assay (K<sub>i</sub> around 8,000 nM) performed with slightly different A $\beta$ [34-42] aggregates. However, when the reference radioligand is changed to chrysamine G (CG; **18**), the K<sub>i</sub> value of CR changes to 48 nM, representing more than 20-fold higher affinity. However, CG is less ionized at physiological pH than CR. When carboxylate groups in CG are replaced by phenolate groups, as in **29**, the K<sub>i</sub> value reduces to 12 nM when the reference radioligand is CG, so excluding, in this case, any necessity for a contribution to binding from di-anion charges.

A model for the interactions of CR and CG with A $\beta$  fibrils has been proposed, which stresses the significance of ionic interaction between the fixed distance di-anions of CR and the repetitive layer structure of A $\beta$  aggregates (Fig. 2). Consistent with this model, structural changes at the central portion of CR do not change the binding affinity significantly (*c.f.* **2**, **16**, **17** and **18**). Changing the distance between the di-anions changes the binding constant (*c.f.* **5**, **8**, **9** and **10**). If one ionizable group is removed (**7**) the binding affinity reduces dramatically. However, other factors play important roles that cannot be explained clearly by the ionic model. If the amino group in CR is replaced by a hydroxyl group, the binding affinity also reduces significantly, as in **6**. Orthogonality is preferred for the central two phenyl rings, as reflected in the stronger binding of **2** compared to that of **4**. The effect of the methyl group in **3** is to weaken binding, suggesting that planarity around the diazo group in CR is important. This is also reflected in the weaker binding of **9** compared to that of **10**. Although the weaker binding of **12-15** may be explained by the increased positive charge in the central portion of CR, the increase in binding affinity for **15** comes from an unidentified source. In summary, compounds **1-17** share a common binding site, where the primary interaction with A $\beta$  is through di-anions, separated by a fixed distance.

A second binding site exists for CR-type ligands, primarily for compounds **18-29**, where ionic interactions are reduced significantly, but the binding affinity for A $\beta$  is generally increased. The notable examples are **28** and **29**, where no ionic form is expected at physiological pH. Compound **19** did not show any binding affinity when competing for the CG binding site, showing that the salicyl carboxylic acid group does not yield an effective ligand. The overall flatness of compounds **18-29** suggests that the primary interaction is probably  $\pi$ - $\pi$  interaction with the  $\beta$ -pleated sheet of A $\beta$  aggregate. Compared with CG and CR derivatives, compounds **20-29** are shorter molecules (generally by the width of one phenyl ring). When ionic interaction is predominant, the distance between the two negative charges appears to be important, as in the reduced binding affinity of **5**.

Another manifestation of the second binding site is the dependence of binding affinity on molecular geometry. For compounds **20-23**, all isomers of the two double bonds have been isolated [70]. These compounds show similar binding affinities with K<sub>i</sub> values ranging from 0.11 to 0.27 nM. Thus, the distance between the two carboxylic acid groups changed significantly among the isomers, but without introducing

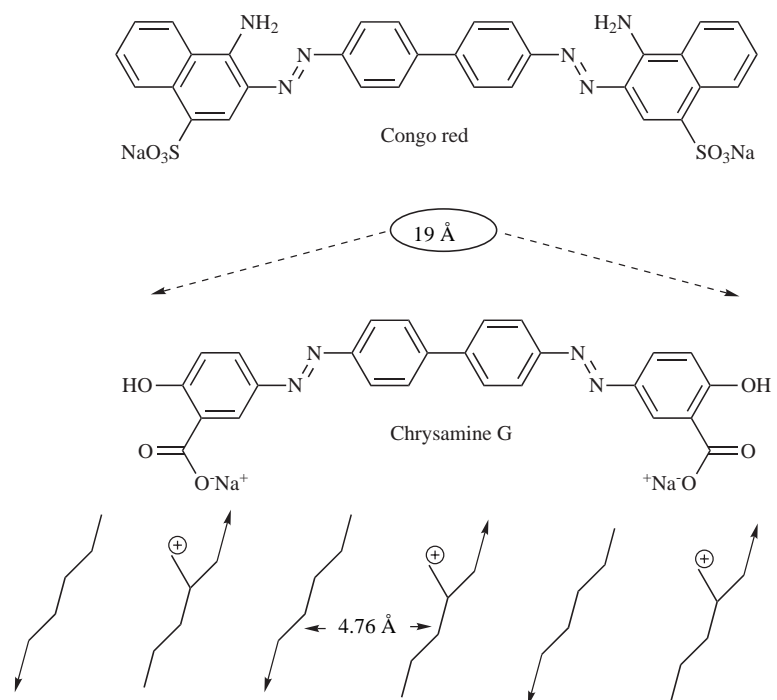
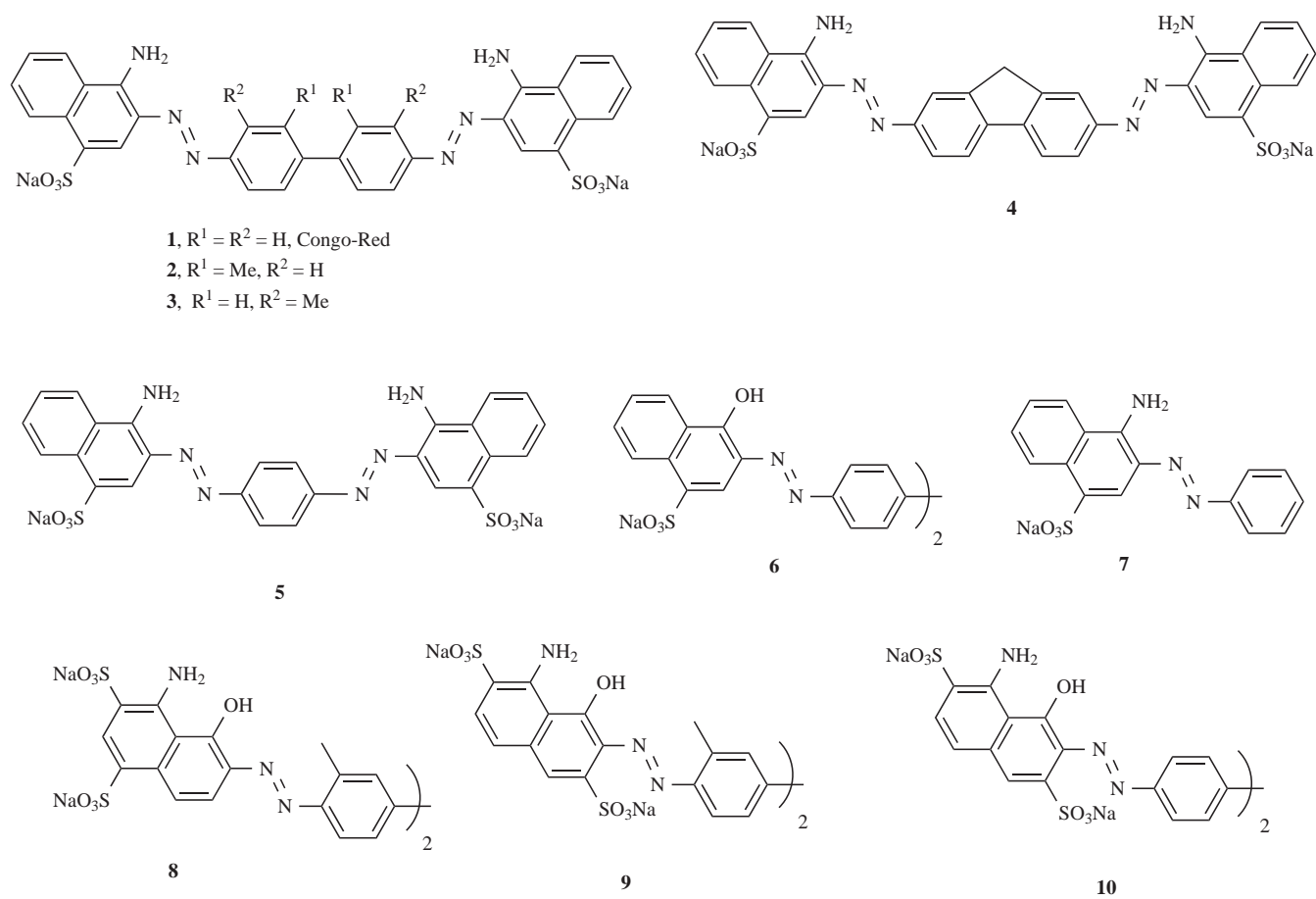
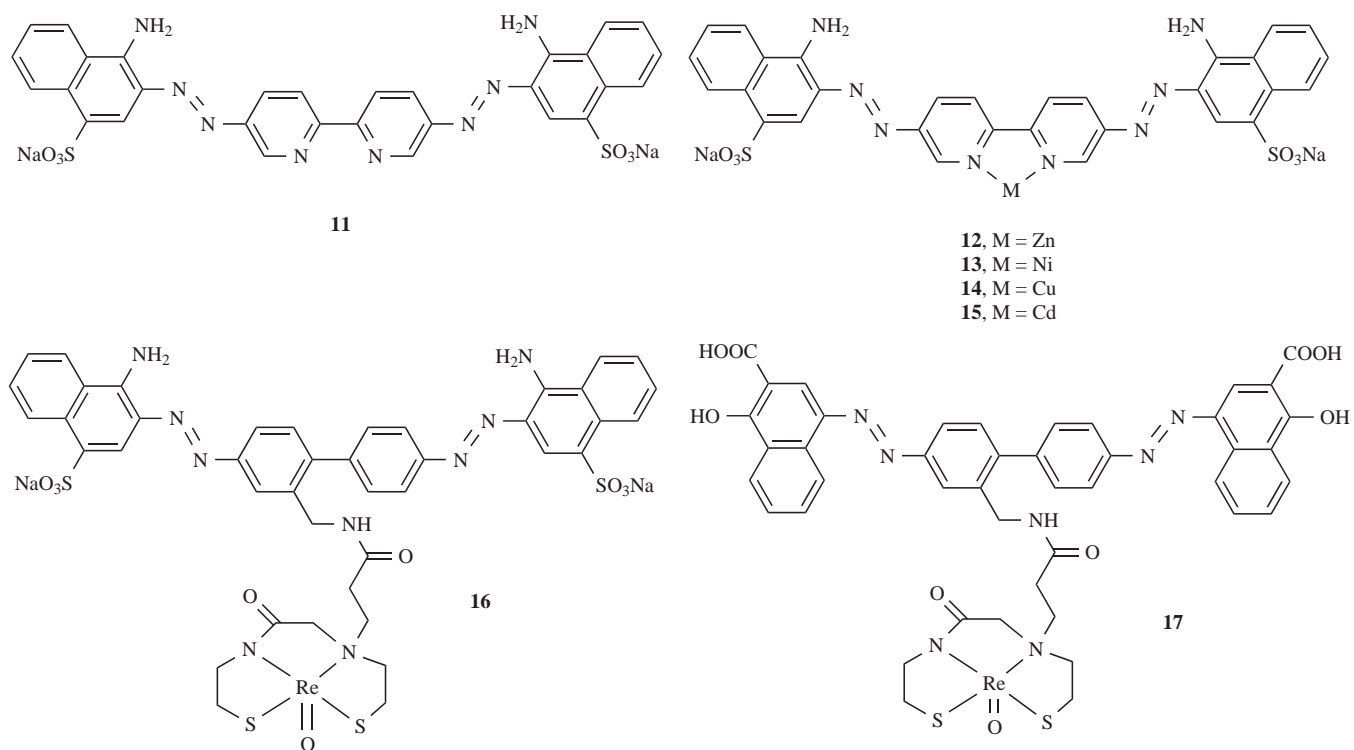


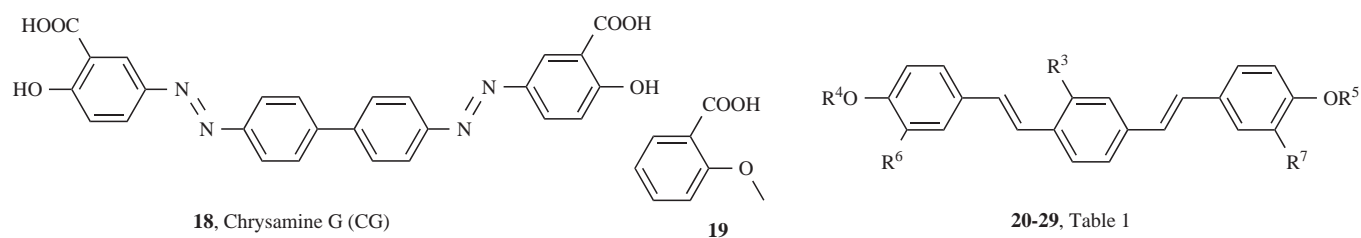
Fig. (2). A hypothetical model of CR (1) and CG (18) interaction with A $\beta$  fibrils. Adapted with permission [69].



Scheme 1. CR ligand series I.



Scheme 2. CR ligand series II.



Scheme 3. CR ligand series III.

Table 1. Structures of Compounds 20-29

| Compound                | R <sup>3</sup> | R <sup>4</sup> | R <sup>5</sup> | R <sup>6</sup> | R <sup>7</sup> |
|-------------------------|----------------|----------------|----------------|----------------|----------------|
| 20, ( <i>E, E</i> )-BSB | Br             | H              | H              | COOH           | COOH           |
| 21, ( <i>E, Z</i> )-BSB | Br             | H              | H              | COOH           | COOH           |
| 22, ( <i>Z, E</i> )-BSB | Br             | H              | H              | COOH           | COOH           |
| 23, ( <i>Z, Z</i> )-BSB | Br             | H              | H              | COOH           | COOH           |
| 24, ISB                 | I              | H              | H              | COOH           | COOH           |
| 25, IMSB                | I              | Me             | Me             | COOH           | COOH           |
| 26, X-34                | H              | H              | H              | COOH           | COOH           |
| 27, MeO-X04             | OMe            | H              | H              | H              | H              |
| 28                      | H              | H              | H              | OH             | OMe            |
| 29                      | H              | H              | H              | OH             | OH             |

ducing significant difference in binding affinity. This is quite different from the characteristics observed from the binding site with an ionic interaction. This reflects the lack of spe-

cific pharmacophore interaction in the second binding site, except for the  $\pi$ - $\pi$  interaction.

Table 2. Binding and LogP Parameters for CR-Type Ligands

| Compound       | Ki (nM)            | Kd (nM)      | PS <sup>a</sup>   | RR <sup>b</sup> | M <sup>c</sup>  | LogD at pH=7.4             | cLogD <sup>d</sup> | Ref.       |
|----------------|--------------------|--------------|-------------------|-----------------|-----------------|----------------------------|--------------------|------------|
| 1, CR          |                    | 1100<br>1500 | A $\beta$ 40      |                 | RT <sup>e</sup> | - 0.80<br>- 0.49<br>- 0.18 | - 0.28             | [71,72]    |
|                | 8000               |              | A $\beta$ [34-42] | CR              | RD <sup>f</sup> |                            |                    | [73]       |
|                | 48                 |              | A $\beta$ 40      | CG              | RD              |                            |                    | [74]       |
|                | infinite           |              | A $\beta$ 40      | FDDNP           | RD              |                            |                    | [75]       |
| 2              | 2300               |              | A $\beta$ [34-42] | CR              | RD              |                            | 0.64               | [73]       |
| 3              | $2.29 \times 10^5$ |              | A $\beta$ [34-42] | CR              | RD              |                            | 0.64               | [73]       |
| 4              | $1.3 \times 10^4$  |              | A $\beta$ [34-42] | CR              | RD              |                            | 0.51               | [73]       |
| 5              | $1.19 \times 10^5$ |              | A $\beta$ [34-42] | CR              | RD              |                            | -1.54              | [73]       |
| 6              | $7.6 \times 10^4$  |              | A $\beta$ [34-42] | CR              | RD              |                            | - 2.63             | [73]       |
| 7              | $> 4 \times 10^6$  |              | A $\beta$ [34-42] | CR              | RD              |                            | - 0.86             | [73]       |
| 8              | $1.07 \times 10^5$ |              | A $\beta$ [34-42] | CR              | RD              |                            | - 3.29             | [73]       |
| 9              | $6.2 \times 10^4$  |              | A $\beta$ [34-42] | CR              | RD              |                            | - 8.21             | [73]       |
| 10             | $4.2 \times 10^4$  |              | A $\beta$ [34-42] | CR              | RD              |                            | - 9.13             | [73]       |
| 11             | $1.96 \times 10^4$ |              | A $\beta$ [34-42] | CR              | RD              |                            | - 2.17             | [73]       |
| 12             | $1.7 \times 10^4$  |              | A $\beta$ [34-42] | CR              | RD              |                            |                    | [73]       |
| 13             | $1.58 \times 10^4$ |              | A $\beta$ [34-42] | CR              | RD              |                            |                    | [73]       |
| 14             | $2.03 \times 10^4$ |              | A $\beta$ [34-42] | CR              | RD              |                            |                    | [73]       |
| 15             | 1500               |              | A $\beta$ [34-42] | CR              | RD              |                            |                    | [73]       |
| 16             |                    | 1100         | A $\beta$ 40      |                 | RT              | - 0.92                     |                    | [71]       |
| 17             |                    | 830          | A $\beta$ 40      |                 | RT              | 0.66                       |                    | [71]       |
| 18, CG         |                    | 350          | AD                |                 | RT              | 0.57<br>1.8                | 2.55               | [64,69,72] |
|                | >1000              |              | AD                | IMPY            | RD              |                            |                    | [65]       |
|                | >1000              |              | AD                | SB-13           | RD              |                            |                    | [65]       |
|                | 0.14               |              | A $\beta$ 40      | IMSB            | RD              |                            |                    | [70,76]    |
|                | 0.4                |              | A $\beta$ 42      | IMSB            | RD              |                            |                    |            |
|                | 25.3               |              | A $\beta$ 40      | MeO-X04         | RD              |                            |                    | [72]       |
|                | >1000              |              | A $\beta$ 40      | TZDM            | RD              |                            |                    | [76]       |
|                | >2000              |              | A $\beta$ 42      | TZDM            | RD              |                            |                    |            |
|                | 3                  |              | A $\beta$ 40      | CG              | RD              |                            |                    | [74]       |
|                | 19                 | >1800        |                   | A $\beta$ 40    | IMSB            | RD                         |                    | -1.43      |
| 20, (E, E)-BSB | 0.11               |              | A $\beta$ 40      | IMSB            | RD              |                            | 4.21               | [70]       |
|                | >1000              |              | AD                | IMPY            | RD              |                            |                    | [65]       |
| 21, (E, Z)-BSB | 0.19               |              | A $\beta$ 40      | IMSB            | RD              |                            | 4.21               | [70]       |
| 22, (Z, E)-BSB | 0.27               |              | A $\beta$ 40      | IMSB            | RD              |                            | 4.21               | [70]       |
| 23, (Z, Z)-BSB | 0.13               |              | A $\beta$ 40      | IMSB            | RD              |                            | 4.21               | [70]       |
| 24, ISB        |                    | 0.08         | A $\beta$ 40      |                 | RT              | 1.54                       | 4.41               | [64,77]    |
|                |                    | 0.15         | A $\beta$ 42      |                 | RT              |                            |                    |            |
| 25, IMSB       |                    | 0.13         | A $\beta$ 40      |                 | RT              | 0.04                       | 2.94               | [64,77]    |
|                |                    | 0.73         | A $\beta$ 42      |                 | RT              |                            |                    |            |
|                | 0.17               |              | A $\beta$ 40      | IMSB            | RD              |                            |                    | [76]       |
|                | 0.8                |              | A $\beta$ 42      | IMSB            | RD              |                            |                    | [76]       |
|                | >1000              |              | A $\beta$ 40      | TZDM            | RD              |                            |                    | [76,77]    |
| 26, X-34       | >1000              |              | A $\beta$ 42      | TZDM            | RD              |                            |                    | [77]       |
|                | 452                |              | A $\beta$ 40      | Th-T            | FD              | 0.477                      | 3.38               | [66]       |
|                | 6                  |              | A $\beta$ 40      | CG              | RD              |                            |                    | [74]       |
| 27, MeO-X04    | 26.8               |              | A $\beta$ 40      | MeO-X04         | RD              | 2.6                        | 3.45               | [72]       |
| 28             | 38                 |              | A $\beta$ 40      | CG              | RD              |                            | 5.68               | [74]       |
| 29             | 12                 |              | A $\beta$ 40      | CG              | RD              |                            | 5.47               | [74]       |

Note: a) PS: protein source; b) RR: reference radioligand; c) M: method; d) cLogD at pH 7.4, calculated using ACD software package version 8.0; e) RT: radioligand titration; f) RD: radioligand displacement.

## 5.2. Thioflavin-T (Th-T) Type Ligands

Derivatives of Thioflavin-T (Th-T; **30**, Scheme 4) have been extensively investigated in the search for PET radioligands for A $\beta$  aggregates. Interestingly, the binding affinities reported for Th-T range widely from 120 to 2,400 nM (Table 4), even though the reference radioligands are supposed to bind to the same site. Generally, synthetic A $\beta$  aggregates give higher binding affinities than human A $\beta$  plaques, although there is no strict comparison from use of the same reference radioligand. These data may reflect structural differences between the two protein sources, with the human A $\beta$  plaques being more regular and uniform overall. Th-T has been in use for tissue staining for many years [78]. However, its positive charge prevents BBB penetration. Removing the charge not only improves brain entry, but also increases binding affinity to A $\beta$  plaques. The first series of ligands (**31-62**) to be considered are derivatives with electron-donating groups at the 6-position (R<sup>8</sup> in Scheme 4). Structures of **31-62** are defined in Scheme 4 with Table 3, and their binding and LogD parameters in Table 4.

A number of factors influence the binding affinity. First, the methylation of the aromatic amino group plays an important role. The first *N*-methyl group increases binding affinity significantly, but a second *N*-methyl group has either a limited or, in one case, an adverse effect (*c.f.* sets **31-33**; **42, 43**; **44-46**; **48, 49**; **50-52**; **53-55**; **57, 58**). The methyl group shows an “iso-steric” effect. Thus, placing a group of similar size to methyl in *o*-position to the aromatic amino group gives a binding affinity similar to the corresponding *N*-methyl compound (*c.f.* pairs **32, 42**; **33, 43**; **45, 48**; **46, 49**; **54, 57**; **55, 58**). A second *N*-methyl group generally increases the binding affinity, but normally by a factor of less than two. 6-Me-BTA-2 (**52**) is an exception. Its binding constant (K<sub>i</sub>) changes dramatically with the reference radioligand.

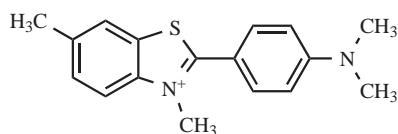
Second, the influence of the substituent at 6-position is generally limited, except for **53**. Substituents at this position have strong influence on lipophilicity, so indicating a lack of general correlation between binding affinity and lipophilicity. By contrast, Wang *et al.* [79] found that the affinity for A $\beta$ 40 fibrils for several benzothiazole derivatives increases with ligand lipophilicity. However, the relationship holds only for limited variations of a given ligand. A general correlation between binding constants and either the measured or calculated LogD value is not established.

The second series of Th-T type ligand (**63-80**) differs from the first in the electronic nature of the substituent at the 6-position (Scheme 5, Table 5). Binding parameters and LogD values for this series of ligands are given in Table 6. Here, the substituents are electron-withdrawing and generally give these compounds higher lipophilicity. The influ-

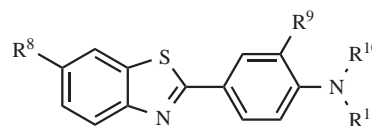
ence of an *N*-methyl group persists, but with the mono *N*-methyl compound as the strongest binder (*c.f.* sets **63-65** and **74-76**). So does the “iso-steric” effect of *N*-methyl and *o*-methyl groups (*c.f.* pairs **64, 68**; **65, 69**; **78, 79**). Generally, the second series of compounds has stronger binding affinity than the first, probably due to increased lipophilicity.

**Table 3. Structures of Compounds 31-62**

| Compound              | R <sup>8</sup>                     | R <sup>9</sup> | R <sup>10</sup>                                   | R <sup>11</sup> |
|-----------------------|------------------------------------|----------------|---|-----------------|
| <b>31</b>             | OH                                 | H              | H   | H               |
| <b>32, PIB</b>        | OH                                 | H              | Me  | H               |
| <b>33</b>             | OH                                 | H              | Me  | Me              |
| <b>34</b>             | OH                                 | H              | (CH <sub>2</sub> ) <sub>2</sub> F                 | H               |
| <b>35</b>             | OH                                 | H              | (CH <sub>2</sub> ) <sub>3</sub> F                 | H               |
| <b>36</b>             | OH                                 | H              | (CH <sub>2</sub> ) <sub>4</sub> F                 | H               |
| <b>37</b>             | OH                                 | H              | CH <sub>2</sub> (C <sub>6</sub> H <sub>4</sub> )F | H               |
| <b>38</b>             | OH                                 | H              | (CH <sub>2</sub> ) <sub>2</sub> F                 | Me              |
| <b>39</b>             | OH                                 | H              | (CH <sub>2</sub> ) <sub>3</sub> F                 | Me              |
| <b>40</b>             | OH                                 | F              | H   | H               |
| <b>41</b>             | OH                                 | F              | Me  | H               |
| <b>42</b>             | OH                                 | I              | H   | H               |
| <b>43</b>             | OH                                 | I              | Me  | H               |
| <b>44, BTA-0</b>      | H                                  | H              | H   | H               |
| <b>45</b>             | H                                  | H              | Me  | H               |
| <b>46</b>             | H                                  | H              | Me  | Me              |
| <b>47</b>             | H                                  | H              | (CH <sub>2</sub> ) <sub>3</sub> F                 | H               |
| <b>48</b>             | H                                  | I              | H   | H               |
| <b>49</b>             | H                                  | I              | Me  | H               |
| <b>50, 6-Me-BTA-0</b> | Me                                 | H              | H   | H               |
| <b>51, 6-Me-BTA-1</b> | Me                                 | H              | Me  | H               |
| <b>52, 6-Me-BTA-2</b> | Me                                 | H              | Me  | Me              |
| <b>53</b>             | OMe                                | H              | H   | H               |
| <b>54</b>             | OMe                                | H              | Me  | H               |
| <b>55</b>             | OMe                                | H              | Me  | Me              |
| <b>56</b>             | OMe                                | F              | H   | H               |
| <b>57</b>             | OMe                                | I              | H   | H               |
| <b>58</b>             | OMe                                | I              | Me  | H               |
| <b>59</b>             | O(CH <sub>2</sub> ) <sub>2</sub> F | H              | H   | H               |
| <b>60</b>             | O(CH <sub>2</sub> ) <sub>2</sub> F | H              | Me  | H               |
| <b>61</b>             | OCH <sub>2</sub> OMe               | H              | H   | H               |
| <b>62</b>             | OCH <sub>2</sub> OMe               | I              | H   | H               |



**30, Thioflavin-T**



**31-62, Table 3**

**Scheme 4.** Th-T ligand series I.

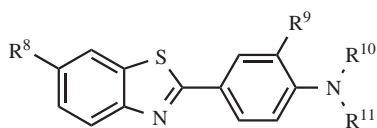
Table 4. The Binding and LogD Parameters of Th-T Ligand Series I

| Compound            | Ki (nM)   | Kd (nM)            | PS           | RR              | M     | LogD at pH = 7.4 | cLogP | Ref.          |
|---------------------|-----------|--------------------|--------------|-----------------|-------|------------------|-------|---------------|
| 30, Th-T            | 890       |                    | A $\beta$ 40 | 6-Me-BTA-1      | RD    | 0.57             | 4.88  | [64,77,80,81] |
|                     | 580       |                    | A $\beta$ 40 | BTA-1           | RD    |                  |       | [81]          |
|                     | 116       |                    | A $\beta$ 40 | TZDM            | RD    |                  |       | [76,77]       |
|                     | 279       |                    | A $\beta$ 40 | TZDM            | RD    |                  |       | [64,65]       |
|                     | 294       |                    | A $\beta$ 42 | TZDM            | RD    |                  |       | [64]          |
|                     | 2310      |                    | AD           | IMPY            | RD    |                  |       | [65]          |
|                     | 2379      |                    | AD           | SB-13           | RD    |                  |       | [65]          |
|                     | >9000     |                    | A $\beta$ 40 | IMSB            | RD    |                  |       | [64,76]       |
|                     | >4000     |                    | A $\beta$ 42 | IMSB            | RD    |                  |       | [64]          |
|                     | infinite  |                    | A $\beta$ 40 | FDDNP           | RD    |                  |       | [75]          |
|                     | 31        | 46                 |              | A $\beta$ 40    | BTA-1 | RD               | 0.66  | 2.74          |
| 32, PIB             | 4.3       |                    | A $\beta$ 40 | BTA-1           | RD    | 1.2              | 3.31  | [79,82,83]    |
|                     | 7         |                    | A $\beta$ 40 | PIB             | RD    | 2.0              | 3.99  | [84]          |
|                     | 2.8       |                    | AD           | IMPY            | RD    |                  |       | [85]          |
|                     |           | 4.7                | A $\beta$ 40 |                 | RT    |                  |       | [82]          |
|                     |           | 1.4                | AD           |                 | RT    |                  |       | [82]          |
| 33                  | 4.4       |                    | A $\beta$ 40 | BTA-1           | RD    | 2.0              | 3.92  | [82]          |
| 34                  | 2 to 80   |                    | A $\beta$ 40 | ?               | RD    |                  | 3.43  | [86]          |
| 35, 6-OH-BTA-NP-F   | 2 to 80   |                    | A $\beta$ 40 | ?               | RD    |                  | 3.83  | [86]          |
| 36                  | 2 to 80   |                    | A $\beta$ 40 | ?               | RD    |                  | 4.26  | [86]          |
| 37                  | 2 to 80   |                    | A $\beta$ 40 | ?               | RD    |                  | 4.89  | [86]          |
| 38                  | 2 to 80   |                    | A $\beta$ 40 | ?               | RD    |                  | 4.05  | [86]          |
| 39                  | 2 to 80   |                    | A $\beta$ 40 | ?               | RD    |                  | 4.44  | [86]          |
| 40                  | 2 to 80   |                    | A $\beta$ 40 | ?               | RD    |                  | 3.26  | [86]          |
| 41                  | 2 to 80   |                    | A $\beta$ 40 | ?               | RD    |                  | 3.45  | [86]          |
| 42                  |           | 16                 | A $\beta$ 40 |                 | RD    | 1.65<br>2.4      | 4.28  | [87]          |
|                     |           | 25                 | AD           |                 | RT    |                  |       | [87]          |
|                     | 11.1      |                    | A $\beta$ 40 | BTA-1           | RD    |                  |       | [79]          |
| 43, 6-OH-BTA-1-3'-I | 3.22      |                    | A $\beta$ 40 | BTA-1           | RD    | 2.35             | 4.44  | [79]          |
|                     | 7.1       |                    | A $\beta$ 40 | 6-OH-BTA-1-3'-I | RD    |                  |       | [88]          |
|                     |           | 1.33 (1)<br>37 (2) | A $\beta$ 40 |                 | RT    |                  |       | [88]          |
| 44, BTA-0           | 37        |                    | A $\beta$ 40 | BTA-1           | RD    | 2.0              | 3.50  | [79,82]       |
| 45, BTA-1           | 11        |                    | A $\beta$ 40 | BTA-1           | RD    | 2.7              | 4.07  | [79,81,82]    |
|                     | 7.6       |                    | AD           | IMPY            | RD    |                  |       | [65]          |
|                     | 6.9       |                    | AD           | SB-13           | RD    |                  |       | [65]          |
|                     |           | 3.0                | A $\beta$ 40 |                 | RT    |                  |       | [77]          |
|                     | 46, BTA-2 | 4.0                |              | A $\beta$ 40    | BTA-1 | RD               | 3.4   | 4.68          |
| 47                  | 1.2 to 12 |                    | A $\beta$ 40 | ???             | RD    |                  | 4.59  | [83,86]       |
| 48                  | 8.32      |                    | A $\beta$ 40 | BTA-1           | RD    | 3.17             | 5.06  | [79]          |

(Table 4) contd.....

| Compound       | Ki (nM)   | Kd (nM) | PS   | RR         | M  | LogD at pH = 7.4 | cLogP | Ref.    |
|----------------|-----------|---------|------|------------|----|------------------|-------|---------|
| 49             | 4.94      |         | Aβ40 | BTA-1      | RD | 3.90             | 5.21  | [79]    |
| 50, 6-Me-BTA-0 | 30.3      |         | Aβ40 | 6-Me-BTA-1 | RD |                  | 3.96  | [89,90] |
|                | 9.5       |         | Aβ40 | BTA-1      | RD | 2.4              |       | [82]    |
| 51, 6-Me-BTA-1 | 20.2      |         | Aβ40 | 6-Me-BTA-1 | RD | 3.36<br>3.1      | 4.53  | [81,91] |
|                | 10        |         | Aβ40 | BTA-1      | RD |                  |       | [81,82] |
| 52, 6-Me-BTA-2 | 143       |         | Aβ40 | 6-Me-BTA-1 | RD | 3.8              | 5.14  | [92]    |
|                | 64        |         | Aβ40 | BTA-1      | RD |                  |       | [82]    |
|                | 2.3       |         | Aβ40 | TZDM       | RD |                  |       | [76,93] |
| 53             | 7.0       |         | Aβ40 | BTA-1      | RD | 1.9              | 3.42  | [79,82] |
| 54             | 4.9       |         | Aβ40 | BTA-1      | RD | 2.7              | 3.98  | [79,82] |
| 55             | 1.9       |         | Aβ40 | BTA-1      | RD | 3.3              | 4.59  | [82]    |
| 56             | 2 to 80   |         | Aβ40 | ???        | RD |                  | 3.95  | [86]    |
| 57             | 4.4       |         | Aβ40 | BTA-1      | RD | 3.08             | 4.98  | [79]    |
| 58             | 1.93      |         | Aβ40 | BTA-1      | RD | 3.80             | 5.13  | [79]    |
| 59             | 1.2 to 12 |         | Aβ40 | ???        | RD |                  | 3.64  | [83,86] |
| 60             | 1.2 to 12 |         | Aβ40 | ???        | RD |                  | 4.21  | [83]    |
| 61             | 53.6      |         | Aβ40 | BTA-1      | RD | 1.86             | 2.82  | [79]    |
| 62             | 15.1      |         | Aβ40 | BTA-1      | RD | 3.03             | 4.38  | [79]    |

Increasing the size and polarity of the substituent at the aromatic amino group has an intriguing influence on binding affinity. Changing from an *N,N*-dimethylamino (**65**) to a 1-methylpiperazino group (**66**) changes binding affinity little. However, change from an *N,N*-dimethylamino to a morpholino group (**67**) reduces the binding affinity more than 20-fold. This suggests that this portion of the ligand is not involved in any specific interaction. In general, both electron-withdrawing ability and polarizability of the substituent at the 6-position, play an important role. The stronger is the electron-withdrawing ability and polarizability, the higher is the binding affinity, as in the group **65**, **70**, **72**, **74** and **77**. However, the binding affinity of **63** is higher than those of **72**, **74** and **77**, suggesting electron-withdrawing ability and polarizability are two independent variables in determination of the binding constants.



63-80, Table 5

Scheme 5. Th-T ligand series II.

Table 5. Structures of Compounds 63-80

| Compound | R <sup>8</sup> | R <sup>9</sup> | R <sup>10</sup> | R <sup>11</sup> |
|----------|----------------|----------------|-----------------|-----------------|
| 63       | Br             | H              | H               | H               |
| 64       | Br             | H              | Me              | H               |

(Table 4) contd.....

| Compound | R <sup>8</sup>  | R <sup>9</sup> | R <sup>10</sup>                                     | R <sup>11</sup>                                     |
|----------|-----------------|----------------|---|---|
| 65       | Br              | H              | Me  | Me  |
| 66       | Br              | H              | (CH <sub>2</sub> CH <sub>2</sub> ) <sub>2</sub> NMe | (CH <sub>2</sub> CH <sub>2</sub> ) <sub>2</sub> NMe |
| 67       | Br              | H              | (CH <sub>2</sub> CH <sub>2</sub> ) <sub>2</sub> O   | (CH <sub>2</sub> CH <sub>2</sub> ) <sub>2</sub> O   |
| 68       | Br              | I              | H   | H   |
| 69       | Br              | I              | Me  | H   |
| 70, TZDM | I               | H              | Me  | Me  |
| 71, TZPI | I               | H              | (CH <sub>2</sub> CH <sub>2</sub> ) <sub>2</sub> NMe | (CH <sub>2</sub> CH <sub>2</sub> ) <sub>2</sub> NMe |
| 72       | COOMe           | H              | H   | H   |
| 73       | COOMe           | I              | H   | H   |
| 74       | CN              | H              | H   | H   |
| 75       | CN              | H              | Me  | H   |
| 76       | CN              | H              | Me  | Me  |
| 77       | NO <sub>2</sub> | H              | H   | H   |
| 78       | NO <sub>2</sub> | H              | Me  | H   |
| 79       | NO <sub>2</sub> | I              | H   | H   |
| 80       | NO <sub>2</sub> | I              | Me  | H   |

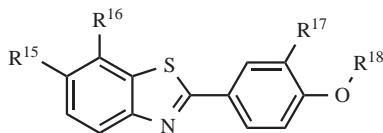
Table 6. The Binding and LogD Parameters of Th-T Ligand Series II

| Compound       | Ki (nM) | Kd (nM) | PS           | RR         | M  | LogD at pH = 7.4 | cLogD | Ref.       |
|----------------|---------|---------|--------------|------------|----|------------------|-------|------------|
| 63             | 7.2     |         | A $\beta$ 40 | BTA-1      | RD | 2.9              | 4.27  | [79,82]    |
| 64             | 1.7     |         | A $\beta$ 40 | BTA-1      | RD | 3.6              | 4.84  | [79,82]    |
| 65             | 2.9     |         | A $\beta$ 40 | BTA-1      | RD | 4.4              | 5.45  | [82]       |
|                | 1.9     |         | A $\beta$ 40 | TZDM       | RD |                  |       | [64]       |
|                | 0.8     |         | A $\beta$ 42 | TZDM       | RD |                  |       | [41]       |
|                | >2000   |         | A $\beta$ 40 | IMSB       | RD |                  |       | [64,94]    |
|                | >3000   |         | A $\beta$ 42 | IMSB       | RD |                  |       | [64]       |
| 66             | 1.6     |         | A $\beta$ 40 | TZDM       | RD |                  | 4.46  | [64]       |
|                | 5.0     |         | A $\beta$ 42 | TZDM       | RD |                  |       |            |
|                | >2000   |         | A $\beta$ 40 | IMSB       | RD |                  |       |            |
|                | >2400   |         | A $\beta$ 42 | IMSB       | RD |                  |       |            |
| 67             | 33.5    |         | A $\beta$ 40 | TZDM       | RD |                  | 4.48  | [94,95]    |
| 68             | 0.67    |         | A $\beta$ 40 | BTA-1      | RD | 4.11             | 5.83  | [79]       |
| 69             | 1.6     |         | A $\beta$ 40 | BTA-1      | RD | 4.86             | 5.99  | [79]       |
| 70, TZDM       |         | 0.06    | A $\beta$ 40 |            | RT | 1.85             | 5.71  | [64,77,94] |
|                |         | 0.14    | A $\beta$ 42 |            | RT |                  |       |            |
|                | 1.9     |         | A $\beta$ 40 | TZDM       | RD |                  |       | [77]       |
|                | 1.6     |         | A $\beta$ 40 | TZDM       | RD |                  |       | [94]       |
|                | 0.9     |         | A $\beta$ 40 | TZDM       | RD |                  |       | [64,76,96] |
|                | 2.2     |         | A $\beta$ 42 | TZDM       | RD |                  |       | [64]       |
|                | >2000   |         | A $\beta$ 40 | IMSB       | RD |                  |       | [64,76,94] |
|                | >5000   |         | A $\beta$ 42 | IMSB       | RD |                  |       | [64]       |
| 71, TZPI       |         | 0.13    | A $\beta$ 40 |            | RT | 2.49             | 4.72  | [64]       |
|                |         | 0.15    | A $\beta$ 42 |            | RT |                  |       | [64]       |
|                | 5.4     |         | A $\beta$ 40 | TZDM       | RD |                  |       | [64]       |
|                | 6.4     |         | A $\beta$ 42 | TZDM       | RD |                  |       | [64]       |
|                | >2000   |         | A $\beta$ 40 | IMSB       | RD |                  |       | [64]       |
|                | >2000   |         | A $\beta$ 42 | IMSB       | RD |                  |       | [64]       |
| 72             | 17.9    |         | A $\beta$ 40 | BTA-1      | RD | 2.07             | 3.48  | [79]       |
| 73             | 3.34    |         | A $\beta$ 40 | BTA-1      | RD | 3.29             | 5.04  | [79]       |
| 74             | 64      |         | A $\beta$ 40 | BTA-1      | RD | 1.8              | 2.94  | [82]       |
| 75, 6-CN-BTA-1 | 8.6     |         | A $\beta$ 40 | BTA-1      | RD | 2.5              | 3.51  | [82]       |
|                | 14      |         | A $\beta$ 40 | 6-CN-BTA-1 | RD | 3.95             | 3.43  | [84]       |
| 76             | 11      |         | A $\beta$ 40 | BTA-1      | RD | 3.2              | 4.11  | [82]       |
| 77             | 17.4    |         | A $\beta$ 40 | BTA-1      | RD | 2.21             | 3.23  | [79]       |
| 78             | 2.75    |         | A $\beta$ 40 | BTA-1      | RD | 2.96             | 3.80  | [79]       |
| 79             | 4.6     |         | A $\beta$ 40 | BTA-1      | RD | 3.33             | 4.79  | [79]       |
| 80             | 1       |         | A $\beta$ 40 | BTA-1      | RD | 4.08             | 4.94  | [79]       |

The third series of Th-T type ligand are those with a phenolate group instead of an aromatic amino group (81-94, Scheme 6 with Table 7). The binding and LogD parameters

for these ligands are presented in Table 8. The most interesting observation is the effect of an iodo group on Ki value. For any 6-substituent except for amino, the introduction of

iodo at either the 3' or 5-position reduces binding affinity (*c.f.* pairs **81**, **82**; **83**, **84**; **83**, **85**; **86**, **87**; **88**, **89**). The reason for this is unclear. However, if the 6-substituent is an amino group, the introduction of iodo at the 5-position increases the binding affinity (*c.f.* pairs **91**, **92**; **93**, **94**). This is consistent with observations for introduction of an iodo substituent into other sub-groups of Th-T type ligands.



81-94, Table 7

### Scheme 6. Th-T ligand series III.

The fourth group of Th-T type ligands comprise analogous benzo[d]oxazole, **95-97**, and benzofuran, **98-107**, derivatives (Scheme 7). Compared with the corresponding benzothiazoles (**51**, **70**, **90**, Tables 4, 6 and 8), **95-97** have very similar or slightly lower binding affinities (Table 9). When substituents at the 6-position and the aromatic amino group are the same, changes in the central five-membered ring have limited influence on binding affinity (*c.f.* **65**, Table 6 with **99**; **70**, Table 6 with **96** and **98**). This is similar to the influence of 6- and 7-position isomers (*c.f.* pairs **98**, **101**; **99**, **103**). As always, there is little difference in the influence of iodo and bromo substituents. In the benzofuran series, the influence of the aromatic amino and phenolate groups is reversed compared with that in the benzothiazole series (*c.f.* **44** ( $K_i = 37$  nM) and **81** ( $K_i = 5.68$  nM) with **100** ( $K_i = 1.1$  nM) and **105** ( $K_i = 4.2$  nM), respectively). However, the influence of a second *N*-methyl group varies and is generally small.

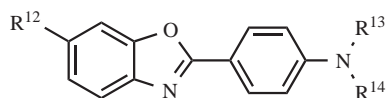
### Table 7. Structures of Compounds 81-94

| Compound  | R <sup>15</sup>                    | R <sup>16</sup> | R <sup>17</sup> | R <sup>18</sup> |
|-----------|------------------------------------|-----------------|-----------------|-----------------|
| <b>81</b> | H                                  | H               | H               | H               |
| <b>82</b> | H                                  | H               | I               | H               |
| <b>83</b> | OH                                 | H               | H               | H               |
| <b>84</b> | OH                                 | H               | I               | H               |
| <b>85</b> | OH                                 | I               | H               | H               |
| <b>86</b> | OH                                 | H               | H               | Me              |
| <b>87</b> | OH                                 | I               | H               | Me              |
| <b>88</b> | OMe                                | H               | H               | H               |
| <b>89</b> | OMe                                | H               | I               | H               |
| <b>90</b> | O(CH <sub>2</sub> ) <sub>2</sub> F | H               | H               | Me              |
| <b>91</b> | NH <sub>2</sub>                    | H               | H               | H               |
| <b>92</b> | NH <sub>2</sub>                    | I               | H               | H               |
| <b>93</b> | NH <sub>2</sub>                    | H               | H               | Me              |
| <b>94</b> | NH <sub>2</sub>                    | I               | H               | Me              |

The fifth group of Th-T type ligands (**108-123**, Scheme 8 with Tables 10) are those derived from stilbene, SB-13 (**109**). The binding affinities and LogD values of this group are shown in Table 11. The effect of an *N*-methyl group is the same as in previous groups. The first *N*-methyl group has a larger influence than the second and increases the binding affinity, except for **118**. The binding site has substantial tolerance for the size of the substituent at the phenolate oxygen, up to a certain limit. Any group other than methyl at the

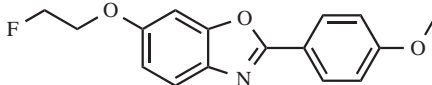
### Table 8. The Binding and LogD Parameters of Th-T Ligand Series III

| Compound  | K <sub>i</sub> (nM) | K <sub>d</sub> (nM) | PS   | RR    | M  | LogD at pH = 7.4 | cLogD | Ref. |
|-----------|---------------------|---------------------|------|-------|----|------------------|-------|------|
| <b>81</b> | 5.68                |                     | Aβ40 | BTA-1 | RD | 1.86             | 3.86  | [79] |
| <b>82</b> | 19.1                |                     | Aβ40 | BTA-1 | RD | 2.22             | 4.80  | [79] |
| <b>83</b> | 16.8                |                     | Aβ40 | BTA-1 | RD | 0.39             | 3.11  | [79] |
| <b>84</b> | 71.2                |                     | Aβ40 | BTA-1 | RD | 1.09             | 4.01  | [79] |
| <b>85</b> | 34.5                |                     | Aβ40 | BTA-1 | RD | 1.01             | 3.44  | [79] |
| <b>86</b> | 6.3                 |                     | Aβ40 | BTA-1 | RD | 1.75             | 3.66  | [79] |
| <b>87</b> | 7.1                 |                     | Aβ40 | BTA-1 | RD | 2.49             | 4.00  | [79] |
| <b>88</b> | 4.2                 |                     | Aβ40 | BTA-1 | RD | 1.8              | 3.78  | [79] |
| <b>89</b> | 15.8                |                     | Aβ40 | BTA-1 | RD | 2.31             | 4.70  | [79] |
| <b>90</b> | 1.2 to 12           |                     | Aβ40 | ???   | RD |                  | 4.57  | [83] |
| <b>91</b> | 52.6                |                     | Aβ40 | BTA-1 | RD | 0.7              | 2.58  | [79] |
| <b>92</b> | 26.3                |                     | Aβ40 | BTA-1 | RD | 1.6              | 3.94  | [79] |
| <b>93</b> | 6.9                 |                     | Aβ40 | BTA-1 | RD | 1.76             | 3.14  | [79] |
| <b>94</b> | 3.6                 |                     | Aβ40 | BTA-1 | RD | 2.95             | 4.50  | [79] |

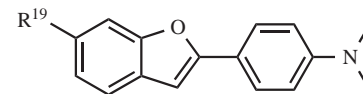


95, R<sup>12</sup> = Me, R<sup>13</sup> = H, R<sup>14</sup> = Me

96, R<sup>12</sup> = I, R<sup>13</sup> = Me, R<sup>14</sup> = Me

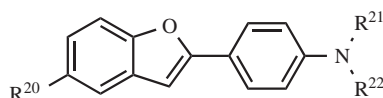


97



98, R<sup>19</sup> = I

99, R<sup>19</sup> = Br

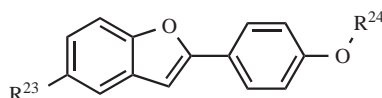


100, R<sup>20</sup> = I, R<sup>21</sup> = H, R<sup>22</sup> = Me

101, R<sup>20</sup> = I, R<sup>21</sup> = Me, R<sup>22</sup> = Me

102, R<sup>20</sup> = Br, R<sup>21</sup> = H, R<sup>22</sup> = Me

103, R<sup>20</sup> = Br, R<sup>21</sup> = Me, R<sup>22</sup> = Me



104, R<sup>23</sup> = I, R<sup>24</sup> = H

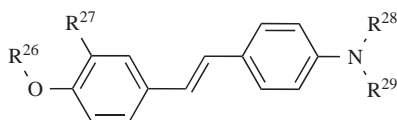
105, R<sup>23</sup> = I, R<sup>24</sup> = Me

106, R<sup>23</sup> = Br, R<sup>24</sup> = H

107, R<sup>23</sup> = Br, R<sup>24</sup> = Me

Scheme 7. Thioflavin-T ligand series IV.

phenolate oxygen reduces binding affinity, as reflected by comparing the set **108-115** with **116-123**. Those observations support the notion that the phenolate portion of the molecule is located outside the binding site.



108-123, Table 10

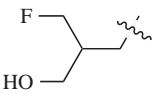
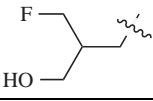
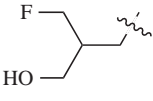
Scheme 8. Th-T ligand series V.

The sixth group of thioflavin-T type ligand (**124-146**) includes more general versions of the styrene derivatives (Scheme 9 with Table 12). Binding and LogD parameters are shown in Table 13. Interestingly, stilbene itself shows quite strong binding with A $\beta$  (K<sub>i</sub> = 535 nM). Electron-Donating groups, such as an aromatic amino or phenolate group, have strong influence on the binding affinity as reflected in **125-128** and **131-141**. The thiolate group has an influence comparable to that of amino or phenolate groups, although thiolate has much less electron-donating ability to the aryl system. However, oxidation of the thioether to sulfone completely abolishes binding affinity (*c.f.* **129** with **130**), either

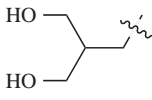
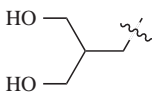
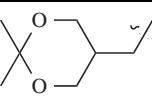
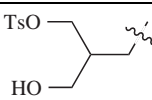
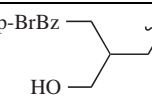
Table 9. The Binding LogD Parameters of Th-T Ligand Series IV

| Compound       | K <sub>i</sub> (nM) | K <sub>d</sub> (nM) | PS           | RR         | M  | LogD at pH = 7.4 | cLogD        | Ref.    |
|----------------|---------------------|---------------------|--------------|------------|----|------------------|--------------|---------|
| 95, 6-Me-BOA-1 | 37                  |                     | A $\beta$ 40 | 6-Me-BOA-1 | RD | 4.21             | 3.70<br>4.28 | [84]    |
| 96, IBOX       | 0.8                 |                     | A $\beta$ 40 | TZDM       | RD | 2.09             | 5.46         | [77,96] |
| 97             | 1.2 to 12           |                     | A $\beta$ 40 | ???        | RD |                  | 4.32         | [83]    |
| 98             | 0.4                 |                     | A $\beta$ 40 | TZDM       | RD | 2.12             | 5.72         | [97,98] |
| 99             | 0.6                 |                     | A $\beta$ 40 | TZDM       | RD |                  | 5.46         | [97,98] |
| 100            | 1.1                 |                     | A $\beta$ 40 | TZDM       | RD | 2.04             | 5.29         | [97,98] |
|                | >3000               |                     | A $\beta$ 40 | IMSB       | RD |                  |              | [97,98] |
| 101            | 7.7                 |                     | A $\beta$ 40 | TZDM       | RD | 2.25             | 5.72         | [97,98] |
|                | >3000               |                     | A $\beta$ 40 | IMSB       | RD |                  |              | [97,98] |
| 102            | 2.7                 |                     | A $\beta$ 40 | TZDM       | RD |                  | 5.03         | [97,98] |
| 103            | 1.6                 |                     | A $\beta$ 40 | TZDM       | RD |                  | 5.46         | [97,98] |
| 104            | 6.5                 |                     | A $\beta$ 40 | TZDM       | RD | 2.97             | 4.83         | [97,98] |
| 105            | 4.2                 |                     | A $\beta$ 40 | TZDM       | RD |                  | 5.42         | [97,98] |
| 106            | 9.0                 |                     | A $\beta$ 40 | TZDM       | RD |                  | 4.57         | [97,98] |
|                | >3000               |                     | A $\beta$ 40 | IMSB       | RD |                  |              | [97,98] |
| 107            | 1.3                 |                     | A $\beta$ 40 | TZDM       | RD |                  | 5.16         | [97,98] |
|                | >3000               |                     | A $\beta$ 40 | IMSB       | RD |                  |              | [97,98] |

**Table 10. Structures of compounds 108-123**

| Compound          | R <sup>26</sup>   | R <sup>27</sup> | R <sup>28</sup> | R <sup>29</sup> |
|-------------------|---|-----------------|-----------------|-----------------|
| <b>108</b>        | H   | H               | H               | H               |
| <b>109, SB-13</b> | H   | H               | H               | Me              |
| <b>110</b>        | H   | H               | Me              | Me              |
| <b>111</b>        | H   | I               | Me              | Me              |
| <b>112</b>        | Me  | H               | O               | O               |
| <b>113</b>        | Me  | H               | H               | H               |
| <b>114</b>        | Me  | H               | H               | Me              |
| <b>115</b>        | Me  | H               | Me              | Me              |
| <b>116</b>        |  | H               | H               | H               |
| <b>117</b>        |  | H               | H               | Me              |
| <b>118</b>        |  | H               | Me              | Me              |

**(Table 10) contd.....**

| Compound   | R <sup>26</sup>   | R <sup>27</sup> | R <sup>28</sup> | R <sup>29</sup> |
|------------|---|-----------------|-----------------|-----------------|
| <b>119</b> |  | H               | H               | Me              |
| <b>120</b> |  | H               | Me              | Me              |
| <b>121</b> |  | H               | Me              | Me              |
| <b>122</b> |  | H               | Me              | Me              |
| <b>123</b> |  | H               | Me              | Me              |

due to non-planar geometry or the electron-withdrawing nature of the sulfone group. An electron-withdrawing group at the opposite end of the molecule increases the binding affini-

**Table 11. The Binding and LogD Parameters of Th-T Ligand Series V**

| Compound             | K <sub>i</sub> (nM) | K <sub>d</sub> (nM) | PS   | RR       | M  | LogD at pH = 7.4 | cLogP        | Ref.    |
|----------------------|---------------------|---------------------|------|----------|----|------------------|--------------|---------|
| <b>108</b>           | 95                  |                     | AD   | IMPY     | RD |                  | 3.01         | [85]    |
| <b>109, SB-13</b>    | 6                   |                     | Aβ40 | SB-13    | RD | 3.17<br>2.36     | 2.98<br>3.67 | [84,99] |
|                      | 1.2                 |                     | AD   | IMPY     | RD |                  |              | [65,85] |
|                      |                     | 2.4                 | AD   |          | RT |                  |              | [65]    |
| <b>110</b>           | 2.2                 |                     | Aβ40 | TZDM     | RD |                  | 4.80         | [99]    |
|                      | 1.7                 |                     | Aβ40 | TZDM     | RD |                  |              | [100]   |
|                      | 1.1                 |                     | AD   | IMPY     | RD |                  |              | [85]    |
| <b>111</b>           | 2.0                 |                     | Aβ40 | TZDM     | RD |                  | 5.95         | [100]   |
| <b>112</b>           | 151                 |                     | Aβ40 | TZDM     | RD |                  | 4.56         | [99]    |
| <b>113</b>           | 36                  |                     | Aβ40 | TZDM     | RD |                  | 3.50         | [99]    |
| <b>114</b>           | 1.2                 |                     | Aβ40 | TZDM     | RD |                  | 4.15         | [99]    |
| <b>115, Me-SB-13</b> | 1.3                 |                     | Aβ40 | TZDM     | RD |                  | 5.28         | [99]    |
|                      | 0.8                 |                     | Aβ40 | TZDM     | RD |                  |              | [100]   |
|                      | 1                   |                     | Aβ40 | Me-SB-13 | RD | 3.85             | 4.97         | [84]    |
| <b>116</b>           | 15                  |                     | AD   | IMPY     | RD |                  | 3.37         | [85]    |
| <b>117</b>           | 5                   |                     | AD   | IMPY     | RD | 2.95             | 4.02         | [85]    |
| <b>118</b>           | 15                  |                     | AD   | IMPY     | RD | 3.14             | 5.15         | [85]    |
| <b>119</b>           | 32.5                |                     | AD   | IMPY     | RD |                  | 3.66         | [85]    |
| <b>120</b>           | 38                  |                     | AD   | IMPY     | RD |                  | 4.79         | [85]    |
| <b>121</b>           | 59                  |                     | AD   | IMPY     | RD |                  | 5.46         | [85]    |
| <b>122</b>           | 150                 |                     | AD   | IMPY     | RD |                  | 6.31         | [85]    |
| <b>123</b>           | 80                  |                     | AD   | IMPY     | RD |                  | 7.86         | [85]    |

ity, as in **131-134**, suggesting that elongated conjugation along the  $\pi$  system, enhanced by an electron-donating group at one end and an electron-withdrawing group at the other, plays an important role. The regioisomers of the iodo group in **133**, **136** and **140** showed similar binding affinities with **140** slightly lower. In **140**, non-planarity arising from the *o*-iodo group may play a role in reducing binding affinity. The geometrical isomers, **133** and **135**, also show similar binding affinity. When a methyl group is introduced at the central double bond of the stilbene derivatives (**137**, **138**), the methyl group closer to the aromatic amino system reduces binding more strongly than a methyl close to the aromatic iodo system. This reflects the critical importance of a co-planar arrangement near the aromatic amino system. When two methyl groups are attached to the central double bond, binding affinity is completely lost (**139**). Use of a naphthalenyl group (**141**) instead of a styrenyl group has little effect on binding affinity. This is consistent with the proposed  $\pi$ - $\pi$  interaction of the ligands with A $\beta$  plaques. The most intriguing results are those from substitution of one phenyl group by a pyridine ring. When the ring nitrogen is at *o*-position (**142**) binding affinity is lost. When the double bond attaches at the *m*-position, the ligands show stronger binding affinity (*c.f.* **143-146** with their phenyl counterparts, **108**, **132** and **133**).

The seventh group of Th-T type ligands (**147-163**) results from insertion of a double bond into the benzo[*d*]thiazole and benzo[*d*]oxazole derivatives (Scheme 10 with Tables 14). Binding parameters and LogD values are shown in Table 15. When the extended benzo[*d*]thiazole derivatives (**147-148**) are compared with their counterparts (**46** and **52**) there is a general small increase in binding affinity. However, for this series, the binding site is tolerant to increasing size of substituent on the aromatic amino group, as in **149**.

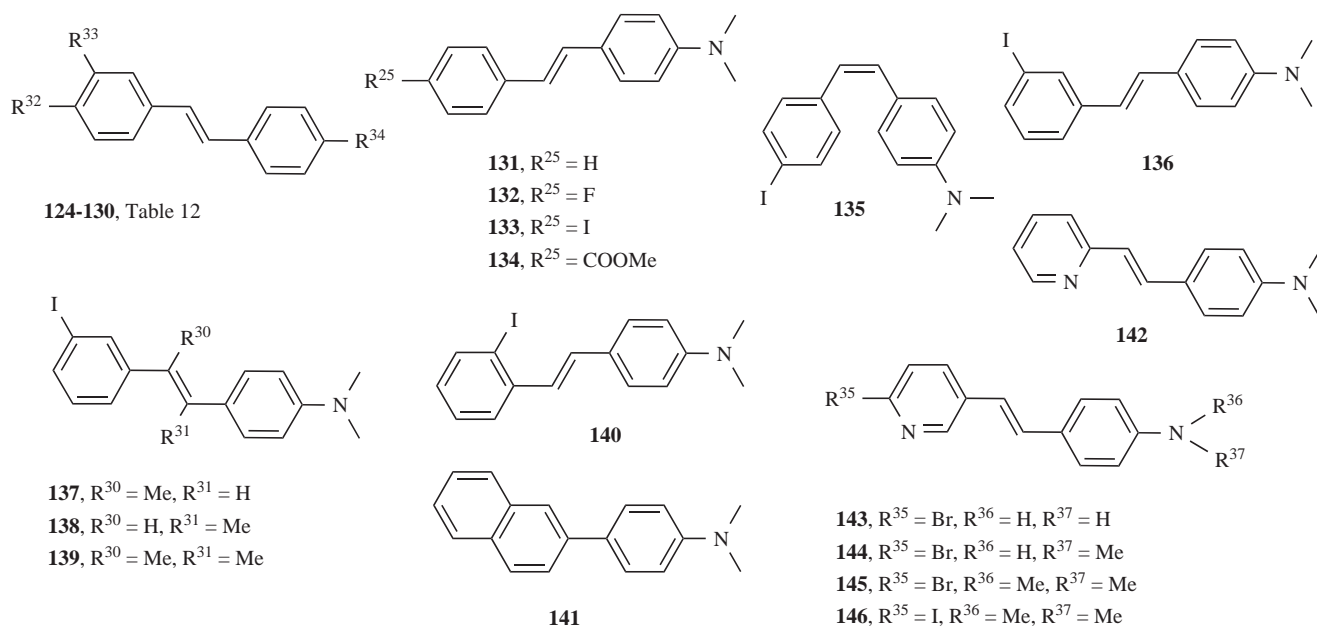
In the extended series of benzo[*d*]oxazole derivatives, **150-161**, the effect of an *N*-methyl group almost disappears. In some cases, the effect is even reversed, as in **150-152**. The

effect of a halogen substituent at either the 6- or 7-position is also small or even reversed, as in **150**, **151**, **154-157**. The most striking observation is that compound **153** has binding affinity comparable to **152**, showing the binding site has steric tolerance for a group larger than methyl at the aromatic amino group, the only example known at this time. However, for this series of compounds the binding site shows intolerance to lack of aromatic amino group. Compounds **162** and **163**, with a halogen substituent in place of the amino group, do not show any binding affinity.

Table 12. Structures of Compounds 124-130

| Compound | R <sup>32</sup> | R <sup>33</sup> | R <sup>34</sup>    |
|----------|-----------------|-----------------|--------------------|
| 124      | H               | H               | H                  |
| 125      | F               | H               | OH                 |
| 126      | H               | H               | OMe                |
| 127      | H               | I               | OH                 |
| 128      | H               | I               | OMe                |
| 129      | H               | I               | SMe                |
| 130      | H               | I               | SO <sub>2</sub> Me |

The eighth series of Th-T type ligands (**164-173**) arises from the elimination of the central five-membered ring, generating *bi*-aryl derivatives (Scheme 11 with Table 16). Binding parameters and LogD values are shown in Table 17. Only those ligands with at least one aromatic amino group have been evaluated. Generally, they have lower binding affinities than those with the central five-membered ring. Other peripheral groups modulate the binding affinity. Among five substituents (Me, Br, I, OH, NO<sub>2</sub>, NH<sub>2</sub>) at the opposite end of the amino group in the *bi*-phenyl series, the bromo substituent promotes strongest binding. It appears that both high electron polarizability and electron-withdrawing



Scheme 9. Th-T ligand series VI.

**Table 13. The Binding and LogD Parameters of Th-T Ligand Series VI**

| Compound     | Ki (nM) | Kd (nM) | PS           | RR      | M  | LogD at pH = 7.4 | cLogD        | Ref.     |
|--------------|---------|---------|--------------|---------|----|------------------|--------------|----------|
| 124          | 535     |         | A $\beta$ 40 | TZDM    | RD |                  | 4.83         | [76]     |
| 125          | 22      |         | A $\beta$ 40 | TZDM    | RD |                  | 4.30         | [100]    |
| 126          | 44      |         | A $\beta$ 40 | TZDM    | RD |                  | 4.78         | [76,100] |
| 127          | 32      |         | A $\beta$ 40 | TZDM    | RD |                  | 5.33         | [76,100] |
|              | >2000   |         | A $\beta$ 40 | IMSB    | RD |                  |              | [76]     |
| 128          | 22      |         | A $\beta$ 40 | TZDM    | RD |                  | 5.81         | [76,100] |
|              | >1000   |         | A $\beta$ 40 | IMSB    | RD |                  |              | [76]     |
| 129          | 7       |         | A $\beta$ 40 | TZDM    | RD |                  | 6.35         | [76,100] |
| 130          | >2000   |         | A $\beta$ 40 | TZDM    | RD |                  | 4.15         | [76,100] |
| 131          | 45      |         | A $\beta$ 40 | TZDM    | RD |                  | 5.34         | [100]    |
| 132          | 22      |         | A $\beta$ 40 | TZDM    | RD |                  | 5.35         | [76]     |
|              | >2000   |         | A $\beta$ 40 | IMSB    | RD |                  |              | [76]     |
| 133          | 2.0     |         | A $\beta$ 40 | TZDM    | RD |                  | 6.37         | [76,100] |
|              | >2000   |         | A $\beta$ 40 | IMSB    | RD |                  |              | [76]     |
| 134, E-SB-13 | 1       |         | A $\beta$ 40 | E-SB-13 | RD | 3.15             | 4.98<br>5.31 | [84]     |
| 135          | 2.2     |         | A $\beta$ 40 | TZDM    | RD |                  | 6.37         | [76,100] |
| 136          | 4.5     |         | A $\beta$ 40 | TZDM    | RD | 2.63             | 6.37         | [76,100] |
|              | >2000   |         | A $\beta$ 40 | IMSB    | RD |                  |              | [76]     |
| 137          | 17.1    |         | A $\beta$ 40 | TZDM    | RD |                  | 6.92         | [100]    |
| 138          | 61.3    |         | A $\beta$ 40 | TZDM    | RD |                  | 6.91         | [100]    |
| 139          | >1000   |         | A $\beta$ 40 | TZDM    | RD |                  | 7.46         | [100]    |
| 140          | 7.7     |         | A $\beta$ 40 | TZDM    | RD |                  | 6.37         | [76,100] |
|              | >3000   |         | A $\beta$ 40 | IMSB    | RD |                  |              | [76]     |
| 141          | 10.6    |         | A $\beta$ 40 | TZDM    | RD |                  | 6.57         | [101]    |
| 142          | >3000   |         | A $\beta$ 40 | TZDM    | RD |                  | 3.98         | [76]     |
| 143          | 210     |         | AD           | IMPY    | RD |                  | 3.23         | [102]    |
| 144          | 7.0     |         | AD           | IMPY    | RD |                  | 3.89         | [102]    |
| 145          | 3.2     |         | AD           | IMPY    | RD |                  | 5.02         | [102]    |
| 146          | 4.8     |         | AD           | IMPY    | RD | 1.92             | 5.19         | [102]    |

ability in these substituents play important roles. A methyl group at either the phenolate or aromatic amino groups increases binding affinity. Interestingly, **173** with five- and six-membered rings has quite strong binding affinity.

The ninth series of Th-T type ligands (**174-196**) comes from the *bi*-aryl system with a tether, and some other miscellaneous compounds related to the Th-T series (Scheme 12

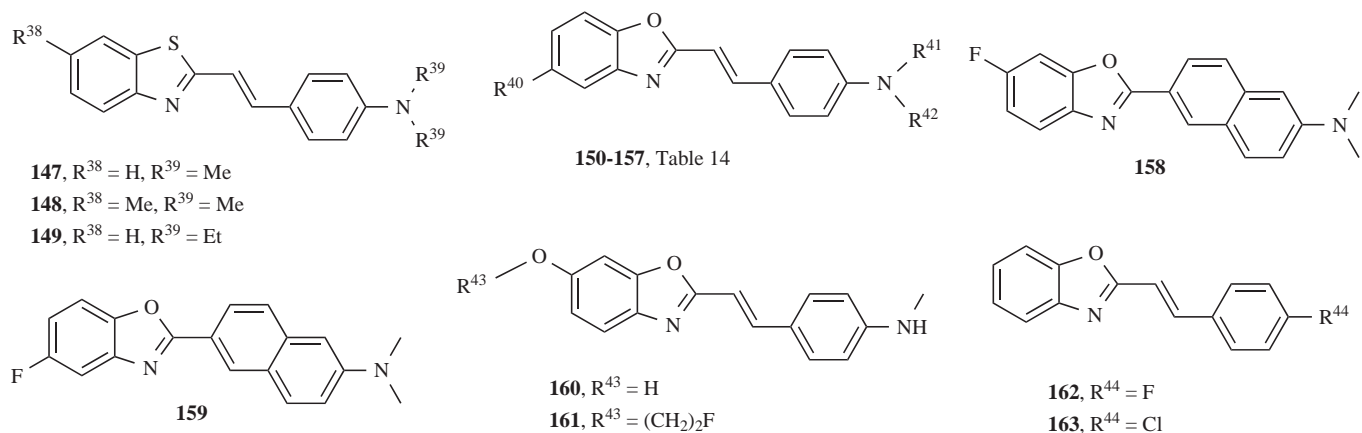
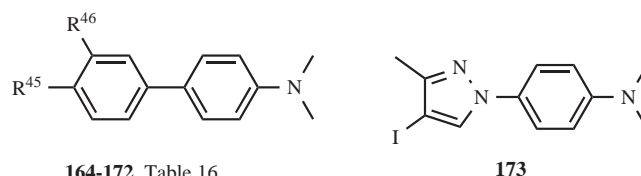
**Scheme 10.** Th-T ligand series VII.

Table 14. Structures of Compounds 150-157

| Compound | R <sup>40</sup> | R <sup>41</sup> | R <sup>42</sup> |
|----------|-----------------|-----------------|-----------------|
| 150      | H               | H               | H               |
| 151      | H               | H               | Me              |
| 152      | H               | Me              | Me              |
| 153      | H               | Et              | Et              |
| 154      | F               | H               | H               |
| 155      | F               | H               | Me              |
| 156      | F               | Me              | Me              |
| 157      | I               | H               | Me              |

with Table 18). Binding and LogD parameters are shown in Table 19. Among compounds 174-180, only a combination of *N,N*-dimethyl and *p*-bromo or *p*-iodo substituents (178-179) gives high binding affinities. Geometrical isomers in 174-184 do not show any significant variation in binding affinity. Introduction of a hydroxyl group into the tethering methylene group (185-188) gave no high affinity compound. When the tethering group was changed to carbonyl, only 190 with *N,N*-dimethyl and *p*-bromo substituents, gave a signifi-

cant binding affinity, but much weaker than that for the methylene-tethered analog, 178. No geometric isomerism can overcome the adverse effect manifested by the carbonyl group. The direct conjugation present in 191 did not result in any significant increase in binding affinity. This may suggest that the dipole moment of the carbonyl group is detrimental to binding. Acridine Orange derivatives (193-195) also show significant binding affinities, but they are generally low, partly from an unfavorable combination of functional groups, such as pyridinyl in the middle ring and two opposed aromatic amino groups. Interestingly, a new type of compound, 196, has been identified showing strong binding affinity. Although the mode of interaction is unclear, it is possible that the phenol group occupies the same site as the aromatic amino group in other series of Th-T type ligands.



Scheme 11. Th-T ligand series VIII.

The tenth series of Th-T type ligands (197-213) is those of 2-phenyl-*H*-imidazo[1,2-*a*]pyridine derivatives, (Scheme

Table 15. The Binding and LogD Parameters of Th-T Ligand Series VII

| Compound    | K <sub>i</sub> (nM) | K <sub>d</sub> (nM) | PS           | RR     | M  | cLogD at pH = 7.4 | Ref.  |
|-------------|---------------------|---------------------|--------------|--------|----|-------------------|-------|
| 147         | 2.3                 |                     | A $\beta$ 40 | TZDM   | RD | 5.64              | [76]  |
| 148         | 1.4                 |                     | A $\beta$ 40 | TZDM   | RD | 6.10              | [76]  |
| 149, BF-124 | 10.9                |                     | A $\beta$ 42 | BF-180 | RD | 6.69              | [103] |
| 150, BF-164 | 0.38                |                     | A $\beta$ 42 | BF-180 | RD | 3.27              | [103] |
| 151, BF-169 | 7.1                 |                     | A $\beta$ 42 | BF-180 | RD | 3.93              | [103] |
| 152, N-282  | 4.3                 |                     | A $\beta$ 42 | BF-180 | RD | 5.06              | [103] |
| 153, BF-125 | 4.9                 |                     | A $\beta$ 42 | BF-180 | RD | 6.11              | [103] |
| 154, BF-140 | 4.7                 |                     | A $\beta$ 40 | BF-180 | RD | 3.32              | [104] |
|             | 2.1                 |                     | A $\beta$ 42 | BF-180 | RD |                   | [104] |
| 155, BF-145 | 3.0                 |                     | A $\beta$ 40 | BF-180 | RD | 3.98              | [104] |
|             | 4.5                 |                     | A $\beta$ 42 | BF-180 | RD |                   | [104] |
| 156, BF-133 | 2.1                 |                     | A $\beta$ 40 | BF-180 | RD | 5.11              | [104] |
|             | 3.4                 |                     | A $\beta$ 42 | BF-180 | RD |                   | [104] |
| 157, BF-180 |                     | 6.8                 | A $\beta$ 40 |        | RT | 4.96              | [104] |
|             |                     | 10.6                | A $\beta$ 42 |        | RT |                   | [104] |
| 158, BF-148 | 4.2                 |                     | A $\beta$ 42 | BF-180 | RD | 5.11              | [103] |
| 159, BF-151 | 1.4                 |                     | A $\beta$ 40 | BF-180 | RD | 5.40              | [104] |
|             | 5.3                 |                     | A $\beta$ 42 | BF-180 | RD |                   | [104] |
| 160, BF-165 | 1.8                 |                     | A $\beta$ 42 | BF-180 | RD | 3.16              | [103] |
| 161, BF-168 | 6.4                 |                     | A $\beta$ 42 | BF-180 | RD | 4.07              | [103] |
| 162, BF-208 | >5000               |                     | A $\beta$ 42 | BF-180 | RD | 4.56              | [103] |
| 163, BF-191 | >5000               |                     | A $\beta$ 42 | BF-180 | RD | 5.08              | [103] |

**Table 16. Structures of compounds 164-172**

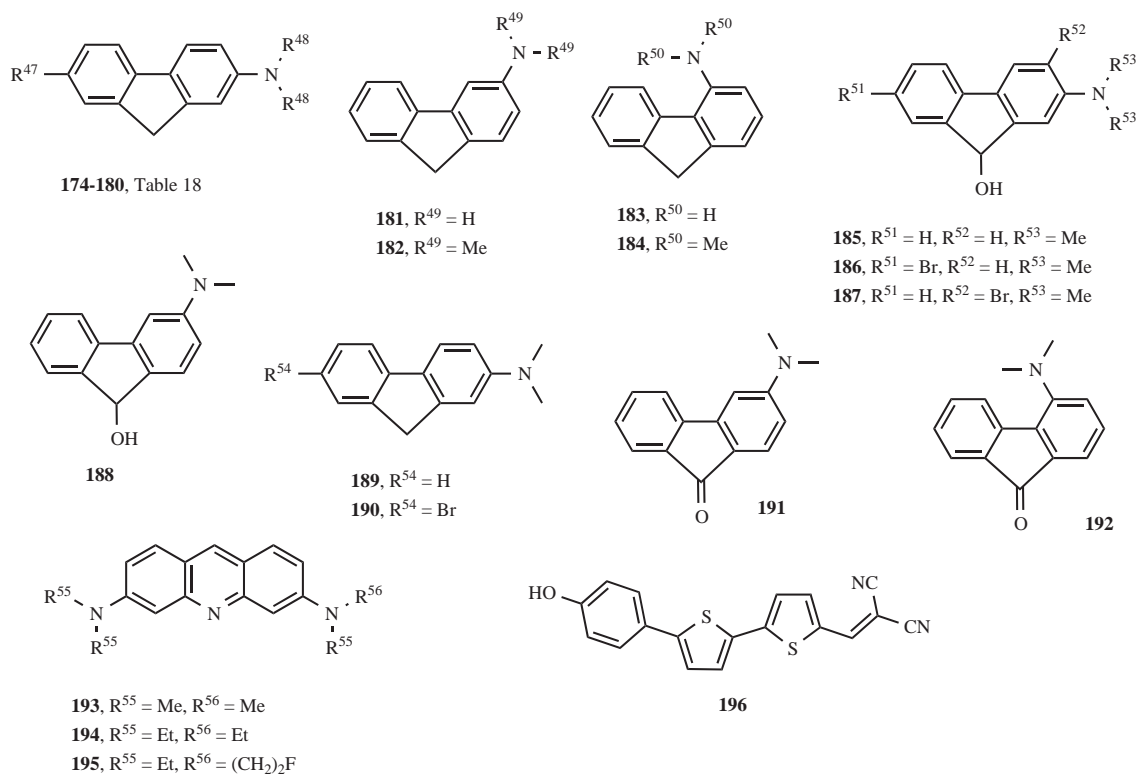
| Compound | R <sup>45</sup>  | R <sup>46</sup> |
|----------|------------------|-----------------|
| 164      | Me               | H               |
| 165      | Br               | H               |
| 166      | I                | H               |
| 167      | OH               | H               |
| 168      | OH               | I               |
| 169      | NO <sub>2</sub>  | H               |
| 170      | NH <sub>2</sub>  | H               |
| 171      | NHMe             | H               |
| 172      | NMe <sub>2</sub> | H               |

**13** with Table 20). Binding and LogD parameters are shown in Table 21. Binding affinity of this series of ligand depends critically on the presence of aromatic amino group. Compounds with phenolate and halogen groups, such as **210-213**, showed lower affinities. Even with an aromatic amino group, the location of the group is also quite critical. Compounds **203** and **213** are isomers, with the amino and bromo substituents in switched positions, but their binding affinities differ by a factor of 15.

Of the 2-phenyl-*H*-imidazo[1,2-*a*]pyridine derivatives with an aromatic amino group (**197-209**), only compounds with 6-halogen substituents showed high binding affinities. Of these compounds, those with a 3-substituent other than hydrogen gave low binding affinity, probably due to distortion from planarity. In the 2-phenyl-*H*-imidazo[1,2-

**Table 17. The Binding and LogD Parameters of Th-T Ligand Series VIII**

| Compound | K <sub>i</sub> (nM) | K <sub>d</sub> (nM) | PS   | RR   | M  | cLogD | Ref.  |
|----------|---------------------|---------------------|------|------|----|-------|-------|
| 164      | 79                  |                     | Aβ40 | TZDM | RD | 4.54  | [101] |
| 165      | 7.9                 |                     | Aβ40 | TZDM | RD | 4.99  | [101] |
| 166      | 17.3                |                     | Aβ40 | TZDM | RD | 5.09  | [101] |
| 167      | 245                 |                     | Aβ40 | TZDM | RD | 3.30  | [101] |
| 168      | 19.1                |                     | Aβ40 | TZDM | RD | 4.40  | [101] |
| 169      | 49                  |                     | Aβ40 | TZDM | RD | 3.70  | [101] |
| 170      | 493                 |                     | Aβ40 | TZDM | RD | 2.87  | [101] |
| 171      | 102                 |                     | Aβ40 | TZDM | RD | 3.75  | [101] |
| 172      | 49                  |                     | Aβ40 | TZDM | RD | 4.17  | [101] |
| 173      | 19.5                |                     | Aβ40 | TZDM | RD | 4.07  | [105] |

**Scheme 12.** Th-T ligand series IX.

*a*]pyridine derivatives, the *N*-methyl group showed significant influence on binding affinity, (*c.f.* pairs **197**, **199**; **198**, **200**). Among the compounds with a 6-halogen substituent, bromo and iodo substituents gave similar binding affinities. Steric bulk at the aromatic amino group has great influence on binding (*c.f.* sets **197**, **198**; **199**, **200**, **201**; **203**, **204**). For IMPY (**199**), and the difference in binding constants for synthetic A $\beta$  aggregates and A $\beta$  plaques from AD reflects amyloid structural difference between the two sources. This contrasts with the observation in benzothiazole series of ligands where the binding constants correlate well between the two protein sources [108].

**Table 18. Structures of Compounds 174-180**

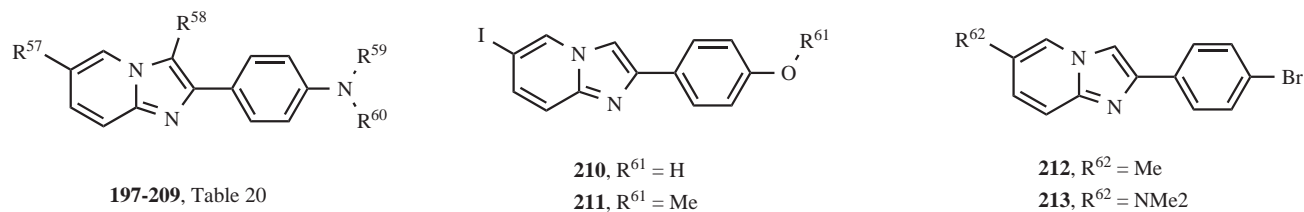
| Compound | R <sup>47</sup>  | R <sup>48</sup> |
|----------|------------------|-----------------|
| 174      | H                | H               |
| 175      | Br               | H               |
| 176      | NH <sub>2</sub>  | H               |
| 177      | H                | Me              |
| 178      | Br               | Me              |
| 179      | I                | Me              |
| 180      | NMe <sub>2</sub> | Me              |

### 5.3. FDDNP Type Ligands

Only ligands **214-222** (Scheme 14) with a naphthalenyl moiety have affinity for the FDDNP binding site (Table 22). For these ligands, it appears that the end of the ligands is the electron-donating group on the naphthalenyl moiety. Probably, this group plays an important role; binding affinity decreases as this group is changed from aromatic amino, to an aryl ether or an alkyl group. The binding affinity of (*S*)-Ibuprofen (**220**) reaches a K<sub>d</sub> in micromolar range. Interestingly, binding affinity depends on chirality at the  $\alpha$ -position of the acid. A similar dependence was also observed for Naproxen (*c.f.* **218**, **219**). Among compounds with an aromatic amino group, the electron-withdrawing ability at the other end of the molecule and the direct conjugation between the donor and acceptor groups play important roles. The best combination so far is found in compound **214**, where the two cyano groups are held in the conformation for direct conjugation with the aromatic amino group by the six-membered ring. Comparison of the binding affinity between **215** and **216** shows the importance of conjugation and co-planarity. Whether or not the steric bulk of substituents at the aromatic amino group has any influence on binding affinity is unclear. This series of ligands also binds with NFTs [75].

**Table 19. The Binding and LogD Parameters of Th-T Ligand Series IX**

| Compound             | K <sub>i</sub> (nM) | PS           | RR    | M  | LogD | cLogD at pH = 7.4 | Ref.  |
|----------------------|---------------------|--------------|-------|----|------|-------------------|-------|
| 174                  | >1000               | A $\beta$ 40 | TZDM  | RD |      | 2.88              | [106] |
| 175                  | 56                  | A $\beta$ 40 | TZDM  | RD |      | 3.65              | [106] |
| 176                  | >1000               | A $\beta$ 40 | TZDM  | RD |      | 1.60              | [106] |
| 177                  | >1000               | A $\beta$ 40 | TZDM  | RD |      | 4.27              | [106] |
| 178                  | 0.85                | A $\beta$ 40 | TZDM  | RD |      | 5.04              | [106] |
| 179                  | 0.92                | A $\beta$ 40 | TZDM  | RD | 2.47 | 5.30              | [106] |
| 180                  | 15.4                | A $\beta$ 40 | TZDM  | RD |      | 4.36              | [106] |
| 181                  | >1000               | A $\beta$ 40 | TZDM  | RD |      | 2.88              | [106] |
| 182                  | 23.5                | A $\beta$ 40 | TZDM  | RD |      | 4.27              | [106] |
| 183                  | >1000               | A $\beta$ 40 | TZDM  | RD |      | 2.88              | [106] |
| 184                  | >1000               | A $\beta$ 40 | TZDM  | RD |      | 4.27              | [106] |
| 185                  | >1000               | A $\beta$ 40 | TZDM  | RD |      | 2.61              | [106] |
| 186                  | 88                  | A $\beta$ 40 | TZDM  | RD |      | 3.39              | [106] |
| 187                  | >1000               | A $\beta$ 40 | TZDM  | RD |      | 3.75              | [106] |
| 188                  | >1000               | A $\beta$ 40 | TZDM  | RD |      | 2.61              | [106] |
| 189                  | >1000               | A $\beta$ 40 | TZDM  | RD |      | 3.79              | [106] |
| 190                  | 16.5                | A $\beta$ 40 | TZDM  | RD |      | 4.76              | [106] |
| 191                  | >1000               | A $\beta$ 40 | TZDM  | RD |      | 3.92              | [106] |
| 192                  | >1000               | A $\beta$ 40 | TZDM  | RD |      | 3.79              | [106] |
| 193, Acridine Orange | 32                  | A $\beta$ 40 | Th-T  | FD | 1.77 | 2.39              | [66]  |
| 194, BF-009          | 167                 | A $\beta$ 40 | Th-T  | FD | 3.01 | 4.55              | [66]  |
| 195, BF-108          | 135                 | A $\beta$ 40 | Th-T  | FD | 2.56 | 4.20              | [66]  |
| 196                  | 10                  | A $\beta$ 40 | BTA-1 | RD |      | 4.87              | [107] |



Scheme 13. Th-T ligand series X.

Table 20. Structures of Compounds 197-209

| Compound  | R <sup>57</sup> | R <sup>58</sup> | R <sup>59</sup>                                   | R <sup>60</sup>                                   |
|-----------|-----------------|-----------------|---|---|
| 197       | I               | H               | Me  | H   |
| 198       | I               | H               | (CH <sub>2</sub> ) <sub>2</sub> F                 | H   |
| 199, IMPY | I               | H               | Me  | Me  |
| 200       | I               | H               | (CH <sub>2</sub> ) <sub>2</sub> F                 | Me  |
| 201       | I               | H               | (CH <sub>2</sub> ) <sub>2</sub> F                 | Me  |
| 202       | I               | I               | Me  | Me  |
| 203       | Br              | H               | Me  | Me  |
| 204       | Br              | H               | (CH <sub>2</sub> CH <sub>2</sub> ) <sub>2</sub> O | (CH <sub>2</sub> CH <sub>2</sub> ) <sub>2</sub> O |
| 205       | Me              | H               | Me  | H   |
| 206       | Me              | H               | Me  | Me  |
| 207       | H               | H               | Me  | H   |
| 208       | H               | H               | Me  | Me  |
| 209       | H               | I               | Me  | Me  |

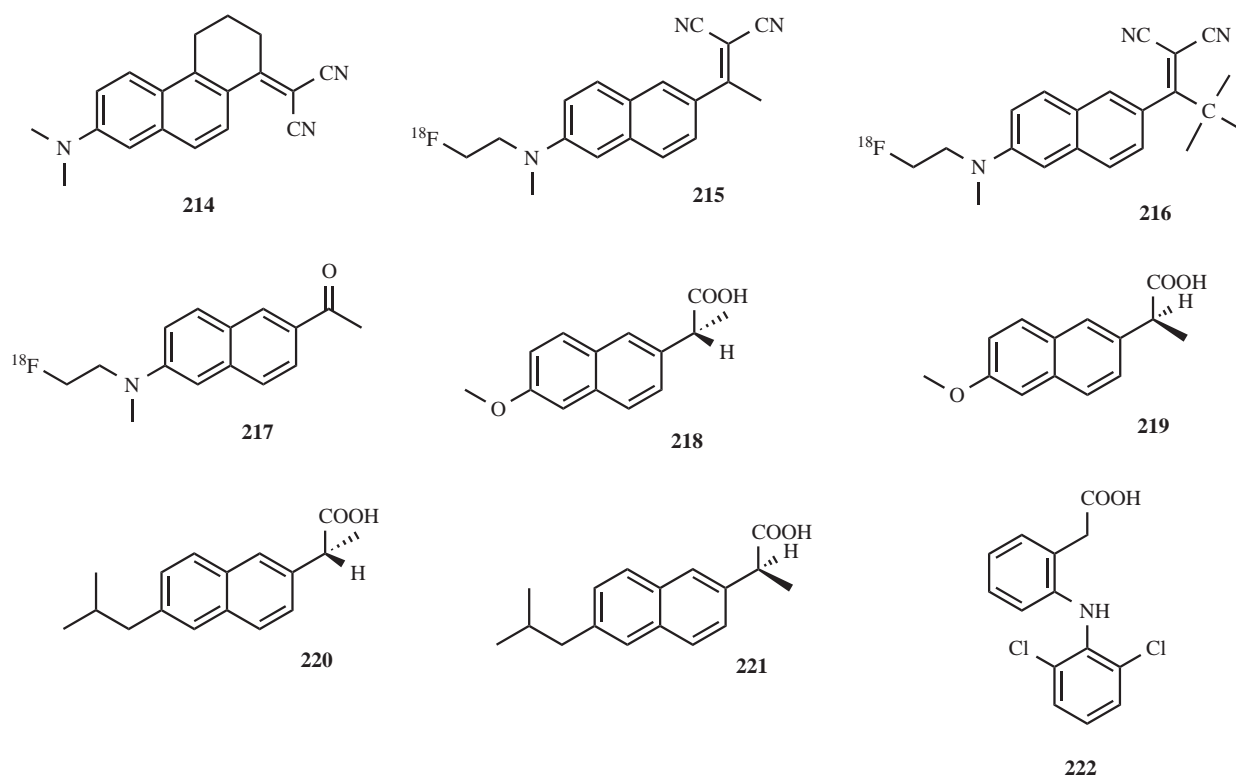
Table 21. Binding and LogD Parameters of Th-T Ligand Series X

| Compound      | K <sub>i</sub> (nM) | K <sub>d</sub> (nM) | PS               | RR       | M  | LogD pH = 7.4 | cLogD | Ref.         |
|---------------|---------------------|---------------------|------------------|----------|----|---------------|-------|--------------|
| 197           | 140                 |                     | Aβ <sub>40</sub> | TZDM     | RD | 4.41          | 4.10  | [109]        |
| 198           | 161                 |                     | Aβ <sub>40</sub> | TZDM     | RD | 4.41          | 4.26  | [109]        |
| 199, IMPY     | 15                  |                     | Aβ <sub>40</sub> | TZDM     | RD | 2.0<br>3.58   | 4.53  | [94,96,110]  |
|               | 5.0                 |                     | AD               | IMPY     | RD |               |       | [65]         |
|               | 1.4                 |                     | AD               | SB-13    | RD |               |       | [65]         |
|               | 152                 |                     | Tg mice          | IMPY     | RD |               |       | [111]        |
| 200, FEM-IMPY | 27                  |                     | Aβ <sub>40</sub> | TZDM     | RD | 4.41          | 4.68  | [109]        |
|               | 83                  |                     | AD               | FEM-IMPY | RD |               |       | [109]        |
| 201, FPM-IMPY | 40                  |                     | Aβ <sub>40</sub> | TZDM     | RD | 4.60          | 5.07  | [109]        |
| 202           | 1000                |                     | Aβ <sub>40</sub> | TZDM     | RD |               | 5.73  | [94,110]     |
|               | >2000               |                     | Aβ <sub>40</sub> | TZDM     | RD |               |       | [112]        |
| 203, BMPY     | 10.3                |                     | Aβ <sub>40</sub> | TZDM     | RD |               | 4.23  | [94,110,112] |
|               | 10                  |                     | Aβ <sub>40</sub> | BMPY     | RD | 3.47          | 4.653 | [84]         |
| 204           | >280                |                     | Aβ <sub>40</sub> | TZDM     | RD |               | 3.25  | [94,110]     |
| 205           | >2000               |                     | Aβ <sub>40</sub> | TZDM     | RD |               | 2.72  | [112]        |
| 206, IMPY/Me  | 242                 |                     | Aβ <sub>40</sub> | TZDM     | RD |               | 3.17  | [96,112]     |
| 207           | >1000               |                     | Aβ <sub>40</sub> | TZDM     | RD |               | 2.50  | [112]        |
| 208, IMPY/H   | 1242                |                     | Aβ <sub>40</sub> | TZDM     | RD |               | 2.95  | [96]         |
|               | >2000               |                     | Aβ <sub>40</sub> | TZDM     | RD |               |       | [112]        |
| 209           | >2000               |                     | Aβ <sub>40</sub> | TZDM     | RD |               | 4.67  | [112]        |
| 210           | >1000               |                     | Aβ <sub>40</sub> | TZDM     | RD | 4.60          | 3.66  | [109]        |
| 211           | 451                 |                     | Aβ <sub>40</sub> | TZDM     | RD | 4.60          | 4.27  | [109]        |
| 212           | 339                 |                     | Aβ <sub>40</sub> | TZDM     | RD |               | 4.75  | [94,110]     |
|               | 638                 |                     | Aβ <sub>40</sub> | TZDM     | RD |               |       | [112]        |
| 213           | 339                 |                     | Aβ <sub>40</sub> | TZDM     | RD |               | 4.38  | [112]        |

## 6. PHARMACOKINETICS OF CANDIDATE PET RADIIOLIGANDS

The pharmacokinetics of candidate PET radioligands have been evaluated using normal animals, such as monkey, rat, and mouse. Promising PET radioligands should have rapid and high initial uptake followed by rapid washout from normal brain. The standard uptake value (SUV), defined as (I. D. /g × g body mass), at three time points (2, 30 and 60 min after injection) were selected to compare the pharmacokinetics of the potential PET radioligands. A list of radioligands evaluated in the literature is shown in Table 23.

From Table 23, it is clear that there is no correlation between ratios of the maximum radioactivity reaching brain to the residual radioactivity at 30 and 60 min with the binding constants of the radioligand. However, there is some correlation between that ratios and lipophilicity (LogD). Given the



Scheme 14. FDDNP ligand series.

widely variable cLogD values reported in the literature for a given compound, values calculated from a single program are used here instead. Of the 14 compounds with the ratios R1 and R2 less than 1, only three compounds, [ $^{123/125}$ I]71, [ $^{123/125}$ I]104, and [ $^{18}$ F]195 have cLogD values less than 5, but

greater than 4.2. All compounds, which gave R1 and R2 values greater than 5, have cLogD values in the range 2.9 to 5.2. Only three compounds, [ $^{11}$ C]PIB ([ $^{11}$ C]32), [ $^{123/125}$ I]42 and [ $^{123/125}$ I]IMPY ([ $^{123/125}$ I]99), have ratios greater than 10. Their cLogD values were 3.31, 4.28 and 4.53, respectively.

Table 22. Binding and LogD Parameters for the FDDNP Ligand Series

| Compound           | Ki (nM)                     | Kd (nM)                      | PS           | RR    | M  | LogD | cLogD        | Ref.         |
|--------------------|-----------------------------|------------------------------|--------------|-------|----|------|--------------|--------------|
| 214                | 0.0066                      |                              | A $\beta$ 40 | FDDNP | RD | 3.2  | 3.27<br>4.52 | [75,113,114] |
| 215, FDDNP         |                             | Site 1: 0.12<br>Site 2: 1.86 | A $\beta$ 40 |       | FT | 3.92 | 3.12<br>4.0  | [68,75,114]  |
|                    | Site 1: 0.2<br>Site 2: 234  |                              | A $\beta$ 40 | FDDNP | RD |      |              | [75,114]     |
|                    | 293                         |                              | AD           | SB-13 | RD |      |              | [65]         |
| 216                | 520                         |                              | A $\beta$ 40 | FDDNP | RD |      | 3.12<br>5.23 | [75,113]     |
|                    | Site 1: 0.91<br>Site 2: 521 |                              | A $\beta$ 40 | FDDNP | RD |      |              | [75]         |
|                    | 457                         |                              | A $\beta$ 40 | Th-T  | FD | 2.39 |              | [66]         |
| 217, FENE          |                             | Site 1: 0.16<br>Site 2: 71.2 | A $\beta$ 40 |       | FT | 3.13 | 3.14         | [68]         |
| 218, (S)-Naproxen  | 5.70                        |                              | A $\beta$ 40 | FDDNP | RD |      | 0.47         | [75,114]     |
| 219, (R)-Naproxen  | 2.76                        |                              | A $\beta$ 40 | FDDNP | RD |      | 0.47         | [75,114]     |
| 220, (S)-Ibuprofen | 11300                       |                              | A $\beta$ 40 | FDDNP | RD |      | 2.4          | [75,114]     |
| 221, (R) Ibuprofen | 44400                       |                              | A $\beta$ 40 | FDDNP | RD |      | 2.4          | [75,114]     |
| 222, Diclofenac    | infinite                    |                              | A $\beta$ 40 | FDDNP | RD |      | 0.95         | [75,114]     |

**Table 23. Pharmacokinetics of PET Radioligands in Normal Animals**

| Radioligand  | 2.0 min  | 30 min | 60 min | R1 <sup>a</sup> | R2 <sup>b</sup> | Ki (nM) <sup>c</sup> | cLogD <sup>d</sup> | Ref.     |
|--|----------|--------|--------|-----------------|-----------------|----------------------|--------------------|----------|
| [ <sup>123/125</sup> I]24, [ <sup>123/125</sup> I]ISB  | 0.27     | 0.06   | 0.04   | 4.5             | <b>6.8</b>      | 0.08                 | 4.41               | [64]     |
|  | 0.14     | 0.06   | 0.04   | 2.3             | 3.5             |                      |                    | [64]     |
| [ <sup>123/125</sup> I]25, [ <sup>123/125</sup> I]IMSB | 0.14     | 0.03   | 0.02   | 4.7             | <b>7</b>        | 0.17                 | 2.94               | [64]     |
| [ <sup>11</sup> C]27, [ <sup>11</sup> C]MeO-X04        | 81 (IDI) | 50     |        | 1.6             |                 | 26.8                 | 3.45               | [72]     |
| [ <sup>11</sup> C]28                                   | 2.25     | 0.71   |        | 3.2             |                 | 38                   | 5.68               | [74]     |
| [ <sup>11</sup> C]32, [ <sup>11</sup> C]PIB            | 0.21     | 0.018  |        | <b>12</b>       |                 | 2.8                  | 3.31               | [82]     |
| [ <sup>11</sup> C]33                                   | 0.32     | 0.10   |        | 3.0             |                 | 4.4                  | 3.92               | [82]     |
| [ <sup>123/125</sup> I]42                              | 5.64     | 0.36   |        | <b>15.7</b>     |                 | 11.1                 | 4.28               | [79,87]  |
| [ <sup>123/125</sup> I]43                              | 7.76     | 2.66   |        | 2.91            |                 | 3.22                 | 4.44               | [79]     |
| [ <sup>11</sup> C]45                                   | 0.43     | 0.057  |        | <b>7.6</b>      |                 | 7.6                  | 4.07               | [82]     |
| [ <sup>11</sup> C]46                                   | 0.19     | 0.078  |        | 2.5             |                 | 4.0                  | 4.68               | [82]     |
| [ <sup>123/125</sup> I]48                              | 9.08     | 3.4    |        | 2.7             |                 | 8.32                 | 5.06               | [79]     |
| [ <sup>123/125</sup> I]49                              | 4.40     | 2.68   |        | 1.6             |                 | 4.94                 | 5.21               | [79]     |
| [ <sup>11</sup> C]51                                   | 0.22     | 0.083  | 0.036  | 2.7             | <b>6.1</b>      | 10                   | 4.53               | [82,115] |
| [ <sup>11</sup> C]52                                   | 0.078    | 0.15   |        | 0.52            |                 | 2.3                  | 5.14               | [82]     |
| [ <sup>11</sup> C]53                                   | 0.32     | 0.084  |        | 3.8             |                 | 7.0                  | 3.42               | [82]     |
| [ <sup>11</sup> C]54                                   | 0.33     | 0.10   |        | 3.2             |                 | 4.9                  | 3.98               | [82]     |
| [ <sup>11</sup> C]55                                   | 0.16     | 0.14   |        | 1.1             |                 | 1.9                  | 4.59               | [82]     |
| [ <sup>11</sup> C]64                                   | 0.12     | 0.12   |        | 1.0             |                 | 1.7                  | 4.84               | [82]     |
| [ <sup>11</sup> C]65                                   | 0.054    | 0.11   |        | 0.49            |                 | 2.9                  | 5.45               | [82]     |
| [ <sup>123/125</sup> I]70, TZDM                        | 0.6      | 0.9    | 1.57   | 0.67            | 0.38            | 0.9                  | 5.71               | [64]     |
|  | 0.67     | 0.97   | 1.57   | 0.69            | 0.43            |                      |                    | [94]     |
| [ <sup>123/125</sup> I]71, TZPI                        | 1.50     | 1.59   | 1.89   | 0.94            | 0.79            | 5.4                  | 4.72               | [64,94]  |
| [ <sup>11</sup> C]75                                   | 0.32     | 0.063  |        | <b>5.0</b>      |                 | 8.6                  | 3.51               | [82]     |
| [ <sup>11</sup> C]76                                   | 0.24     | 0.097  |        | 2.5             |                 | 11                   | 4.11               | [82]     |
| [ <sup>123/125</sup> I]96                              | 1.43     | 2.08   | 1.26   | 0.69            | 1.1             | 0.8                  | 5.46               | [77]     |
| [ <sup>123/125</sup> I]98                              | 0.48     | 0.80   | 1.0    | 0.6             | 0.48            | 0.4                  | 5.72               | [77]     |
| [ <sup>123/125</sup> I]100                             | 0.78     | 1.19   | 1.20   | 0.66            | 0.65            | 1.1                  | 5.29               | [77]     |
| [ <sup>123/125</sup> I]101                             | 0.51     | 0.90   | 1.08   | 0.57            | 0.47            | 7.7                  | 5.72               | [98]     |
| [ <sup>123/125</sup> I]104                             | 1.40     | 1.83   | 1.51   | 0.77            | 0.93            | 6.5                  | 4.83               | [98]     |
| [ <sup>11</sup> C]109, SB-13                           | 1.15     | 0.42   | 0.30   | 2.7             | 3.8             | 1.2                  | 3.67               | [99]     |
| [ <sup>18</sup> F]117                                  | 9.75     | 1.70   | 0.72   |                 |                 | 5                    | 4.02               | [85]     |
| [ <sup>18</sup> F]118                                  | 5.55     | 5.21   | 2.97   |                 |                 | 15                   | 5.15               | [85]     |
| [ <sup>123/125</sup> I]129                             | 0.72     | 1.12   | 1.08   | 0.64            | 0.67            | 4.5                  | 6.37               | [100]    |
| [ <sup>11</sup> C]145                                  | 1.68     | 0.36   | 0.22   | 4.7             | <b>7.6</b>      | 4.8                  | 5.19               | [102]    |
| [ <sup>18</sup> F]154, BF-140                          | 5.5      | 1.1    |        | <b>5.0</b>      |                 | 4.7                  | 3.32               | [102]    |
| [ <sup>18</sup> F]155, BF-145                          | 4.4      | 1.6    |        | 2.8             |                 | 3.0                  | 3.98               | [102]    |
| [ <sup>18</sup> F]156, BF-133                          | 5.5      | 3.8    |        | 1.4             |                 | 2.1                  | 5.11               | [104]    |
| [ <sup>18</sup> F]159, BF-151                          | 1.1      | 1.6    |        | 0.67            |                 | 1.4                  | 5.40               | [104]    |
| [ <sup>18</sup> F]161, BF-168                          | 3.9      | 1.6    | 1.3    | 2.4             | 3.0             | 6.4                  | 4.07               | [103]    |
| [ <sup>123/125</sup> I]173                             | 2.2      |        | 0.2    |                 | <b>11</b>       | 19.5                 | 4.07               | [105]    |
| [ <sup>123/125</sup> I]179                             | 1.13     | 1.26   | 0.72   | 0.90            | 1.6             | 0.92                 | 5.30               | [106]    |
| [ <sup>18</sup> F]195, BF-108                          | 0.42     | 1.53   | 1.39   | 0.27            | 0.30            | 135                  | 4.20               | [116]    |
| [ <sup>123/125</sup> I]199, IMPY                       | 2.88     | 0.26   | 0.2    | <b>11</b>       | <b>14</b>       | 5.0                  | 4.53               | [96,105] |

Note: <sup>a</sup>The ratio of the radioactivity of the brain at 2 and 30 min. <sup>b</sup>The ratio of the radioactivity of the brain at 2 and 60 min. <sup>c</sup>Only those Ki values that approximate brain tissue were selected. <sup>d</sup>Calculated using ACD software package 8.0.

Only [ $^{11}\text{C}$ ]PIB has been evaluated in human subjects. [ $^{11}\text{C}$ ]SB-13 ([ $^{11}\text{C}$ ]109) was selected for human trial based on different criteria [84]. Previously, it was established that the optimal LogD values for compounds to enter the brain were 2 to 3 [82]. However, this range only applies to the specific method used to measure the LogD values.

If a radioligand has sufficient binding affinity, such that the empirical relationship of  $\text{BP} = \text{B}_{\text{max}}/\text{K}_d > 6$  holds (where BP is binding potential and  $\text{B}_{\text{max}}$  is the concentration of target binding sites), and the dissociation of the radioligand from the target binding site is insignificant over a short period of time (such as 60 min), ratios of R1 and R2 would be a measure of maximum attainable signal (specific to non-specific binding) [117]. The pharmacokinetic evaluation described above for normal animals could be used for the selection of PET radioligands for further evaluation, such as in human trials.

## 7. STRUCTURE OF A $\beta$ PLAQUES AND SYNTHETIC A $\beta$ AGGREGATES

The above survey demonstrates that ligands from different structural classes bind to different binding sites in A $\beta$  aggregates, and that different aggregates present a different profile of binding sites for ligand binding. Ultimately, these observations may be rationalized in terms of the architecture and density of each binding site in each type of aggregate. Hence, it is pertinent with regard to PET radioligand development to consider present knowledge of the structure of such aggregates.

Different levels of structures are describable for A $\beta$  plaques, except for the level of cross-linking due to oxidation such as super oxide, hydroxyl radical, hydroperoxyl radical and/or singlet oxygen species. The first is the primary sequence of A $\beta$ 40 and A $\beta$ 42, the second the  $\beta$ -sheet, the third the interface among sheets to form a bundle called protofibril, fourth the 3D arrangement of bundles called fibril. The full length A $\beta$  peptides associated with AD were demonstrated to be those with 39 to 43 amino acid residues derived from secretases, with the sequence: [1]DAEFR, HDSGY, EVHHQ, KLVFF, AEDVG, SNKGA, IIGLM, VGGVV, IA[42] (where 1 and 42 refer to the numbering of the polypeptide sequence) [118-121]. An X-ray crystal structure of A $\beta$  plaques has not been obtained. In combination with other techniques, including X-ray fiber diffraction and solid state NMR, electron microscopy has revealed that the internal structure of the A $\beta$  fibril is a ladder of  $\beta$ -sheet structure arranged in a cross- $\beta$  structural motif [122], with extended  $\beta$ -sheets where the  $\beta$ -strand segments run almost perpendicular to, and the intermolecular hydrogen bonds run almost parallel to, the long axis of the fibril [123-125]. Atomic force microscopic imaging showed that there is a family of A $\beta$  oligomers, of heterogeneous length, that differ from the much longer product fibrils in their length and morphology [126-129]. These oligomers are collectively called protofibrils. It has been shown that the protofibril to fibril transition is nucleation-dependent and that protofibril winding is involved in that transition [126]. The observation that both protofibril and fibril showed helical twist which depends on the chirality of A $\beta$  monomer suggests the winding of  $\beta$ -sheet in the formation of protofibril and fibril.

Only recently, the atomic structures of the aggregates from small synthetic peptides, GNNQQNY and NNQQNY, have been obtained (Fig. 3) [130]. The molecules in the structures are extended in conformation, and hydrogen bonded to each other in standard Pauling-Corey parallel  $\beta$ -sheets. The GNNQQNY  $\beta$ -strands within each sheet are parallel and exactly in register (Fig. 3). The side chains extending from a strand in a sheet nestle between side chains extending from two strands of the mating sheet. Two distinctly different interfaces have been identified and termed dry and wet interface, depending on the number of water molecules involved. The dry interface comes from van der Waals interaction involving inter-digitating side chains, as a "steric zipper", while the wet interface is formed by polar side chains hydrated by water. The wet interfaces are separated by 15 Å, and the dry interfaces by 8.5 Å. The separation between adjacent  $\beta$ -strands is 4.87 Å.

Similar parallel, in register arrangement is also seen for other A $\beta$  molecules in their fibrils, but not through single crystal X-ray diffraction study. Solid state nuclear magnetic resonance (NMR) study of  $^{13}\text{C}$ -labeled poly peptide A $\beta$ [10-35] [131-133] and A $\beta$ 40 [134] together with X-ray diffraction measurement showed that it had a parallel in register arrangement within the  $\beta$ -sheet with the inter-strand distance of 5 Å. However, analogous study of the fibrils formed from A $\beta$ [16-22] [135] and A $\beta$ [34-42] [136] showed anti-parallel arrangement. It was proposed that the hydrophobic interaction may favor the parallel, in register arrangement, and electrostatic interaction may favor the anti-parallel structure [135]. "Polar zipper" interaction has also been proposed to rationalize some anti-parallel structures of A $\beta$  fibrils [137]. Recent studies of fibrils with solid state NMR of fibrils formed by A $\beta$  associated with AD [134,138-143], by various A $\beta$  fragments [131-133,135,136,144-147] and by other A $\beta$ -forming peptides indicates that the  $\beta$ -sheets in A $\beta$  fibrils have structures that tend to maximize contacts among hydrophobic residues when the component peptides contain continuous hydrophobic segments.

The fibril structure model of A $\beta$ 40 has been proposed based on experimental constraints from solid state NMR [139]. The basic structural feature is amazingly consistent with the X-ray single crystal study described above for GNNQQNY. However, there are additional features for this structure. Given that the sequences of A $\beta$ 40 and A $\beta$ 42 are as follows: [1]DAEFR, HDSGY, EVHHQ, KLVFF, AEDVG, SNKGA, IIGLM, VGGVV, IA[42] [118], the structure has two separate, parallel  $\beta$ -sheets, created by residues 9-24 and 30-40, separated by a 180° angle bend formed by residues 25-29 (Figs. 4 and 5). Solid-state NMR using dipolar-assisted rotational resonance (DARR) revealed the presence of a turn structure at positions 22 and 23 in E22K-A $\beta$ 42 (Italian mutation) fibrils [148]. The formation of a salt bridge between Lys-22 and Asp-23 in the minor conformer might be a reason why E22K-A $\beta$ 42 is more pathogenic than wild-type A $\beta$ 42. The prediction of the protofilaments as dimers and tetramers coincided with the molecular mass measurement for ADDLs [149].

Using sequence searches in the Protein Data-Bank (PDB, <http://www.rcsb.org>) and physicochemical profile matching, Mathura *et al.* [150] suggested a model of A $\beta$  as an anti-parallel  $\beta$ -sheet similar to the  $\beta$ -turn- $\beta$  conformation of the

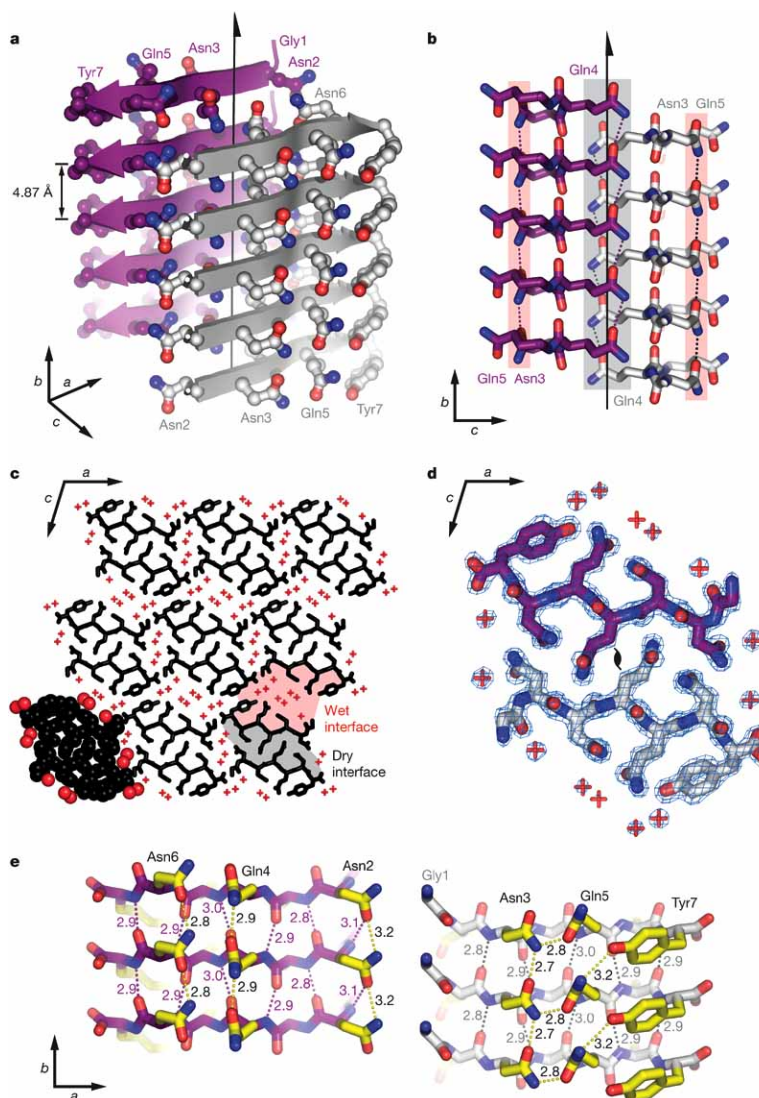


**Fig. (3).** X-ray crystal structure of A $\beta$  aggregates from GNNQQNY. Unless otherwise noted, carbon atoms are coloured in purple or grey/white, oxygen in red, nitrogen in blue. **a**, The pair-of-sheets structure, showing the backbone of each  $\beta$ -strand as an arrow, with side chains protruding. The dry interface is between the two sheets, with the wet interfaces on the outside surfaces. Side chains Asn 2, Gln 4, and Asn 6 point inwards, forming the dry interface. The  $2_1$  screw axis of the crystal is shown as the vertical line. It rotates one of these strands of the near sheet  $180^\circ$  about the axis and moves it up  $4.87 \text{ \AA}$  so that it is superimposed on one of the strands of the far sheet. **b**, The steric zipper viewed edge on down the  $a$  axis. Note the vertical shift of one sheet relative to the other, allowing interdigitation of the side chains emanating from each sheet. The amide stacks of the dry interface are shaded in grey at the centre, and those of the wet interface are shaded in pale red on either side. **c**, The GNNQQNY crystal viewed down the sheets from the top of panel **a**, along the  $b$  axis. Six rows of  $\beta$ -sheets run horizontally. Peptide molecules are shown in black and water molecules are red plus signs. The atoms in the lower left unit cell are shown as spheres representing van der Waals radii. **d**, The steric zipper. This is a close-up view of a pair of GNNQQNY molecules from the same view as panel **c**, showing the remarkable shape complementarity of the Asn and Gln side chains protruding into the dry interface.  $2F_o - F_c$  electron density is shown, and the position of the central screw axis is indicated. **e**, Views of the  $\beta$ -sheets from the side down the  $c$  axis, showing three  $\beta$ -strands with the inter-strand hydrogen bonds. Side-chain carbon atoms are yellow. Backbone hydrogen bonds are shown by purple or grey dots and side-chain hydrogen bonds by yellow dots. Hydrogen bond lengths are noted in  $\text{\AA}$ . Views of these interfaces are close to views of panel **a**. The left-hand set is viewed from the centre of the dry interface; the right-hand set is viewed from the wet interface. Note the amide stacks in both interfaces. Adapted by permission from Macmillan Publishers Ltd: Nature (435: 773-778), copyright (2005) [130].

RNA binding protein AF-Sm1. IR absorption spectroscopy has also been applied to elucidate the amyloid fibril structure of the #21-31 fragment of  $\beta 2$ -microglobulin [ $^{21}\text{NFLNCYVSGFH}^{31}$ ]. Hiramatsu *et al.* [151] suggested parallel  $\beta$ -sheet stacking instead of anti-parallel  $\beta$ -sheet, since no band is seen around  $1690 \text{ cm}^{-1}$ , but a two-residual displacement between molecules and the disulfide bridge have also been

suggested. X-ray diffraction study of the fibril formed by the variants of the B1 domain of IgG binding protein G of streptococcus suggested a model of four  $\beta$  sheets in a bundle with a diameter of  $45 \text{ \AA}$  [152]. The fibril has an overall helical twist with a periodicity of about  $154 \text{ \AA}$ . In all of these studies one must keep separate results obtained from peptides isolated from plaques and synthetic peptides.

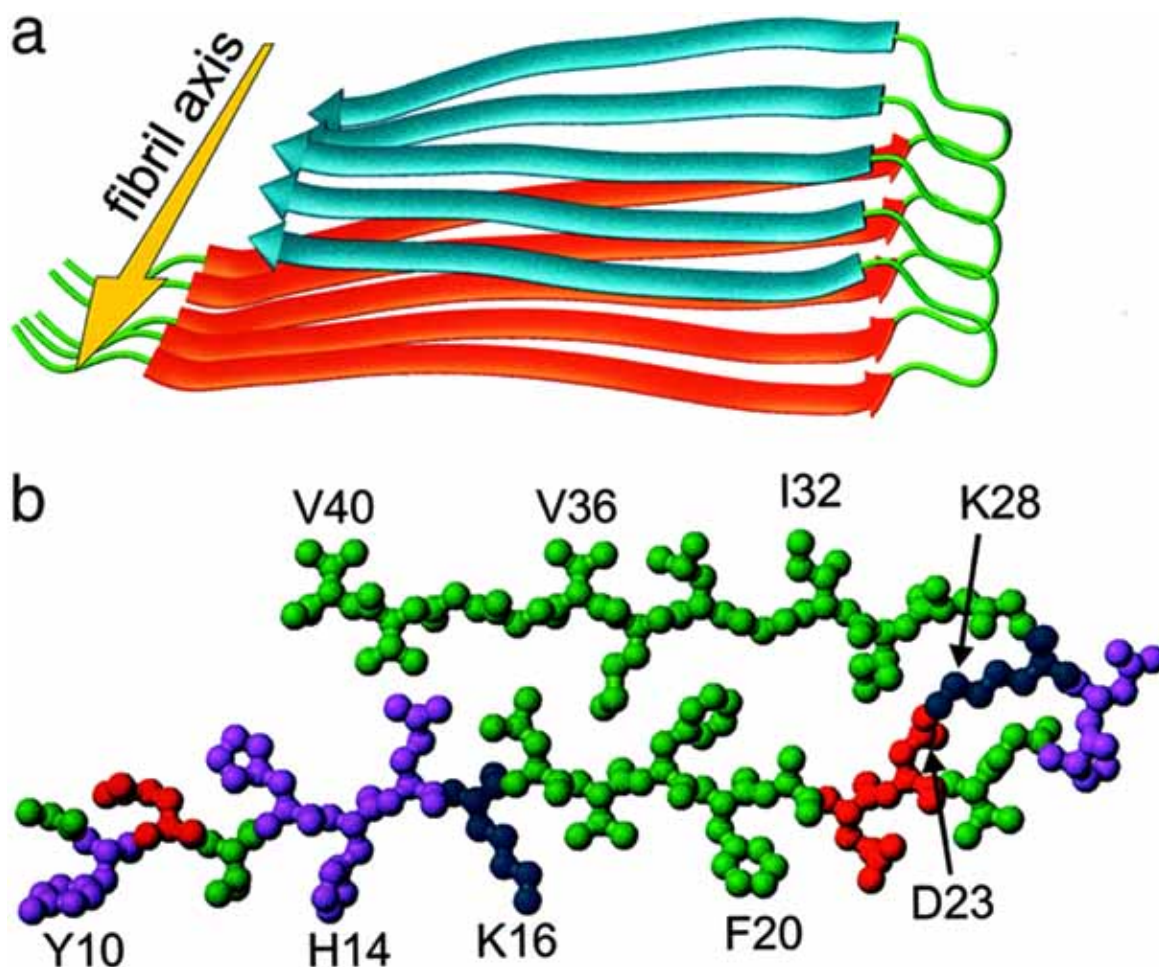


**Fig. (4).** Structural model for A $\beta$ 40 fibrils consistent with solid state NMR constraints on the molecular conformation and intermolecular distances and incorporating the cross- $\beta$  motif common to all amyloid fibrils. Residues 1-8 are considered fully disordered and are omitted. (a) Schematic representation of a single molecular layer, or cross- $\beta$  unit. The yellow arrow indicates the direction of the long axis of the fibril, which coincides with the direction of intermolecular backbone hydrogen bonds. The cross- $\beta$  unit is a double-layered structure, with in-register parallel  $\beta$ -sheets formed by residues 12-24 (orange ribbons) and 30-40 (blue ribbons). (b) Central A $\beta$ 40 molecule from the energy-minimized, five-chain system, viewed down the long axis of the fibril. Residues are color-coded according to their side-chains as hydrophobic (green), polar (magenta), positive (blue), or negative (red). Adapted by permission (Copyright 2002 National Academy of Sciences, USA) [139].

Although no atomic structure for aggregates of A $\beta$  are known, we anticipate that possible positions for planar hydrophobic PET radioligands interaction should be around amino acids with aromatic side chains, such as F[4], Y[10] and FF[19-20], with the last two positions being the most probable. However, no detailed knowledge of this interaction is available at this time.

## 8. PET IMAGING OF A $\beta$ AGGREGATES IN TG ANIMALS

PET imaging in Tg mice models of AD has many aspects of significance for diagnostic and therapeutic developments. It may allow for the direct correlation of the imaging signal to the amount of A $\beta$  deposit determined from *in vitro* measurement and provides an animal model for therapeutic evaluation of new compounds targeting specific aspects of AD pathology [62]. Various Tg rodents have been developed, including APP23 [153], Tg2576 [154], PS/APP [155], CRND8 [156], and double and triple Tg rats [157]. A number of radioligands have been reported to show *in vitro* and

*ex vivo* binding with A $\beta$  plaques from Tg rodents [96,99]. Wang *et al.* [74] reported an NOR- $\beta$  (normal A $\beta$ ) Tg mice (available from Aventis Pharmaceuticals, Inc.) study of compound **28** *ex vivo*, and observed up to about 2:1 ratio of the radioactivity in the pancreas of Tg vs. control mice. Kung, *et al.* [111] reported the *ex vivo* study of IMPY on PS/APP Tg mice, and observed up to about 2:1 ratio of the radioactivity in the brain of Tg vs. control mice. Wilson, *et al.* [84] evaluated both [ $^{11}\text{C}$ ]PIB and [ $^{11}\text{C}$ ]SB-13 using CRND8 *ex vivo*, and obtained a radioactivity ratio of 1.7:1 between cerebrum and cerebellum.

Kepe *et al.* [157] used a triple Tg rat, developed by Cephalon, Inc. and Xenogen Bioscience, and [ $^{18}\text{F}$ ]FDDNP in brain PET imaging. They obtained a radioactivity ratio of up to 1.32 between different regions of gray matter and cerebellum. In our initial effort, we evaluated [ $^{11}\text{C}$ ]PIB for imaging Tg2576 [158]. We did not observe any specific binding in cerebrum, only non-specific binding comparable to that in cerebellum; *in vitro* A $\beta$  plaques are found to be abundant in

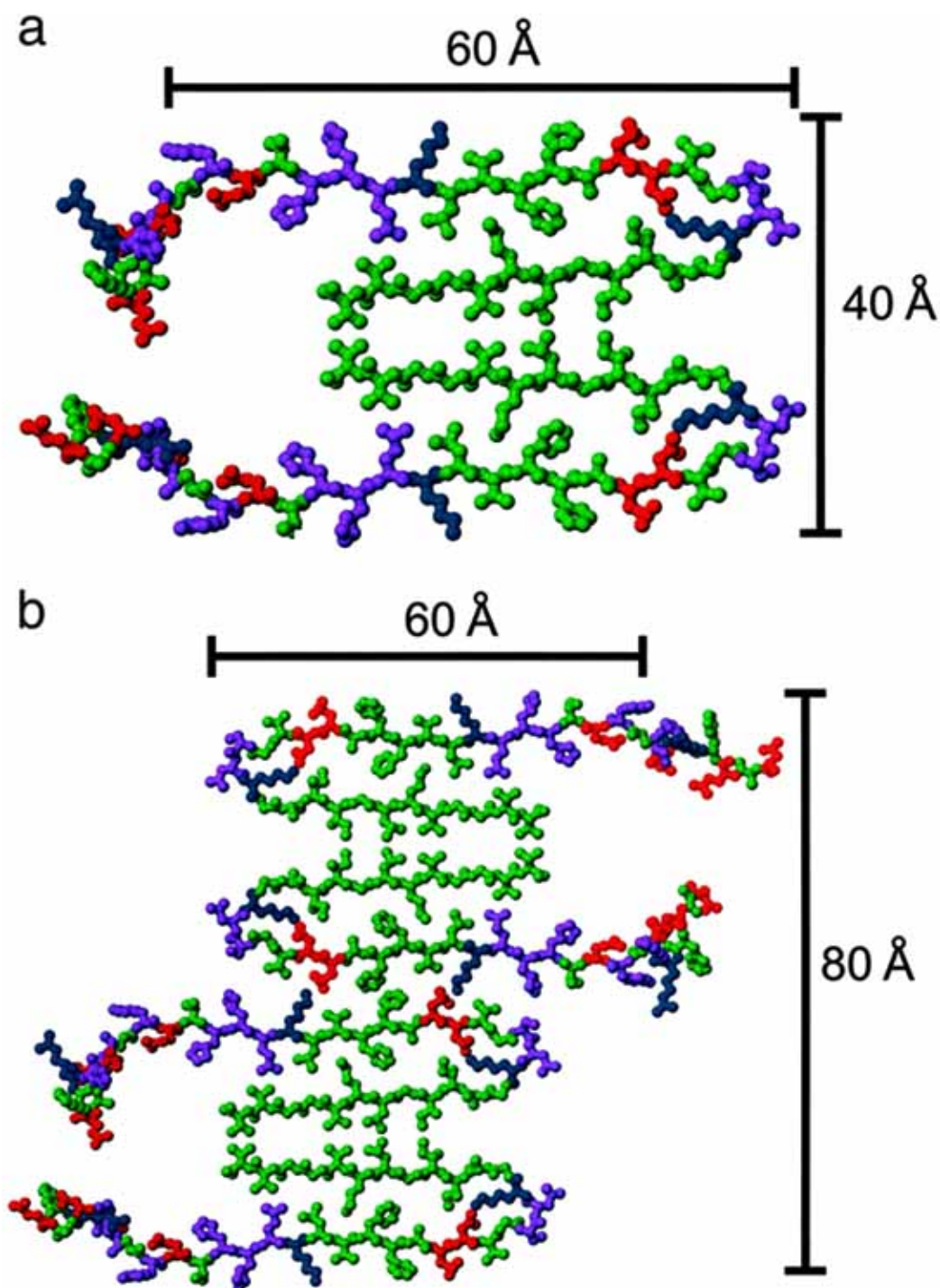


**Fig. (5).** (a) Cross section of an Aβ40 fibril with the minimal mass-per-length (MPL) indicated by scanning transmission electron microscopy (13, 29), formed by juxtaposing the hydrophobic faces of two cross-β units from Fig. 4. Residues 1-8 are included with randomly assigned conformations. (b) Possible mode of lateral association to generate fibrils with greater MPL and greater cross-sectional dimensions. Adapted by permission (Copyright 2002 National Academy of Sciences, USA) [139].

cerebrum but very much less prevalent in cerebellum. However, in three animals greater than 28 months of age, we found moderate levels of activity in neocortex compared to cerebellum, which was displaced by saturating doses of cold carrier (unpublished data). These preliminary data suggest that [<sup>11</sup>C]PIB can successfully image Aβ in transgenic animals only if excessive quantities are present.

## 9. AMYLOID OF SYNTHETIC AGGREGATES, TG PLAQUES AND HUMAN AD PLAQUES

The most intriguing question about animal models of AD and *in vitro* experiments with synthetic Aβ aggregates is how these studies relate to human AD conditions. We are focusing on the aspect of the binding of small molecules with Aβ. Klunk *et al.* [108] compared the binding of ten structurally

related BTA derivatives (Tables 4 and 6) to synthetic A $\beta$ 40 fibrils and to AD brain frontal gray matter. A good correlation was found between the Ki values determined using [<sup>3</sup>H]BTA-1 as reference radioligand binding to synthetic A $\beta$ 40 fibrils and to the AD brain homogenate in a wide range of 1.8 to 3030 nM. This suggests that the synthetic fibrils and AD brain tissue shares a common structural motif. Genetic mutation of the APP gene in Tg mice and rats as described above generates significant amount of A $\beta$  plaques in these animals. Here, we focus on the differences among those A $\beta$  plaques which may create the difference in PET imaging.

The number of binding sites among the three sources of A $\beta$  differs significantly. Mathis *et al.* [82] demonstrated that the Bmax value of BTA derivatives determined in homogenates taken from post mortem AD brain were strikingly higher (~ 400-fold) than for synthetic A $\beta$ 40 fibrils and resulted in a ligand-to-A $\beta$  peptide stoichiometry of about 1 to 1. We also measured the binding constants of [<sup>3</sup>H]PIB with A $\beta$  plaques from TgCRND8 and Tg2576 mice and Tg rat, and showed less than 1 to 2 orders of magnitude in the number of binding sites and lower than 1 order of magnitude of the binding constant as compared with AD brain homogenates (unpublished results). Klunk *et al.* [159] also evaluated PS1/APP transgenic mice, and showed much reduced binding of PIB as compared with human AD. Binding of the PET tracer PIB reflects the amount of amyloid-beta in Alzheimer's disease brain but not in transgenic mouse brain [160]. The physical and chemical properties of the A $\beta$  plaques are also quite different. Prolonged incubation (< 20 h) at room temperature in each of the following reagents failed to solubilize quantitatively the A $\beta$  fibers from AD brain: urea (9 M); guanidine HCl (6 M); guanidine HCl (5 M) in acetic acid (1 M); lithium bromide (7 M); potassium thiocyanate (7 M); 2% SDS; chelating molecules (such as EDTA); and chloroform/methanol (2:1) [161]. In contrast, the A $\beta$  cores from Tg2576 and APP23 Tg mice were completely soluble in SDS solutions containing EDTA [162]. In the  $\beta$ APP Tg mice, EDTA increased the solubility of A $\beta$  amyloid. APP23 Tg mice produced high levels of water-soluble A $\beta$ , amounting to over 50  $\mu$ g/g of brain tissue, that was apparent at the age of 2 months and persisted during the entire life of these Tg mice. No appreciable amount of posttranslational modification and N-terminal degradation has been measured in Tg mice and rats. Indeed, abundant structural alteration has been demonstrated in A $\beta$  plaques from AD, especially the alteration in aspartyl residue [163].

## 10. HUMAN PET IMAGING

Three radioligands, [<sup>11</sup>C]PIB, [<sup>11</sup>C]SB-13, and [<sup>18</sup>F]FDDNP, have reached clinical stage, and part of their PET imaging results have been reviewed recently [164].

**[<sup>11</sup>C]PIB.** [<sup>11</sup>C]PIB is the most thoroughly investigated PET radioligand for human A $\beta$  plaques. Klunk *et al.* [56] reported the human study of [<sup>11</sup>C]PIB in 16 patients with diagnosed mild AD and 9 controls (Fig. 6). For SUV [<sup>11</sup>C]PIB images summed over 40 to 60 min, the ratio of PIB retention in a number of brain areas of AD versus control were 1.94 fold ( $p = 0.0001$ ) in frontal cortex, 1.71 fold in parietal cortex ( $p = 0.0002$ ), 1.52 fold in temporal cortex ( $p =$

0.002), 1.54 fold in occipital cortex ( $p = 0.002$ ), 1.76 fold in striatum ( $p = 0.0001$ ), 1.08 fold in pons ( $p = 0.3563$ ), 1.03 in subcortical white matter ( $p = 0.7238$ ), and 1.17 fold in cerebellum ( $p = 0.0205$ ). The [<sup>11</sup>C]PIB retention matches the distribution of A $\beta$  deposits in post mortem studies of human AD brain [165-177], and correlates inversely with cerebral glucose metabolism determined with [<sup>18</sup>F]FDG, especially in parietal cortex area ( $r = -0.72$ ,  $p = 0.0001$ ) [178].

The most comprehensive model that was applied to the [<sup>11</sup>C]PIB data was a 3-tissue 6-parameter (3T-6k) configuration [179]. For specific binding areas, a 2-tissue compartment 4-parameter (2T-4k) model was applied assuming that free and nonspecific tracer kinetics were indistinguishable (Fig. 7). The distribution volume ratio (DVR) that is the regional DV value ( $DV_{ROI}$ ) normalized by the nonspecific retention in the reference region ( $DV_{REF}$ ) was significant for the PCG (posterior cingulate gyrus), PAR (parietal), LTC (lateral temporal), and FRT (frontal) regions before and after CSF (MR-based partial volume correction) correction, but not after FDR (false discovery rate) correction ( $p = 0.08$ ) [178]. The Logan graphical [180] and Ichise MA1 analyses [181] were also performed over the 35 to 90 min PET scan interval. The increase in [<sup>11</sup>C]PIB retention in AD subjects versus controls was evident in the tissue ratio data, the quantitative compartment modeling, and graphical analyses. This verifies that the specific binding differences were not likely results of plasma clearance or nonspecific effects.

**[<sup>11</sup>C]SB-13.** As shown above, SB-13 occupies the same binding site as PIB with comparable binding affinities (Kd of 2.4 nM vs. 1.4 nM in AD brain homogenates). Verhoeff *et al.* [182] studied [<sup>11</sup>C]SB-13 in comparison with [<sup>11</sup>C]PIB in AD patients and controls. A significantly higher retention of radioactivity in the frontal cortex of AD patients versus comparative controls was observed for both [<sup>11</sup>C]SB-13 and [<sup>11</sup>C]PIB. As in PIB case, the two-tissue compartment model  $DV_{2T}$  estimates were superior to the one-tissue compartment model  $DV_{1T}$  estimates for both AD patients and comparison subjects. The non-invasive Ichise Rv values [181] were dramatically increased in the AD patients versus controls in association cortex regions and striatum but not in other subcortical areas for both [<sup>11</sup>C]SB-13 and [<sup>11</sup>C]PIB. The significance of difference for Rv between AD patients and controls was quantitatively evaluated using Cohen's measure for effect size (the average value for AD patients minus the average value for comparison subjects divided by the pooled standard deviation) [183]. Effect sizes for Rv to discriminate AD patients from controls met heuristic "benchmark" criteria: 3.0 for five ROIs with a maximum of 6.07 (SB-13), and nine ROIs with a maximum of 5.91 (PIB).

**[<sup>18</sup>F]FDDNP.** [<sup>18</sup>F]FDDNP was the first PET radioligand put into human trial. Its binding site on A $\beta$  deposits differs from that of [<sup>11</sup>C]PIB or [<sup>11</sup>C]SB-13. [<sup>18</sup>F]FDDNP was also reported to bind to NFTs [75]. The brain regions with limited neuropathological lesions are pons, instead of cerebellum in A $\beta$  PET imaging. Shoghi-Jadid *et al.* [184] used a modified Logan plot approach to measure [<sup>18</sup>F]FDDNP localization in brain regions. They measured the relative residence time (RRT) of the radioligand in a target region relative to that in pons. The MMSE (Mini-Mental State Exam) scores were plotted against RRT values of the hippocampus-amygdala-

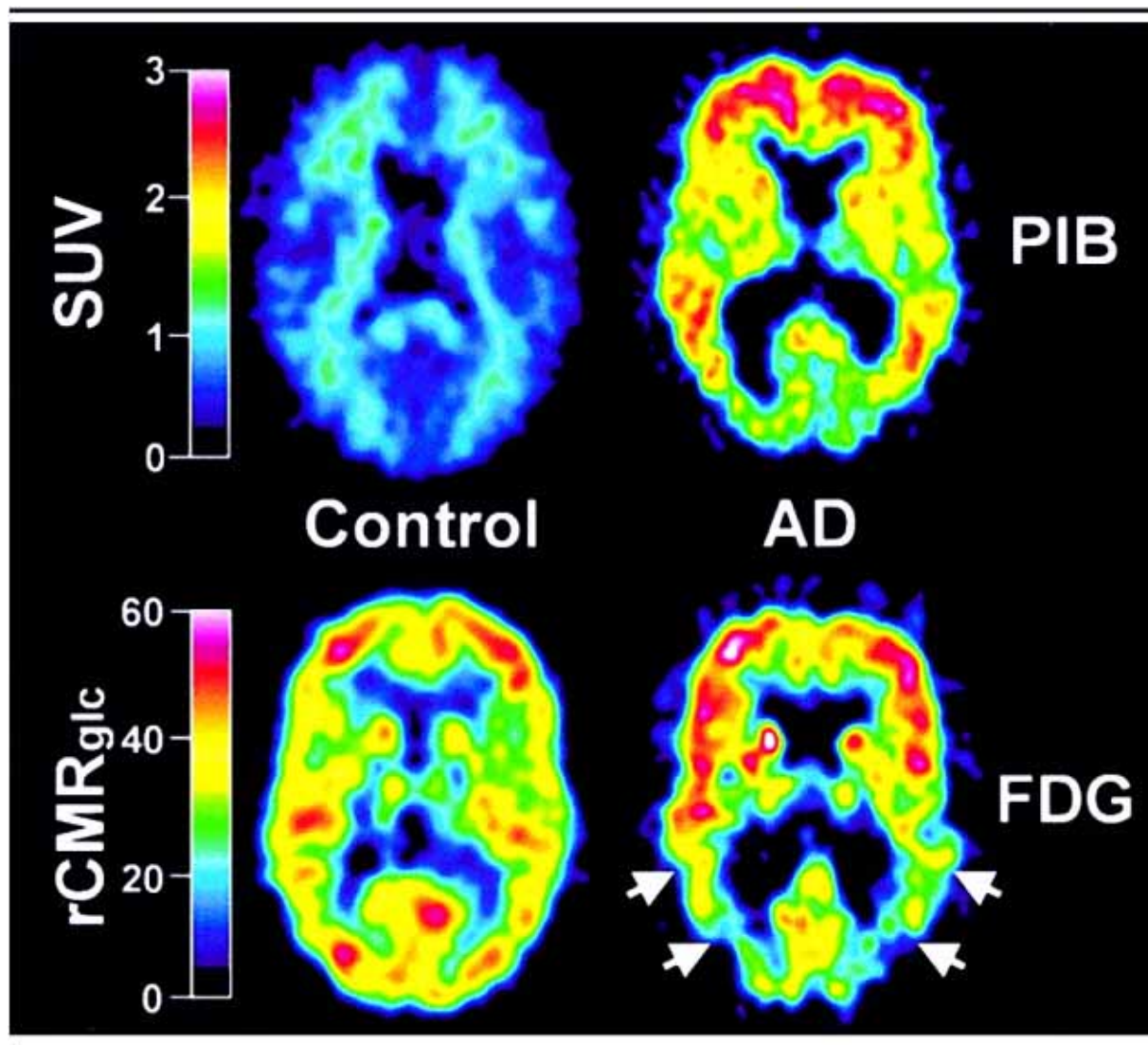


**Fig. (6).** [ $^{11}\text{C}$ ]PIB SUV images demonstrate a marked difference between PIB retention in AD patients and healthy control (HC) subjects. PET images of a 67-year-old HC subject (left) and a 79-year-old AD patient (AD6; MMSE = 21; right). (top) SUV [ $^{11}\text{C}$ ]PIB images summed over 40 to 60 min; (bottom)  $^{18}\text{F}$ FDG rCMR<sub>glc</sub> images ( $\mu\text{mol}/\text{min}/100\text{ ml}$ ). The left column shows lack of PIB retention in the entire gray matter of the HC subject (top left) and normal  $^{18}\text{F}$ FDG uptake (bottom left). Nonspecific [ $^{11}\text{C}$ ]PIB retention is seen in the white matter (top left). The right column shows high [ $^{11}\text{C}$ ]PIB retention in the frontal and temporoparietal cortices of the AD patient (top right) and a typical pattern of  $^{18}\text{F}$ FDG hypometabolism present in the temporoparietal cortex (arrows; bottom right) along with preserved metabolic rate in the frontal cortex. [ $^{11}\text{C}$ ]PIB and  $^{18}\text{F}$ FDG scans were obtained within 3 days of each other. Adapted by permission [56].

entorhinal regions, the highest RRT values in brain. There is a strong correlation between RRT and MMSE scores with a Spearman correlation coefficient  $r_s = -0.87$  (exact  $p < 0.0001$ ;  $n = 16$ ), as shown in Fig. 8.

In summary, there are three PET radioligands for A $\beta$  plaques and tangles for AD. For the first time these pathological lesions have been imaged in living brains. These radioligands are not optimal in any sense, but are a start for future development.

## 11. PERSPECTIVE AND FUTURE DEVELOPMENTS

Recent findings suggest that ADDLs are the primary lesions in AD brain [44,185]. Relatively stable forms of ADDLs from synthetic A $\beta$ 42 have been produced and reported [149]. Atomic force microscopy study of the A $\beta$ 42 fibrillogenesis *in vitro* has generated a model for the process (Fig. 9) [186].

Dimer, trimer, tetramer, and larger heterogeneous oligomers have been identified as SDS insoluble species. A

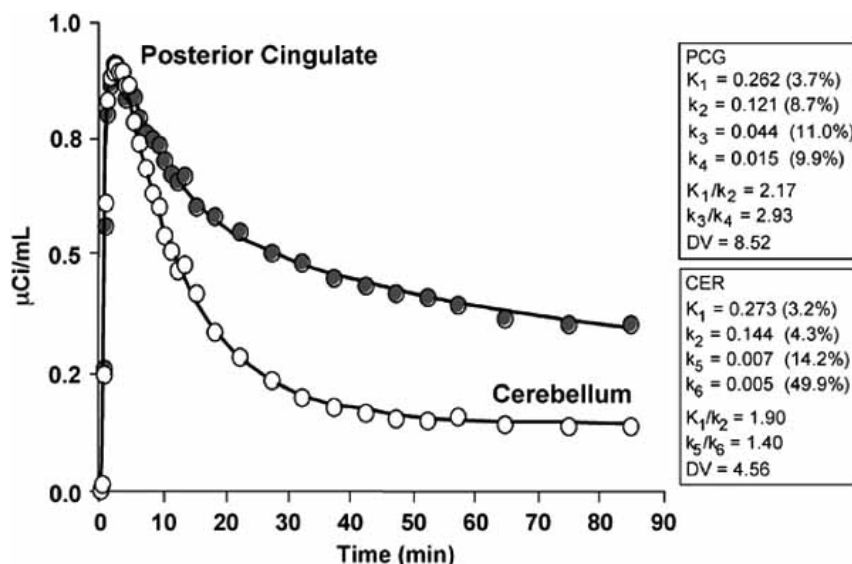


**Fig. (7).** Compartmental modeling results obtained using a 2-tissue compartment model (4 parameters, 2T-4k). The graph shows an example curve fit (solid line) to the posterior cingulate Pittsburgh Compound-B (PIB) data (gray circles) of an AD subject (AD-3, 15 mCi injection), along with the cerebellar data (white circles) for comparison. The kinetic parameters (standard errors) obtained for the posterior cingulate (specific binding:  $k_3$ ,  $k_4$ ) and cerebellar fits are listed in the text boxes. The regional data were generally well described by the 2T-4k model, across regions and subjects. Adapted by permission from Macmillan Publishers Ltd: J Cereb Blood Flow Metab (25: 1528-1547), copyright (2005) [178].

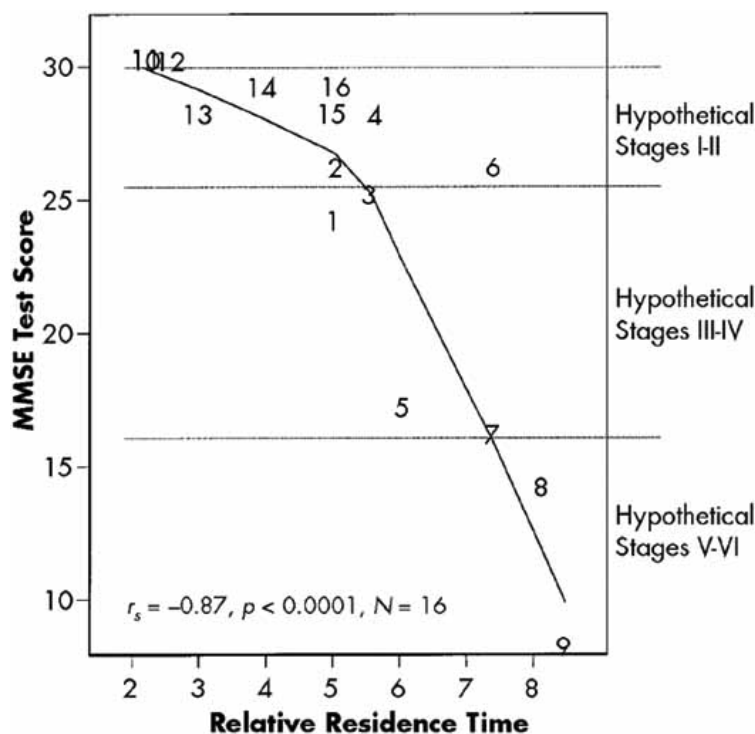


**Fig. (8).** Plot of Mini-Mental State Exam (MMSE) scores versus relative residence time (RRT) values. Note: the solid line represents the pseudo-saturation model fitted to these data. These data-points are plotted using the study numbers. RRT values of control subjects are localized at the apex of the saturation model. With increasing RRT, MMSE scores decrease. The Spearman correlation coefficient is  $r_s = -0.87$  (exact  $p < 0.0001$ ;  $n = 16$ ). When subjects diagnosed with possible AD are excluded from the analysis, the Spearman correlation value remains the same ( $r_s = -0.87$ ; exact  $p = 0.0001$ ;  $n = 14$ ). It is widely accepted that MMSE scores below 25 are indicative of AD. The dashed lines represent hypothetical staging of a brain region afflicted early in the evolution of AD. Under this hypothetical model, during the early stages, there is a greater sensitivity to "binding capacity" compared with later stages, at which point the region's resources have been exhausted. Note that both RRT and MMSE are functions of a continuous plaque density-distribution and that these values are samples from the joint distribution of Immediate Paragraph Recall (IPR), Delayed Figure Recall (DFR), relative residence time (RRT), and plaque density. The designations "AD" and "normal-control" are thus macro-labels used in the clinical setting. Adapted by permission [184].

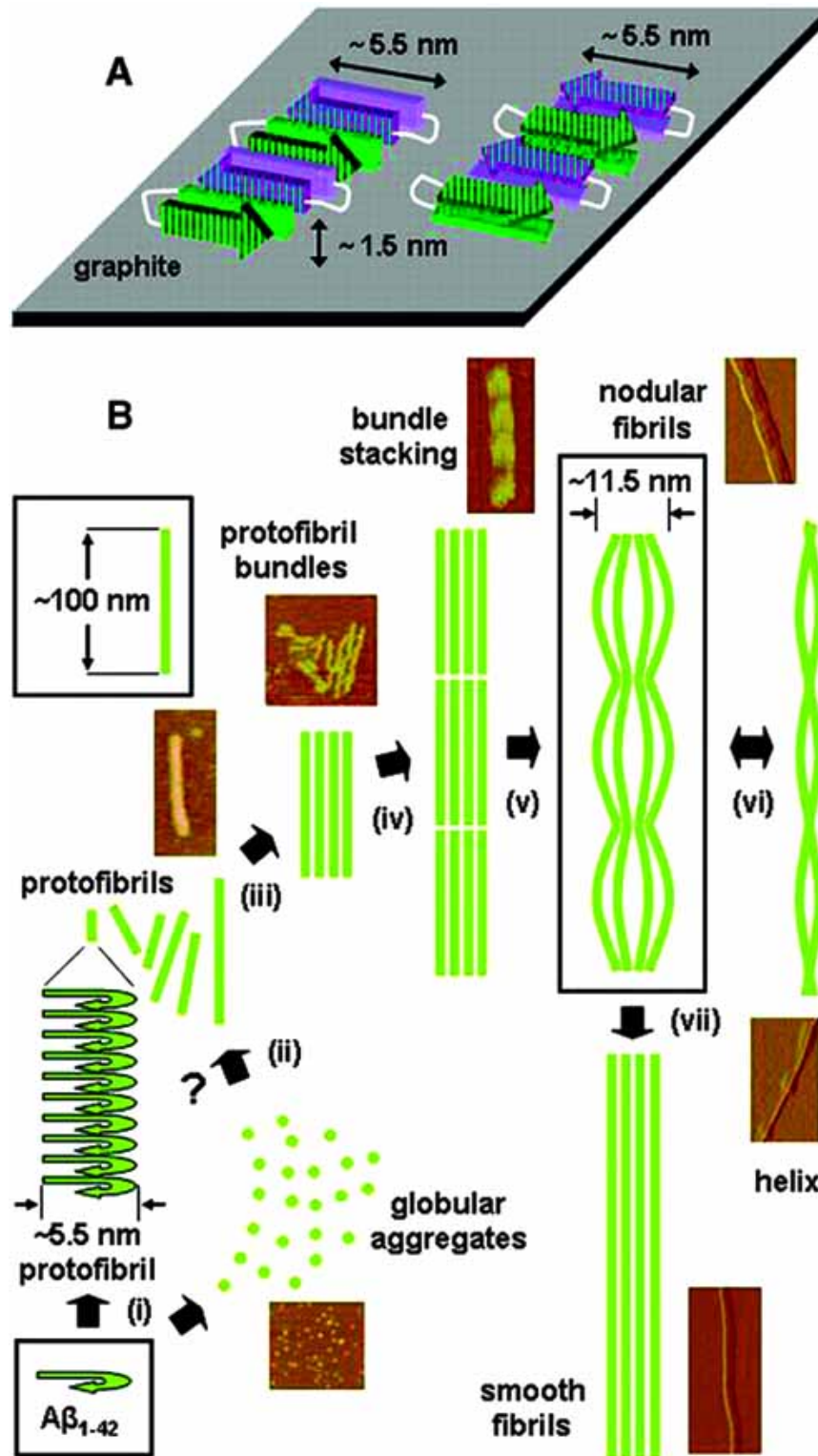


**Fig. (9).** Proposed model for  $A\beta_{42}$  fibrillogenesis *in vitro*. **A)** Cartoon illustrating two possible models for the formation of an  $A\beta_{42}$  protofibril on graphite. The height of the protofibril (~1.5 nm) is provided by the thickness of the peptide adopting a hairpin (for each model, 4 peptide molecules are represented), and the width of the protofibril (~5.5 nm) corresponds to the length of the hairpin. On the left scheme, both strands of the hairpin are in contact with the graphite, whereas on the right scheme only one strand of the hairpin is facing the surface. **B)** Schematic model proposal of the different stages in the amyloid fibril formation process: (i) monomeric  $A\beta_{42}$  associates to form protofibrils and globular oligomers; data presented here do not provide evidence for the incorporation of oligomers into growing protofibrils (ii); protofibrils that reach ~100 nm can form bundles (iii) that through end-to-end stacking (iv) generate the nodular type fibrils (v), which may be related to a helical structure formed by intertwined protofilaments (vi); finally, nodular fibrils might evolve further to yield smooth fibrils (vii). Adapted with permission [186].

new and highly stable A $\beta$  oligomer species has been prepared *in vitro* and is present in the brains of patients with AD and A $\beta$  overproducing Tg mice [187]. Physicochemical characterization reveals a pure, highly water-soluble globular 60 kDa oligomer named as "A $\beta$ 42 globulomer." The globulomer was demonstrated to be a persistent structural entity formed independently of the fibrillar aggregation pathway, and binds specifically to dendritic processes of neurons but not glia in hippocampal cell cultures and completely blocks long-term potentiation in rat hippocampal slices. This provides the basis for *in vitro* assay to evaluate and select proper radioligands to detect such species.

#### ACKNOWLEDGEMENT

This research was supported by the Intramural Research Program of the NIH, NIMH.

#### REFERENCES

- [1] Hebert, L. E.; Scherr, P. A.; Bienias, J. L.; Bennett, D. A.; Evans, D. A. *Arch. Neurol.* **2003**, *60*, 1119-1122.
- [2] Selkoe, D. J. *Ann. Intern. Med.* **2004**, *140*, 627-638.
- [3] Villemagne, V. L.; Rowe, C. C.; Macfarlane, S.; Novakovic, K. E.; Masters, C. L. *J. Clin. Neurosci.* **2005**, *12*, 221-230.
- [4] Selkoe, D. J. *Physiol. Rev.* **2001**, *81*, 741-766.
- [5] Cummings, J. L. *N. Engl. J. Med.* **2004**, *351*, 56-67.
- [6] Mosconi, L.; De Santi, S.; Rusinek, H.; Convit, A.; de Leon, M. J. *Expert. Rev. Neurother.* **2004**, *4*, 831-849.
- [7] Bertram, L.; Tanzi, R. E. *Curr. Neurol. Neurosci. Rep.* **2001**, *1*, 442-450.
- [8] Holmes, C. *Br. J. Psychiatry* **2002**, *180*, 131-134.
- [9] Holmes, C.; Lovestone, S. *Int. J. Geriatr. Psychiatry* **2002**, *17*, 146-149.
- [10] Corder, E. H.; Saunders, A. M.; Strittmatter, W. J.; Schmechel, D. E.; Gaskell, P. C.; Small, G. W.; Roses, A. D.; Haines, J. L.; Pericak-Vance, M. A. *Science* **1993**, *261*, 921-923.
- [11] Corder, E. H.; Woodbury, M. A. *Genet. Epidemiol.* **1993**, *10*, 495-499.
- [12] Mahley, R. W. *Science* **1988**, *240*, 622-630.
- [13] Igbavboa, U.; Hamilton, J.; Kim, H. Y.; Sun, G. Y.; Wood, W. G. *J. Neurochem.* **2002**, *80*, 255-261.
- [14] Boyles, J. K.; Pitas, R. E.; Wilson, E.; Mahley, R. W.; Taylor, J. M. *J. Clin. Invest.* **1985**, *76*, 1501-1513.
- [15] Pitas, R. E.; Boyles, J. K.; Lee, S. H.; Foss, D.; Mahley, R. W. *Biochim. Biophys. Acta* **1987**, *917*, 148-161.
- [16] Pitas, R. E.; Innerarity, T. L.; Weinstein, J. N.; Mahley, R. W. *Arteriosclerosis* **1981**, *1*, 177-185.
- [17] Holtzman, D. M. *J. Mol. Neurosci.* **2001**, *17*, 147-155.
- [18] Saunders, A. M.; Schmechel, K.; Breitner, J. C.; Benson, M. D.; Brown, W. T.; Goldfarb, L.; Goldgaber, D.; Manwaring, M. G.; Szymanski, M. H.; McCown, N. *Lancet* **1993**, *342*, 710-711.
- [19] Dekroon, R. M.; Armati, P. J. *Glia* **2001**, *33*, 298-305.
- [20] Carter, D. B.; Dunn, E.; McKinley, D. D.; Stratman, N. C.; Boyle, T. P.; Kuiper, S. L.; Oostveen, J. A.; Weaver, R. J.; Boller, J. A.; Gurney, M. E. *Ann. Neurol.* **2001**, *50*, 468-475.
- [21] Brendza, R. P.; Bales, K. R.; Paul, S. M.; Holtzman, D. M. *Mol. Psychiatry* **2002**, *7*, 132-135.
- [22] Nathan, B. P.; Jiang, Y.; Wong, G. K.; Shen, F.; Brewer, G. J.; Struble, R. G. *Brain Res.* **2002**, *928*, 96-105.
- [23] Veinbergs, I.; Everson, A.; Sagara, Y.; Masliah, E. *J. Neurosci. Res.* **2002**, *67*, 379-387.
- [24] Bertram, L.; Tanzi, R. E. *J. Mol. Neurosci.* **2001**, *17*, 127-136.
- [25] Tanzi, R. E.; Bertram, L. *Neuron* **2001**, *32*, 181-184.
- [26] Luna-Munoz, J.; Garcia-Sierra, F.; Falcon, V.; Menendez, I.; Chavez-Macias, L.; Mena, R. *J. Alzheimers. Dis.* **2005**, *8*, 29-41.
- [27] Fishel, M. A.; Watson, G. S.; Montine, T. J.; Wang, Q.; Green, P. S.; Kulstad, J. J.; Cook, D. G.; Peskind, E. R.; Baker, L. D.; Goldgaber, D.; Nie, W.; Asthana, S.; Plymate, S. R.; Schwartz, M. W.; Craft, S. *Arch. Neurol.* **2005**, *62*, 1539-1544.
- [28] Schliebs, R. *Neurochem. Res.* **2005**, *30*, 895-908.
- [29] Cardoso, S. M.; Santana, I.; Swerdlow, R. H.; Oliveira, C. R. *J. Neurochem.* **2004**, *89*, 1417-1426.
- [30] Swerdlow, R. H.; Khan, S. M. *Med. Hypotheses* **2004**, *63*, 8-20.
- [31] Trimmer, P. A.; Keeney, P. M.; Borland, M. K.; Simon, F. A.; Almeida, J.; Swerdlow, R. H.; Parks, J. P.; Parker, W. D. Jr.; Bennett, J. P., Jr. *Neurobiol. Dis.* **2004**, *15*, 29-39.
- [32] Humpel, C.; Marksteiner, J. *Curr. Neurovasc. Res.* **2005**, *2*, 341-347.
- [33] Naslund, J.; Haroutunian, V.; Mohs, R.; Davis, K. L.; Davies, P.; Greengard, P.; Buxbaum, J. D. *JAMA* **2000**, *283*, 1571-1577.
- [34] Mok, S. S.; Clippingdale, A. B.; Beyreuther, K.; Masters, C. L.; Barrow, C. J.; Small, D. H. *J. Neurosci. Res.* **2000**, *61*, 449-457.
- [35] Miller, L. M.; Wang, Q.; Telivala, T. P.; Smith, R. J.; Lanzirrotti, A.; Miklossy, J. *J. Struct. Biol.* **2006**, *155*, 30-37.
- [36] da Silva, G. F.; Ming, L. J. *Angew. Chem. Int. Ed. Engl.* **2005**, *44*, 5501-5504.
- [37] da Silva, G. F.; Tay, W. M.; Ming, L. J. *J. Biol. Chem.* **2005**, *280*, 16601-16609.
- [38] Palavicini, S.; Granata, A.; Monzani, E.; Casella, L. *J. Am. Chem. Soc.* **2005**, *127*, 18031-18036.
- [39] Solomon, E. I.; Sundaram, U. M.; Machonkin, T. E. *Chemical Reviews* **1996**, *96*, 2563-2605.
- [40] Barnham, K. J.; McKinstry, W. J.; Multhaup, G.; Galatis, D.; Morton, C. J.; Curtain, C. C.; Williamson, N. A.; White, A. R.; Hinds, M. G.; Norton, R. S.; Beyreuther, K.; Masters, C. L.; Parker, M. W.; Cappai, R. *J. Biol. Chem.* **2003**, *278*, 17401-17407.
- [41] Bayer, T. A.; Schafer, S.; Simons, A.; Kemmling, A.; Kamer, T.; Tepest, R.; Eckert, A.; Schussel, K.; Eikenberg, O.; Sturchler-Pierrat, C.; Abramowski, D.; Staufenbiel, M.; Multhaup, G. *Proc. Natl. Acad. Sci. USA* **2003**, *100*, 14187-14192.
- [42] Liu, B.; Hong, J. S. *J. Pharmacol. Exp. Ther.* **2003**, *304*, 1-7.
- [43] Marchesi, V. T. *Proc. Natl. Acad. Sci. USA* **2005**, *102*, 9093-9098.
- [44] Klein, W. L.; Krafft, G. A.; Finch, C. E. *Trends Neurosci.* **2001**, *24*, 219-224.
- [45] McLean, C. A.; Cherny, R. A.; Fraser, F. W.; Fuller, S. J.; Smith, M. J.; Beyreuther, K.; Bush, A. I.; Masters, C. L. *Ann. Neurol.* **1999**, *46*, 860-866.
- [46] Lue, L. F.; Kuo, Y. M.; Roher, A. E.; Brachova, L.; Shen, Y.; Sue, L.; Beach, T.; Kurth, J. H.; Rydel, R. E.; Rogers, J. *Am. J. Pathol.* **1999**, *155*, 853-862.
- [47] Mucke, L.; Masliah, E.; Yu, G. Q.; Mallory, M.; Rockenstein, E. M.; Tatsuno, G.; Hu, K.; Kholodenko, D.; Johnson-Wood, K.; McConlogue, L. *J. Neurosci.* **2000**, *20*, 4050-4058.
- [48] Lee, B. C.; Mintun, M.; Buckner, R. L.; Morris, J. C. *J. Neuroimaging* **2003**, *13*, 199-214.
- [49] Small, G. W. *CNS. Spectr.* **2004**, *9*, 20-23.
- [50] Zamrini, E.; De Santi, S.; Tolar, M. *Neurobiol. Aging* **2004**, *25*, 685-691.
- [51] Mosconi, L.; Tsui, W. H.; De Santi, S.; Li, J.; Rusinek, H.; Convit, A.; Li, Y.; Boppana, M.; de Leon, M. J. *Neurology* **2005**, *64*, 1860-1867.
- [52] Mosconi, L. *Eur. J. Nucl. Med. Mol. Imaging* **2005**, *32*, 486-510.
- [53] Herholz, K.; Heiss, W. D. *Mol. Imaging Biol.* **2004**, *6*, 239-269.
- [54] Mathis, C. A.; Klunk, W. E.; Price, J. C.; DeKosky, S. T. *Arch. Neurol.* **2005**, *62*, 196-200.
- [55] Mathis, C. A.; Wang, Y.; Klunk, W. E. *Curr. Pharm. Des.* **2004**, *10*, 1469-1492.
- [56] Klunk, W. E.; Engler, H.; Nordberg, A.; Wang, Y.; Blomqvist, G.; Holt, D. P.; Bergstrom, M.; Savitcheva, I.; Huang, G. F.; Estrada, S.; Ausen, B.; Debnath, M. L.; Barletta, J.; Price, J. C.; Sandell, J.; Lopresti, B. J.; Wall, A.; Koivisto, P.; Antoni, G.; Mathis, C. A.; Langstrom, B. *Ann. Neurol.* **2004**, *55*, 306-319.
- [57] Nordberg, A. *Lancet Neurol.* **2004**, *3*, 519-527.
- [58] Nordberg, A. *Eur. J. Nucl. Med. Mol. Imaging* **2004**, *31*, 1540-1543.
- [59] Klunk, W. E.; Engler, H.; Nordberg, A.; Bacskai, B. J.; Wang, Y.; Price, J. C.; Bergstrom, M.; Hyman, B. T.; Langstrom, B.; Mathis, C. A. *Neuroimaging Clin. N. Am.* **2003**, *13*, 781-9, ix.
- [60] Sair, H. I.; Doraiswamy, P. M.; Petrella, J. R. *Neuroradiology* **2004**, *46*, 93-104.
- [61] Schmidt, B.; Braun, H. A.; Narlawar, R. *Curr. Med. Chem.* **2005**, *12*, 1677-1695.
- [62] Desai, A. K.; Grossberg, G. T. *Neurology* **2005**, *64*, S34-S39.
- [63] Pike, V. W. *J. Psychopharmacology* **1993**, *7*, 139-158.

- [64] Zhuang, Z. P.; Kung, M. P.; Hou, C.; Skovronsky, D. M.; Gur, T. L.; Plossl, K.; Trojanowski, J. Q.; Lee, V. M.; Kung, H. F. *J. Med. Chem.* **2001**, *44*, 1905-1914.
- [65] Kung, M. P.; Hou, C.; Zhuang, Z. P.; Skovronsky, D.; Kung, H. F. *Brain Res* **2004**, *1025*, 98-105.
- [66] Suemoto, T.; Okamura, N.; Shiomitsu, T.; Suzuki, M.; Shimadzu, H.; Akatsu, H.; Yamamoto, T.; Kudo, Y.; Sawada, T. *Neurosci. Res.* **2004**, *48*, 65-74.
- [67] Lockhart, A.; Ye, L.; Judd, D. B.; Merritt, A. T.; Lowe, P. N.; Morgenstern, J. L.; Hong, G.; Gee, A. D.; Brown, J. *J. Biol. Chem.* **2005**, *280*, 7677-7684.
- [68] Agdeppa, E. D.; Kepe, V.; Liu, J.; Flores-Torres, S.; Satyamurthy, N.; Petric, A.; Cole, G. M.; Small, G. W.; Huang, S. C.; Barrio, J. R. *J. Neurosci.* **2001**, *21*, RC189.
- [69] Klunk, W. E.; Debnath, M. L.; Pettegrew, J. W. *Neurobiol. Aging* **1995**, *16*, 541-548.
- [70] Lee, C. W.; Zhuang, Z. P.; Kung, M. P.; Plossl, K.; Skovronsky, D.; Gur, T.; Hou, C.; Trojanowski, J. Q.; Lee, V. M.; Kung, H. F. *J. Med. Chem.* **2001**, *44*, 2270-2275.
- [71] Zhen, W.; Han, H.; Anguiano, M.; Lemere, C. A.; Cho, C. G.; Lansbury, P. T., Jr. *J. Med. Chem.* **1999**, *42*, 2805-2815.
- [72] Klunk, W. E.; Bacskai, B. J.; Mathis, C. A.; Kajdasz, S. T.; McLellan, M. E.; Frosch, M. P.; Debnath, M. L.; Holt, D. P.; Wang, Y.; Hyman, B. T. *J. Neuropathol. Exp. Neurol.* **2002**, *61*, 797-805.
- [73] Ashburn, T. T.; Han, H.; McGuinness, B. F.; Lansbury, P. T., Jr. *Chem. Biol.* **1996**, *3*, 351-358.
- [74] Wang, Y. M.; Mathis, C. A.; Huang, G. F.; Holt, D. P.; Debnath, M. L.; Klunk, W. E. *J. Labelled Comp. Radiopharm.* **2002**, *45*, 647-664.
- [75] Agdeppa, E. D.; Kepe, V.; Liu, J.; Small, G. W.; Huang, S. C.; Petric, A.; Satyamurthy, N.; Barrio, J. R. *Mol. Imaging Biol.* **2003**, *5*, 404-417.
- [76] Kung, H. F.; Lee, C. W.; Zhuang, Z. P.; Kung, M. P.; Hou, C.; Plossl, K. *J. Am. Chem. Soc.* **2001**, *123*, 12740-12741.
- [77] Zhuang, Z. P.; Kung, M. P.; Hou, C.; Plossl, K.; Skovronsky, D.; Gur, T. L.; Trojanowski, J. Q.; Lee, V. M.; Kung, H. F. *Nucl. Med. Biol.* **2001**, *28*, 887-894.
- [78] Ono, K.; Noguchi, M.; Matsumoto, Y.; Yanase, D.; Iwasa, K.; Naiki, H.; Yamada, M. *Neurobiol. Dis.* **2005**, *20*, 233-240.
- [79] Wang, Y.; Mathis, C. A.; Huang, G. F.; Debnath, M. L.; Holt, D. P.; Shao, L.; Klunk, W. E. *J. Mol. Neurosci.* **2003**, *20*, 255-260.
- [80] Klunk, W. E.; Wang, Y.; Huang, G. F.; Debnath, M. L.; Holt, D. P.; Mathis, C. A. *Life Sci.* **2001**, *69*, 1471-1484.
- [81] Mathis, C. A.; Bacskai, B. J.; Kajdasz, S. T.; McLellan, M. E.; Frosch, M. P.; Hyman, B. T.; Holt, D. P.; Wang, Y.; Huang, G. F.; Debnath, M. L.; Klunk, W. E. *Bioorg. Med. Chem. Lett.* **2002**, *12*, 295-298.
- [82] Mathis, C. A.; Wang, Y.; Holt, D. P.; Huang, G. F.; Debnath, M. L.; Klunk, W. E. *J. Med. Chem.* **2003**, *46*, 2740-2754.
- [83] Mathis, C. A.; Holt, D. P.; Wang, Y.; Huang, G. F.; Debnath, M. L.; Klunk, W. E. *Soc. Nucl. Med.* **2002**, Abstract No. 605.
- [84] Wilson, A. A.; Nobrega, J.; Houle, S.; Westaway, D.; Verhoeff, N. P. L. G.; Zhuang, Z. P.; Kung, M. P.; Kung, H. F. *J. Labelled Comp. Radiopharm.* **2003**, *45*, S61.
- [85] Zhang, W.; Oya, S.; Kung, M. P.; Hou, C.; Maier, D. L.; Kung, H. F. *J. Med. Chem.* **2005**, *48*, 5980-5988.
- [86] Mathis, C. A.; Wang, Y.; Holt, D. P.; Huang, G. F.; Shao, L.; Debnath, M. L.; Klunk, W. E. *J. Labelled Comp. Radiopharm.* **2003**, *46*, S62.
- [87] Wang, Y.; Klunk, W. E.; Huang, G. F.; Debnath, M. L.; Holt, D. P.; Mathis, C. A. *J. Mol. Neurosci.* **2002**, *19*, 11-16.
- [88] Wang, Y.; Klunk, W. E.; Debnath, M. L.; Huang, G. F.; Holt, D. P.; Shao, L.; Mathis, C. A. *J. Mol. Neurosci.* **2004**, *24*, 55-62.
- [89] Klunk, W. E.; Wang, Y.; Huang, G. F.; Debnath, M. L.; Holt, D. P.; Mathis, C. A. *Life Sci.* **2001**, *69*, 1471-1484.
- [90] Mathis, C. A.; Holt, D. P.; Wang, Y.; Huang, G. F.; Debnath, M. L.; Klunk, W. E. *J. Labelled Comp. Radiopharm.* **2001**, *44*, S26-S28.
- [91] Klunk, W. E.; Wang, Y.; Huang, G. F.; Debnath, M. L.; Holt, D. P.; Mathis, C. A. *Life Sci.* **2001**, *69*, 1471-1484.
- [92] Klunk, W. E.; Wang, Y.; Huang, G. F.; Debnath, M. L.; Holt, D. P.; Mathis, C. A. *Life Sci.* **2001**, *69*, 1471-1484.
- [93] Klunk, W. E.; Wang, Y.; Huang, G. F.; Debnath, M. L.; Holt, D. P.; Mathis, C. A. *Life Sci.* **2001**, *69*, 1471-1484.
- [94] Zhuang, Z. P.; Kung, M. P.; Hou, C.; Lee, C. W.; Trojanowski, J. Q.; Lee, V. M. Y.; Kung, H. F. *J. Labelled Comp. Radiopharm.* **2001**, *44*, S29-S32.
- [95] Kung, H. F.; Kung, M. P.; Zhuang, Z. P. Amyloid plaque aggregation inhibitors and diagnostic imaging agents. PCT Int. Appl. (WO 2002085903). 2002. Ref. Type: Patent.
- [96] Kung, M. P.; Hou, C.; Zhuang, Z. P.; Zhang, B.; Skovronsky, D.; Trojanowski, J. Q.; Lee, V. M.; Kung, H. F. *Brain Res.* **2002**, *956*, 202-210.
- [97] Kung, H. F. *Society of Nuclear Medicine* **2002**, Abstract No. 1451.
- [98] Ono, M.; Kung, M. P.; Hou, C.; Kung, H. F. *Nucl. Med. Biol.* **2002**, *29*, 633-642.
- [99] Ono, M.; Wilson, A.; Nobrega, J.; Westaway, D.; Verhoeff, P.; Zhuang, Z. P.; Kung, M. P.; Kung, H. F. *Nucl. Med. Biol.* **2003**, *30*, 565-571.
- [100] Kung, H. F. *Society of Nuclear Medicine* **2002**, Abstract No. 1442.
- [101] Kung, H. F.; Zhuang, Z. P.; Kung, M. P.; Hou, C. *J. Labelled Comp. Radiopharm.* **2003**, *46*, S150.
- [102] Ono, M.; Haratake, M.; Nakayama, M.; Kaneko, Y.; Kawabata, K.; Mori, H.; Kung, M. P.; Kung, H. F. *Nucl. Med. Biol.* **2005**, *32*, 329-335.
- [103] Okamura, N.; Suemoto, T.; Shimadzu, H.; Suzuki, M.; Shiomitsu, T.; Akatsu, H.; Yamamoto, T.; Staufenbiel, M.; Yanai, K.; Arai, H.; Sasaki, H.; Kudo, Y.; Sawada, T. *J. Neurosci.* **2004**, *24*, 2535-2541.
- [104] Okamura, N.; Suemoto, T.; Shiomitsu, T.; Suzuki, M.; Shimadzu, H.; Akatsu, H.; Yamamoto, T.; Arai, H.; Sasaki, H.; Yanai, K.; Staufenbiel, M.; Kudo, Y.; Sawada, T. *J. Mol. Neurosci.* **2004**, *24*, 247-255.
- [105] Kung, M. P.; Zhuang, Z. P.; Hou, C.; Jin, L. W.; Kung, H. F. *J. Mol. Neurosci.* **2003**, *20*, 249-254.
- [106] Lee, C. W.; Kung, M. P.; Hou, C.; Kung, H. F. *Nucl. Med. Biol.* **2003**, *30*, 573-580.
- [107] Nesterov, E. E.; Skoch, J.; Hyman, B. T.; Klunk, W. E.; Bacskai, B. J.; Swager, T. M. *Angew. Chem. Int. Ed Engl.* **2005**, *44*, 5452-5456.
- [108] Klunk, W. E.; Wang, Y.; Huang, G. F.; Debnath, M. L.; Holt, D. P.; Shao, L.; Hamilton, R. L.; Ikonovic, M. D.; DeKosky, S. T.; Mathis, C. A. *J. Neurosci.* **2003**, *23*, 2086-2092.
- [109] Cai, L.; Chin, F. T.; Pike, V. W.; Toyama, H.; Liow, J. S.; Zoghbi, S. S.; Modell, K.; Briard, E.; Shetty, H. U.; Sinclair, K.; Donohue, S.; Tipre, D.; Kung, M. P.; Dagostin, C.; Widdowson, D. A.; Green, M.; Gao, W.; Herman, M. M.; Ichise, M.; Innis, R. B. *J. Med. Chem.* **2004**, *47*, 2208-2218.
- [110] Kung, H. F. *Soc. Nucl. Med.* **2002**, Abstract No. 603.
- [111] Kung, M. P.; Hou, C.; Zhuang, Z. P.; Cross, A. J.; Maier, D. L.; Kung, H. F. *Eur. J. Nucl. Med. Mol. Imaging* **2004**, *31*, 1136-1145.
- [112] Zhuang, Z. P.; Kung, M. P.; Wilson, A.; Lee, C. W.; Plossl, K.; Hou, C.; Holtzman, D. M.; Kung, H. F. *J. Med. Chem.* **2003**, *46*, 237-243.
- [113] Agdeppa, E. D.; Kepe, V.; Petric, A.; Liu, J.; Satyamurthy, N.; Shoghi-Jadid, K.; Small, G. W.; Huang, S. C.; Barrio, J. R. *Soc. Nucl. Med.* **2002**, Abstract No. 604.
- [114] Agdeppa, E. D.; Kepe, V.; Petric, A.; Satyamurthy, N.; Liu, J.; Huang, S. C.; Small, G. W.; Cole, G. M.; Barrio, J. R. *Neuroscience* **2003**, *117*, 723-730.
- [115] Klunk, W. E.; Wang, Y.; Huang, G. F.; Debnath, M. L.; Holt, D. P.; Mathis, C. A. *Life Sci.* **2001**, *69*, 1471-1484.
- [116] Shimadzu, H.; Suemoto, T.; Suzuki, M.; Shiomitsu, T.; Okamura, N.; Kudo, Y.; Sawada, T. *J. Labelled Comp. Radiopharm.* **2003**, *46*, 765-772.
- [117] Laruelle, M.; Slifstein, M.; Huang, Y. *Mol. Imaging Biol.* **2003**, *5*, 363-375.
- [118] Lovestone, S.; McLoughlin, D. M. *J. Neurol. Neurosurg. Psychiatry* **2002**, *72*, 152-161.
- [119] Glenner, G. G.; Wong, C. W. *Biochem. Biophys. Res Commun.* **1984**, *120*, 885-890.
- [120] Glenner, G. G.; Wong, C. W. *Biochem. Biophys. Res Commun.* **1984**, *122*, 1131-1135.

- [121] Iwatsubo, T.; Odaka, A.; Suzuki, N.; Mizusawa, H.; Nukina, N.; Ihara, Y. *Neuron* **1994**, *13*, 45-53.
- [122] Stromer, T.; Serpell, L. C. *Microsc. Res. Tech.* **2005**, *67*, 210-217.
- [123] Sunde, M.; Serpell, L. C.; Bartlam, M.; Fraser, P. E.; Pepys, M. B.; Blake, C. C. *J. Mol. Biol.* **1997**, *273*, 729-739.
- [124] Sunde, M.; Blake, C. *Adv. Protein Chem.* **1997**, *50*, 123-159.
- [125] Inouye, H.; Fraser, P. E.; Kirschner, D. A. *Biophys. J.* **1993**, *64*, 502-519.
- [126] Harper, J. D.; Lieber, C. M.; Lansbury, P. T., Jr. *Chem. Biol.* **1997**, *4*, 951-959.
- [127] Harper, J. D.; Wong, S. S.; Lieber, C. M.; Lansbury, P. T. *Chem. Biol.* **1997**, *4*, 119-125.
- [128] Harper, J. D.; Lansbury, P. T., Jr. *Annu. Rev. Biochem.* **1997**, *66*, 385-407.
- [129] Walsh, D. M.; Lomakin, A.; Benedek, G. B.; Condron, M. M.; Teplow, D. B. *J. Biol. Chem.* **1997**, *272*, 22364-22372.
- [130] Nelson, R.; Sawaya, M. R.; Balbirnie, M.; Madsen, A. O.; Riekel, C.; Grothe, R.; Eisenberg, D. *Nature* **2005**, *435*, 773-778.
- [131] Benzinger, T. L.; Gregory, D. M.; Burkoth, T. S.; Miller-Auer, H.; Lynn, D. G.; Botto, R. E.; Meredith, S. C. *Proc. Natl. Acad. Sci. USA* **1998**, *95*, 13407-13412.
- [132] Benzinger, T. L.; Gregory, D. M.; Burkoth, T. S.; Miller-Auer, H.; Lynn, D. G.; Botto, R. E.; Meredith, S. C. *Biochemistry* **2000**, *39*, 3491-3499.
- [133] Gregory, D. M.; Benzinger, T. L.; Burkoth, T. S.; Miller-Auer, H.; Lynn, D. G.; Meredith, S. C.; Botto, R. E. *Solid State Nucl. Magn. Reson.* **1998**, *13*, 149-166.
- [134] Antzutkin, O. N.; Balbach, J. J.; Leapman, R. D.; Rizzo, N. W.; Reed, J.; Tycko, R. *Proc. Natl. Acad. Sci. USA* **2000**, *97*, 13045-13050.
- [135] Balbach, J. J.; Ishii, Y.; Antzutkin, O. N.; Leapman, R. D.; Rizzo, N. W.; Dyda, F.; Reed, J.; Tycko, R. *Biochemistry* **2000**, *39*, 13748-13759.
- [136] Lansbury, P. T., Jr.; Costa, P. R.; Griffiths, J. M.; Simon, E. J.; Auger, M.; Halverson, K. J.; Kocisko, D. A.; Hendsch, Z. S.; Ashburn, T. T.; Spencer, R. G.; *Nat. Struct. Biol.* **1995**, *2*, 990-998.
- [137] Chan, J. C.; Oyler, N. A.; Yau, W. M.; Tycko, R. *Biochemistry* **2005**, *44*, 10669-10680.
- [138] Balbach, J. J.; Petkova, A. T.; Oyler, N. A.; Antzutkin, O. N.; Gordon, D. J.; Meredith, S. C.; Tycko, R. *Biophys. J.* **2002**, *83*, 1205-1216.
- [139] Petkova, A. T.; Ishii, Y.; Balbach, J. J.; Antzutkin, O. N.; Leapman, R. D.; Delaglio, F.; Tycko, R. *Proc. Natl. Acad. Sci. USA* **2002**, *99*, 16742-16747.
- [140] Antzutkin, O. N.; Balbach, J. J.; Tycko, R. *Biophys. J.* **2003**, *84*, 3326-3335.
- [141] Oyler, N. A.; Tycko, R. *J. Am. Chem. Soc.* **2004**, *126*, 4478-4479.
- [142] Petkova, A. T.; Leapman, R. D.; Guo, Z.; Yau, W. M.; Mattson, M. P.; Tycko, R. *Science* **2005**, *307*, 262-265.
- [143] Tycko, R. *Biochemistry* **2003**, *42*, 3151-3159.
- [144] Burkoth, T. S.; Benzinger, T. L. S.; Urban, V.; Morgan, D. M.; Gregory, D. M.; Thiyagarajan, P.; Botto, R. E.; Meredith, S. C.; Lynn, D. G. *J. Am. Chem. Soc.* **2000**, *122*, 7883-7889.
- [145] Antzutkin, O. N.; Leapman, R. D.; Balbach, J. J.; Tycko, R. *Biochemistry* **2002**, *41*, 15436-15450.
- [146] Gordon, D. J.; Balbach, J. J.; Tycko, R.; Meredith, S. C. *Biophys. J.* **2004**, *86*, 428-434.
- [147] Petkova, A. T.; Buntkowsky, G.; Dyda, F.; Leapman, R. D.; Yau, W. M.; Tycko, R. *J. Mol. Biol.* **2004**, *335*, 247-260.
- [148] Masuda, Y.; Irie, K.; Murakami, K.; Ohigashi, H.; Ohashi, R.; Takegoshi, K.; Shimizu, T.; Shirasawa, T. *Bioorg. Med. Chem.* **2005**, *13*, 6803-6809.
- [149] Lambert, M. P.; Barlow, A. K.; Chromy, B. A.; Edwards, C.; Freed, R.; Liosatos, M.; Morgan, T. E.; Rozovsky, I.; Trommer, B.; Viola, K. L.; Wals, P.; Zhang, C.; Finch, C. E.; Krafft, G. A.; Klein, W. L. *Proc. Natl. Acad. Sci. USA* **1998**, *95*, 6448-6453.
- [150] Mathura, V. S.; Paris, D.; Ait-Ghezala, G.; Quadros, A.; Patel, N. S.; Kolippakkam, D. N.; Volmar, C. H.; Mullan, M. J. *Biochem. Biophys. Res. Commun.* **2005**, *332*, 585-592.
- [151] Hiramatsu, H.; Kitagawa, T. *Biochim. Biophys. Acta* **2005**, *1753*, 100-107.
- [152] Wang, J.; Gulich, S.; Bradford, C.; Ramirez-Alvarado, M.; Regan, L. *Structure. (Camb.)* **2005**, *13*, 1279-1288.
- [153] Sturchler-Pierrat, C.; Abramowski, D.; Duke, M.; Wiederhold, K. H.; Mistl, C.; Rothacher, S.; Ledermann, B.; Burki, K.; Frey, P.; Paganetti, P. A.; Waridel, C.; Calhoun, M. E.; Jucker, M.; Probst, A.; Staufenbiel, M.; Sommer, B. *Proc. Natl. Acad. Sci. USA* **1997**, *94*, 13287-13292.
- [154] Hsiao, K.; Chapman, P.; Nilsen, S.; Eckman, C.; Harigaya, Y.; Younkin, S.; Yang, F.; Cole, G. *Science* **1996**, *274*, 99-102.
- [155] Matsuo, Y.; Picciano, M.; Malester, B.; LaFrancois, J.; Zehr, C.; Daeschner, J. M.; Olschowka, J. A.; Fonseca, M. I.; O'Banion, M. K.; Tenner, A. J.; Lemere, C. A.; Duff, K. *Am. J. Pathol.* **2001**, *158*, 1345-1354.
- [156] Chishti, M. A.; Yang, D. S.; Janus, C.; Phinney, A. L.; Horne, P.; Pearson, J.; Strome, R.; Zuker, N.; Loukides, J.; French, J.; Turner, S.; Lozza, G.; Grilli, M.; Kunicki, S.; Morissette, C.; Paquette, J.; Gervais, F.; Bergeron, C.; Fraser, P. E.; Carlson, G. A.; George-Hyslop, P. S.; Westaway, D. *J. Biol. Chem.* **2001**, *276*, 21562-21570.
- [157] Kepe, V.; Cole, G. M.; Liu, J.; Flood, D. G.; Trusko, S. P.; Satyamurthy, N.; Huang, S. -C.; Small, G. W.; Petric, A.; Phelps, M. E.; Barrio, J. R. *J. Label. Compd. Radiopharm.* **2005**, *48*, S43.
- [158] Toyama, H.; Ye, D.; Ichise, M.; Liow, J. S.; Cai, L.; Jacobowitz, D.; Musachio, J. L.; Hong, J.; Crescenzo, M.; Tipre, D.; Lu, J. Q.; Zoghbi, S.; Vines, D. C.; Seidel, J.; Katada, K.; Green, M. V.; Pike, V. W.; Cohen, R. M.; Innis, R. B. *Eur. J. Nucl. Med. Mol. Imaging* **2005**, *32*, 593-600.
- [159] Klunk, W. E.; Lopresti, B. J.; Debnath, M. L.; Holt, D. P.; Wang, Y.; Huang, G. -F.; Shao, L.; Lefterov, I.; Koldamova, R.; Ikonovic, M.; DeKosky, S. T.; Mathis, C. A. *Neurobiol. Aging* **2004**, *25*, 232-233.
- [160] Klunk, W. E.; Lopresti, B. J.; Ikonovic, M. D.; Lefterov, I. M.; Koldamova, R. P.; Abrahamson, E. E.; Debnath, M. L.; Holt, D. P.; Huang, G. F.; Shao, L.; DeKosky, S. T.; Price, J. C.; Mathis, C. A. *J. Neurosci.* **2005**, *25*, 10598-10606.
- [161] Selkoe, D. J.; Abraham, C. R.; Podlisny, M. B.; Duffy, L. K. *J. Neurochem.* **1986**, *46*, 1820-1834.
- [162] Kalback, W.; Watson, M. D.; Kokjohn, T. A.; Kuo, Y. M.; Weiss, N.; Luehrs, D. C.; Lopez, J.; Brune, D.; Sisodia, S. S.; Staufenbiel, M.; Emmerling, M.; Roher, A. E. *Biochemistry* **2002**, *41*, 922-928.
- [163] Roher, A. E. *J. Biol. Chem.* **1993**, *268*, 3072-3083.
- [164] Wei, J.; Wu, C.; Lankin, D.; Gulrati, A.; Valyi-Nagy, T.; Cochran, E.; Pike, V. W.; Kozikowski, A.; Wang, Y. *Curr. Alzheimer Res* **2005**, *2*, 109-114.
- [165] Wolf, D. S.; Gearing, M.; Snowdon, D. A.; Mori, H.; Markesbery, W. R.; Mirra, S. S. *Alzheimer Dis. Assoc. Disord.* **1999**, *13*, 226-231.
- [166] Brilliant, M. J.; Elble, R. J.; Ghobrial, M.; Struble, R. G. *Neuropathol. Appl. Neurobiol.* **1997**, *23*, 322-325.
- [167] Suenaga, T.; Hirano, A.; Llena, J. F.; Yen, S. H.; Dickson, D. W. *Acta Neuropathol. (Berl)* **1990**, *80*, 280-286.
- [168] Suenaga, T.; Hirano, A.; Llena, J. F.; Ksiezak-Reding, H.; Yen, S. H.; Dickson, D. W. *J. Neuropathol. Exp. Neurol.* **1990**, *49*, 31-40.
- [169] Braak, H.; Braak, E. *Acta Neuropathol. (Berl)* **1991**, *82*, 239-259.
- [170] Braak, H.; Braak, E. *J. Neuropathol. Exp. Neurol.* **1990**, *49*, 215-224.
- [171] Braak, H.; Braak, E. *Acta Neuropathol. (Berl)* **1990**, *80*, 479-486.
- [172] Joachim, C. L.; Morris, J. H.; Selkoe, D. J. *Am. J. Pathol.* **1989**, *135*, 309-319.
- [173] Joachim, C. L.; Selkoe, D. J. *J. Gerontol.* **1989**, *44*, B77-B82.
- [174] Yamaguchi, H.; Hirai, S.; Morimatsu, M.; Shoji, M.; Nakazato, Y. *Acta Neuropathol. (Berl)* **1989**, *77*, 314-319.
- [175] Arnold, S. E.; Hyman, B. T.; Flory, J.; Damasio, A. R.; Van Hoesen, G. W. *Cereb. Cortex* **1991**, *1*, 103-116.
- [176] Braak, H.; Braak, E. *Neurobiol. Aging* **1997**, *18*, 351-357.
- [177] Thal, D. R.; Rub, U.; Orantes, M.; Braak, H. *Neurology* **2002**, *58*, 1791-1800.
- [178] Price, J. C.; Klunk, W. E.; Lopresti, B. J.; Lu, X.; Hoge, J. A.; Ziolkowski, S. K.; Holt, D. P.; Meltzer, C. C.; DeKosky, S. T.; Mathis, C. A. *J. Cereb. Blood Flow Metab.* **2005**, *25*, 1528-1547.

- [179] Koeppe, R. A.; Frey, K. A.; Mulholland, G. K.; Kilbourn, M. R.; Buck, A.; Lee, K. S.; Kuhl, D. E. *J. Cereb. Blood Flow Metab.* **1994**, *14*, 85-99.
- [180] Logan, J.; Fowler, J. S.; Volkow, N. D.; Wolf, A. P.; Dewey, S. L.; Schlyer, D. J.; MacGregor, R. R.; Hitzemann, R.; Bendriem, B.; Gatley, S. J.; *J. Cereb. Blood Flow Metab.* **1990**, *10*, 740-747.
- [181] Ichise, M.; Toyama, H.; Innis, R. B.; Carson, R. E. *J. Cereb. Blood Flow Metab.* **2002**, *22*, 1271-1281.
- [182] Verhoeff, N. P.; Wilson, A. A.; Takeshita, S.; Trop, L.; Hussey, D.; Singh, K.; Kung, H. F.; Kung, M. P.; Houle, S. *Am. J. Geriatr. Psychiatry* **2004**, *12*, 584-595.
- [183] Zakzanis, K. K. *Arch. Clin. Neuropsychol.* **2001**, *16*, 653-667.
- [184] Shoghi-Jadid, K.; Small, G. W.; Agdeppa, E. D.; Kepe, V.; Ercoli, L. M.; Siddarth, P.; Read, S.; Satyamurthy, N.; Petric, A.; Huang, S. C.; Barrio, J. R. *Am. J. Geriatr. Psychiatry* **2002**, *10*, 24-35.
- [185] Valeo, T. *Sci. Am.* **2004**, *290*, 26, 28.
- [186] Arimon, M.; Diez-Perez, I.; Kogan, M. J.; Durany, N.; Giralt, E.; Sanz, F.; Fernandez-Busquets, X. *FASEB J.* **2005**, *19*, 1344-1346.
- [187] Barghorn, S.; Nimmrich, V.; Striebinger, A.; Krantz, C.; Keller, P.; Janson, B.; Bahr, M.; Schmidt, M.; Bitner, R. S.; Harlan, J.; Barlow, E.; Ebert, U.; Hillen, H. *J. Neurochem.* **2005**, *95*, 834-847.

---

Received: June 22, 2006

Revised: September 24, 2006

Accepted: September 25, 2006